SMALL-ANGLE X-RAY SCATTERING STUDIES ON ORDERED STRUCTURE OF POLYELECTROLYTE SOLUTIONS

HIDEKI MATSUOKA

Department of Polymer Chemistry
Kyoto University
Kyoto

1987

SMALL-ANGLE X-RAY SCATTERING STUDIES

ON

ORDERED STRUCTURE OF POLYELECTROLYTE SOLUTIONS

HIDEKI MATSUOKA

Department of Polymer Chemistry

Kyoto University

Kyoto

1987

CONTENTS

Chapter 1

General Introduction

The knowledge of the distribution of the solutes is indispensable for the understanding of the solution properties. The distribution is essentially governed by the solute-solute and solute-solvent interactions. In polyelectrolyte solutions, the solute components are macroions and counterions, and there are strong, long-range interactions of electrostatic nature between them. Under no-salt or low salt conditions, these interactions are so enhanced that the solutions have very unique properties, which neutral polymer solutions do not have. To investigate the distribution of the polymer molecules in solution, small-angle X-ray scattering (SAXS) is one of the most powerful techniques. The SAXS curves from polymer solution contain the information of the conformation and the distribution of the polymer molecule.

About 45 years ago, Bernal and Fankuchen[1] performed SAXS measurements on tabacco mosaic virus in dry and wet gel states and in concentrated solution, and obtained distinct intermolecular diffraction peak or peaks. Riley and Oster[2] carried out SAXS measurements on concentrated solutions of bovine serum albumin, and found clear intermolecular scattering peaks. They suggested that the molecules distributed equidistantly.

Recently, X-ray scattering and small-angle neutron scattering (SANS) techniques have developed; small-angle scattering measurements can now be performed also on dilute

solutions of polyelectrolytes[3-7]. A scattering peak, though single and broad, was observed even for dilute solutions and it was attributed to the intermolecular interference.[5-7] The intermolecular distance ($2D_{exp}$) could be evaluated from the peak position by the Bragg equation, and found to be smaller beyond experimental error than the average intermolecular distance ($2D_0$) calculated from the concentration with an assumption of a uniform distribution. From this fact, Ise et al. suggested that the distribution of polyions was not random, but, unexpectedly, there were dense ordered regions in which the polyions were distributed in order, and less dense regions in which the polyions were distributed at random. This was called the "two-state structure".[5]

For relatively small polymer latex particles in suspension, it has been known that the suspension shows iridescence under suitable condition.[8] It has been demonstrated that the iridescence is due to Bragg diffraction of visible light by an ordered array of the latex particles in suspension.[9] For relatively large latex particles Hachisu et al. made an epochal study ; they observed the ordered structure of latex particles by naked eye with a metallurgical microscope as an ultramicroscope.[10] For highly charged latex particles in dilute suspension, the particles usually formed a hexagonal array, and not only the ordered regions but also the disordered region could be observed.[11] The interparticle distance ($2D_{exp}$) was also smaller than $2D_0$.

The ordered arrangement of polyions in solution by the electrostatic interaction had already been predicted by Ise et al.[12,13] based on the experimental data of the mean activity

coefficients (γ) ; logγ was linearly proportional to the cube-root of the concentration (so-called cube-root rule). This fact was taken as suggesting a more or less regular distribution of macroions.

Lin et al. observed an unusual salt concentration dependence of the appearent diffusion coefficient (D_{app}) of poly-L-lysine by dynamic light scattering method.[14] With decreasing salt concentration, D_{app} decreased dramatically at a certain salt concentration. They called this phenomena "ordinary-extraordinary phase transition". The fairly small D_{app} value at low salt concentrations has been attributed to the formation of a structure of macroions by electrostatic interaction.

Concerning these experimental findings, the formation of structure of polyelectrolytes is thought to be a general and fundamental phenomenon. However, to clarify the nature of the structure, more detailed investigations are necessary and indispensable. In this thesis, SAXS observations of ordered structure of polyelectrolytes and the interaction between polyions in solutions will be discussed with respect to the dependences on the polyelectrolyte concentration, the salt concentration, the solution temperature etc. The SAXS profiles will also be discussed. In chapter 2, SAXS observation on dilute solutions of sodium polystyrenesulfonate, which is a typical anionic polyelectrolyte, will be discussed. Details of SAXS apparatus used will also be described in chapter 2. In chapter 3, SAXS investigation on solutions of some biological poly-electrolytes, such as bovine serum albumin, lysozyme, transfer-ribonucleic acid and chondoroitin sulfate, will be described. In

Chapter 4, SAXS observation on solutions of polyallylamine hydrochloride will be treated. A single, broad SAXS peak, which is reminiscent of the ordered arrangement of polyions, was observed for solutions of this novel cationic polyelectrolyte. In Chapter 5, SAXS investigations of the ordered distribution of allkyltrimethylammonium chlorides, which form cationic spherical micelles above the critical micelle concentration (cmc), will be described. Since the spherical nature of the micelle particle, more detalied analysis of SAXS curves becomes feasible, and hence more exact information on the distribution of micelle particles in solutions is obtained. The experimental and theoretical SAXS curves will also be compared, which makes it possible to estimate the lattice system and the distortion of the ordered structure. In chapter 6, SAXS observations on the ordered structure of colloidal silica particles in suspensions and theoretical considerations will be described. In chapter 7, a theory of scattering from distorted crystals will be presented.

Reference

1 J.P.Bernal, and J.Fankuchen, J.Gen.Physiol., 25, 111 (1941).

2 D.P.Riley, and G.Oster, Discuss. Faraday Soc., 11, 107 (1951).

3 M.Nierlich. C.E.Williams, F.Boue, J.P.Cotton, M.Daoud, B.Farnoux, G.Jannink, C.Picot, M.Moan, C.Wolff, M.Rinaudo, and P.G. de Gennes, J.Physique, 40, 701 (1979).

4 J.Plestil, J.Mikes, and K.Dusek, Acta Polym., 30, 29 (1979).

5 N.Ise, T.Okubo, Y.Hiragi, H.Kawai, T.Hashimoto, M.Fujimura, A.Nakajima, and H.Hayashi, J.Am.Chem.Soc., 101, 5836 (1979).

6 N.Ise, T.Okubo, K.Yamamoto, H.Kawai, T.Hashimoto, M.Fujimura, and Y.Hiragi, J.Am.Chem.Soc., 102, 7901 (1980).

7 N.Ise, T.Okubo, K.Yamamoto, H.Matsuoka, H.Kawai, T.Hashimoto, and M.Fujimura, J.Chem.Phys., 78, 541 (1983).

8 T.Alfrey,Jr., E.B.Bradford, J.W.Vanderhoff, and G.Oster, J.Opt.Soc.Am., 44 603 (1954).

9 W.Luck, M.Klier, and H.Wesslau, Ber. Bunsenges. Phys. Chem., 67, 75 (1963).

10 A.Kose, M.Ozaki, K.Takano, Y.Kobayashi, and S.Hachisu, J. Colloid Int. Sci., 44, 1330 (1973).

11 N.Ise, T.Okubo, M.Sugimura, K.Ito, and H.J.Nolte, J.Chem.Phys., 78, 536 (1983).

12 N.Ise, and T.Okubo, J.Phys.Chem., 71, 1287 (1967).

13 N.Ise, and T.Okubo, J.Phys.Chem., 72, 1370 (1968).

14 S.-C. Lin, W.I.Lee, and J.M.Schurr, Biopolymers, 14, 1041 (1978).

Chapter 2

"Ordered" Structure in Dilute Solutions of Sodium Polystyrenesulfonates

I. Introduction

X-ray scattering experiments on dilute and/or concentrated solutions of synthetic macroions, proteins, polynucleotide, ionic micelles, and tabacco mosaic virus show a broad single peak in small angle regions.[1] The peak has been taken to suggest that the solute macroions form ordered structures in the solutions.[2-5] By using the Bragg equation, the intermacroion spacing ($2D_{exp}$) has been evaluated and found to be much smaller than a theoretical distance ($2D_0$) calculated from the solute concentration on the assumption that the highly charged macroions (such as polyacrylate,[3,4] poly-L-lysine[5]) are uniformly distributed. At low polymer concentrations, the $2D_0/2D_{exp}$ amounted to two, while the experimental uncertainty in $2D_{exp}$ was estimated to be $\pm 5\%$ from repeated runs. Recent laser light scattering experiments by Kato et al.[6] on solutions of highly charged polymer latex (having a relatively small diameter) also showed a single broad peak. For a 93%-sulfonated polystyrene latex of a diameter of 1540A, $2D_{exp}$ values were 8×10^3, 3.8×10^3, 2.9×10^3, and 2.8×10^3 A at concentrations of 1.81×10^{-4}, 5.45×10^{-4}, 1.09×10^{-3}, and 2.18×10^{-3} g/ml, respectively, while the $2D_0$ values were 1.5×10^4, 5.2×10^3,

4.1×10^3, and 3.3×10^3A. Thus, the relation $2D_0/2D_{exp} > 1$ is believed to hold for highly charged solutes in general at low concentrations, which suggests that there must exist a two-state structure. In other words, the ordered regions have to coexist with disordered regions in dilute solutions, as was shown in Fig.4 of Ref.1(a).

An EXAFS study on solutions of $ZnBr_2$ disclosed that the interionic distances between Zn^{2+} and Br^- are 2.37 and 2.30 A at 0.089 M in water and at 0.05 M in ethyl acetate, respectively, both being very close to the value in a solid crystal (2.40A). This observation indicates that a local ordering similar to that in the solid crystal persists even at these concentrations.[7] Although the lifetime of the ordered structures is unknown, there must also exist a two-state structure for the $ZnBr_2$ solutions. Furthermore, a two-state structure was observed with the naked eye for dilute solutions of electrically charged polymer latex particles.[8] This system allows us to employ a microscopic method for the investigation of solute distribution. Thus it seems plausible that ionic solutes commonly form an ordered structure, regardless of the molecular mass and geometry, and that the two-state structure is maintained under suitable conditions.[9] If so, the experimental finding implies that an attraction must exist between these ionic species inspite of the like-sign charges thereon. Though it came as a surprise, Ise et al. concluded the existence of such an intermacroion attraction about 20 years ago on the bases of the cube-root dependence of the mean activity coefficient of polyelectrolytes and of the drastic decrease of

the single-ion activity of macroions with increasing concentration.[10] (It should be recalled that the activity increases linearly with increasing concentration in the ideal solution according to Raoult's law. The activity is defined to be the ratio of vapor pressures of the species concerned at the given and reference concentrations. Thus, the observed decrease of the macroion activity indicates that there must naturally exist an interaction - repulsive or attractive - between macroions and the net interaction is an attraction which hinders the transfer of the macroions from the solution phase to the gas phase more and more substantially with increasing concentration.) It is noted that this attraction comes into existence through the intermediary of counterions, though detailed discussion will be given later. For colloid systems, Langmuir emphasized the important role of the attraction between charged micelles and an ion atmosphere of opposite sign, which exceeds the repulsive force between the micelles.[11]

The present chapter deals with the small-angle x-ray scattering of sodium salts of polystyrenesulfonate (NaPSS) with various molecular weights and examines further the above stated, rather unexpected observation and conclusion. This polyelectrolyte is chosen because samples of narrow molecular weight distributions are commercially available.

II Experimental

II-1 Materials

NaPSS was purchased from Pressure Chemical Co., Pittsburgh, Pennsylvania. Four samples with molecular weights of 4600, 18000,

74000, and 780000 (only in part) were used. The polydispersity indexes, M_w/M_n, were 1.07, 1.14. 1.17, and 2.10, respectively. The materials were carefully washed with purified water by using an ultrafiltration cell (model 202, Amicon Co. Lexington, Mass.) until the filtrate ceased to show UV absorbance. Then the materials were treated with cation- and anion-exchange resins (Amberlite IR-120-B and IRA-400) and freeze dried. The water used for the purification and preparation fo solutions was obtained by a Milli-Q system (Type I Millipore, Ltd., Bedford, Mass.). The specific conductance of the water was 8×10^{-8} mho/cm. The ion-exchange resins were purified as follows: The resins were brought into the purified water and heated to $40^{\circ}C$ for 3 h. Then the water was exchanged with HCl or NaOH solution and with the pure water thoroughly before use.

Sodium polyacrylate (NaPAA) was the same sample as used in privious experiments by Ise et al.[3,4] (M_w=97000). Polyvinylpyrrolidone (PVP) (M_w=40000) was purchased from the Tokyo Kasei, Tokyo, and purfied by ultrafiltration. NaCl and KCl (analytical grade) were purchased from Merck. $CaCl_2$ and $BaCl_2$ were of guaranteed grade.

II-2 Small-angle X-ray scattering (SAXS) measurement

In the present experiments, a Kratky U-slit system was employed with a position-sensitive-proportional counter (PSPC) for the SAXS measurements. Figure 1 shows the outline of the SAXS apparatus. A 12 kW rotating-anode generator (RU-200A, Rigaku Denki, Tokyo) was used. The CuK_α beam was monochromatized by a

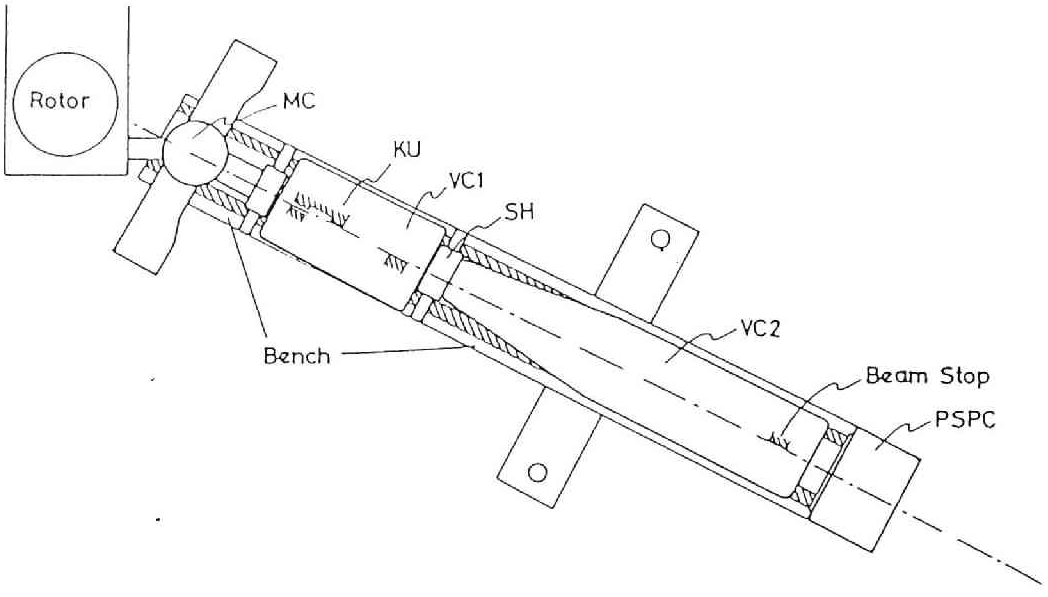

Fig.1 The optical system of the small-angle X-ray scattering apparatus: MC: monochrometer, KU: Kratky U-slit, VC1 and VC2: vacuum chambers, SH: sample holder.

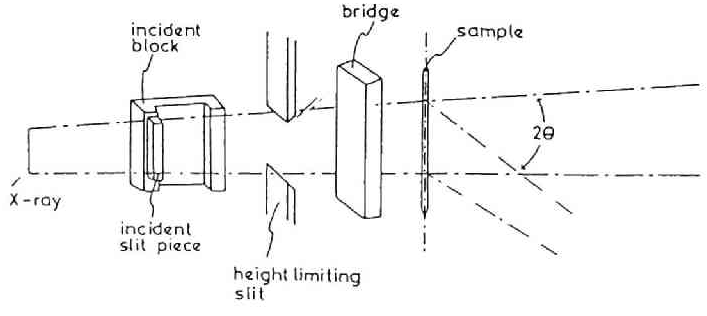

Fig.2 A schematic diagram of the Kratky U-slit system.

graphite crystal (12x25x2 mm, Union Carbide Corporation, Ohio) with a glancing angle of 26.5^{o}. Then the X-ray beam was collimated by a Kratky U-slit (Manual No. MJ210HD, Rigaku Denki, Tokyo) and hit on the sample solution in a glass capillary. The intensity of the scattered X-ray was detected by a PSPC (Manual No. MJ510EM, Rigaku Denki, Tokyo). The camera distance was 525 mm. The vacuum chambers (VC1, VC2) and sample holder (SH) were connected and the entrance window of VC2 were sealed with beryllium(BW). The sample cell was thus kept under vacuum. Inside the vacuum path (VC2), the incident beam stop was mounted in front of the beryllium window.

The optical bench on which the Kratky U-slit (KU), sample holder (SH), vacuum chambers (VC1, VC2) with a beam stop and PSPC were mounted had level- and position-adjusting screws on both front and back parts. The bench could be rotated around the center of the graphite monochrometer. The alignment of the bench with respect to the incident X-ray beam could be adjusted without great difficulity. Each part of the apparatus is described in more detail below.

Kratky U-slit

Figure 2 shows the Kratky U-slit system. The incident CuK_{α} beam was 13 mm high. The entrance slit width was varied in tree steps, 10, 30, and 70 μm, by changing the incident slit piece. A 70 μm slit was used in this experiment. The height limiting slit was varied between 10 and 40 mm with a screw, and in this experiment, adjusted to 30 mm.

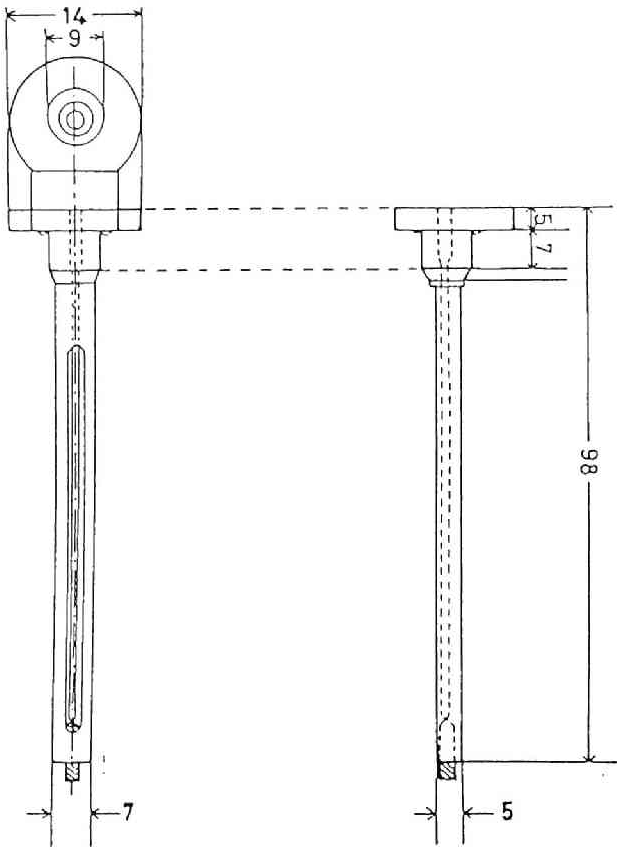

Fig.3 A schematic diagram of the sample cell.

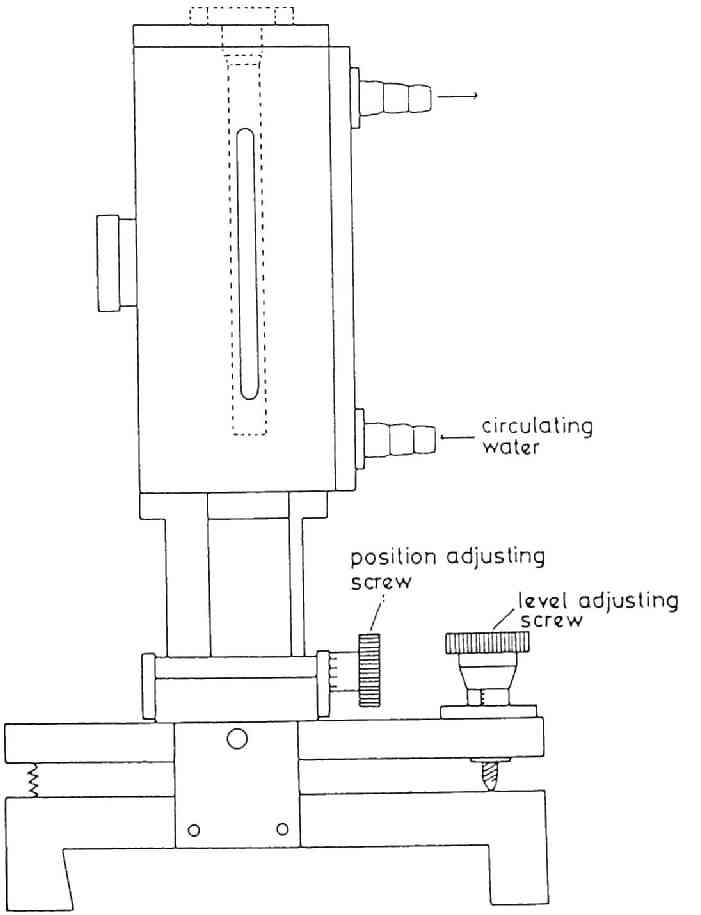

Fig.4 The holder of the sample cell.

Sample cell

A Mark glass capillary (diameter 1.5 mm, thichness 10 μm) was used as the sample cell, which is shown in Fig.3. Figure 4 is a sample holder (SH). Inside of the SH could be kept under vacuum during the measurements. The temperature of the sample was monitored by a thermocouple and controlled by circulating water from a constant temperature bath (Lauda K2R).

PSPC

The linear position-sensitve-proportional-counter (PSPC) could detect X-ray beam scattered in the whole measuring range simultaneously. PSPC had a 10x50 mm window, and the detector holder was designed to enable horizontal movement by 40 mm with a micrometer screw. The quantum effeciency of the detector for CuK_{α} radiation was 38% for PR gas flow (Ar 90% and CH_4 10%) at 3.0 atm pressure and 20°C, and the position resolution was better than 200μm.

This detector used the time-to-amplitude converter (TAC) method. The principle of this system is schematically illustrated in Fig.5. An electric pulse which reached to both ends of the delay line was converted to a voltage signal and amplified by preamplifiers (PA). Then the pulses were doubly differentiated by amplifiers (AMP). The outputs from AMP became 0 V after a certain time (in this case 0.3μs) regardless of pulse heights. The zero cross detectors (ZC) in the timing single channel analyzers (TSCA) gave trigger pulses at the time when the outputs of AMP crossed zero. According to the position of the incident

photon at the PSPC window, the outputs from ZC had a certain time lag. The time-to-amplitude converter (TAC) outputs a voltage signal whose height was proportional to the time lag. The output from TAC was converted into channel number by a multichannel analyzer (MCA).

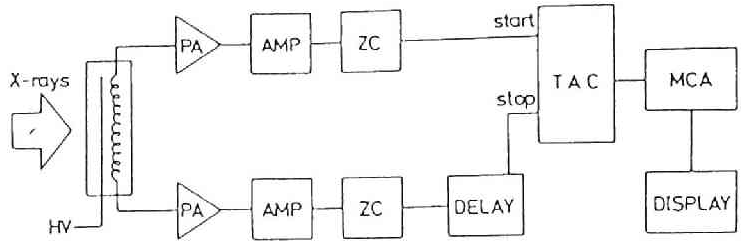

Fig.5 A diagram showing the principle of scattering detection by the PSPC.

Data analyses

A microcomputer (SORD M223 Mark III) multichannel analyzer (MCA, Manual No. MJ520PS, Rigaku Denki) system was used for data analyses. Information in MCA was transferred to microcomputer and stored on 5(1/4)in. diskette, then sent to the University Computer Center through an acoustic coupler for further analyses of data such as absorption correction and sensitivity correction of PSPC. For smoothing and desmearing, Lake's method[12] was employed.

Cooling system

For cooling target. tube and diffusion pump (DP), a cooling water system (Order No. 06h09k1069, Daikin, Osaka) was used, which was composed of a cold water tank, water supplying pump,

circulating pump, and water chilling unit (air cooling, UWA 5GB, Daikin, Osaka). The water was ion exchanged, and its temperature was controlled at 20 $\pm$ 1.0°C.

III Results

III-1 Control SAXS experiments

Dr. J.Plestil and Professor K.Dusek, Institute of Macromolecular Chemistry, Czechoslovak Academy of Science, Prague, kindly performed independent SAXS measurements on one of our samples by using their own apparatus[2]. The peak position observed in Prague agree very satisfactorily with those found in Kyoto within 1.5%. From repeated runs, the experimental uncertainty in $2D_{exp}$ was estimated to be $\pm$ 5% at the highest.

III-2 Polymer concentration dependence

Typical scattering curves of NaPSS (M_w=74000) at various polymer concentrations are shown in Fig.6. In the concentration range between 0.01 and 0.08 g/ml, there appeared a single broad peak, the q_m shifted toward wider angle and the relative intensity at q_m increased with increasing polymer concentration, as was observed for polyacrylate,[2,4], poly-L-lysine,[5] and t-RNA.[13] At 0.16 g/ml, a peak was observed but the intensity was lowered. The tendency for the intensity to increase with increasing polymer concentration and to decrease after passing a maximum was also noted for other samples.

III-3 Salt concentration dependence

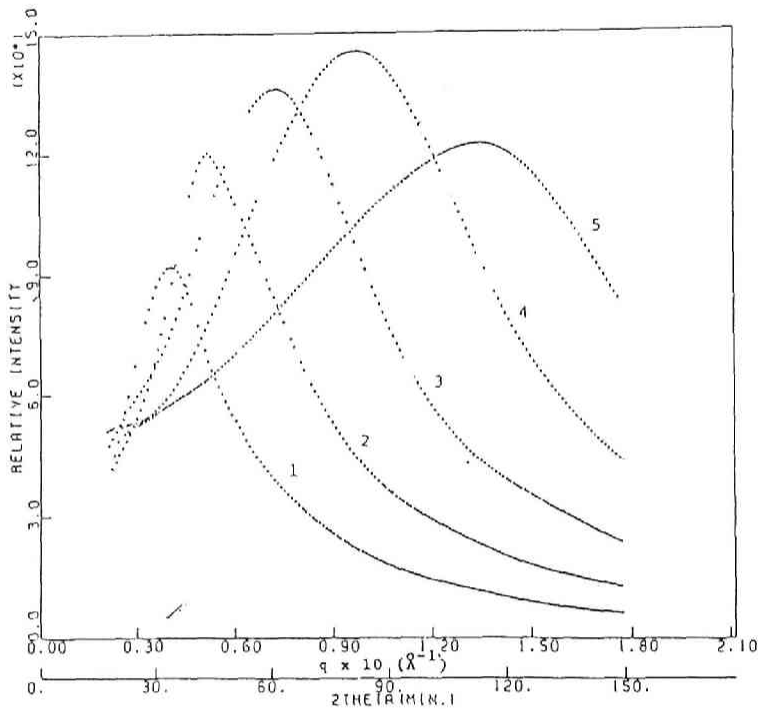

Fig.6 Concentration dependence of scattering curves of NaPSS. M_w=74000, polymer concentration; curve 1: 0.01 g/ml, 2:0.02 g/ml, 3:0.04 g/ml, 5:0.16 g/ml.

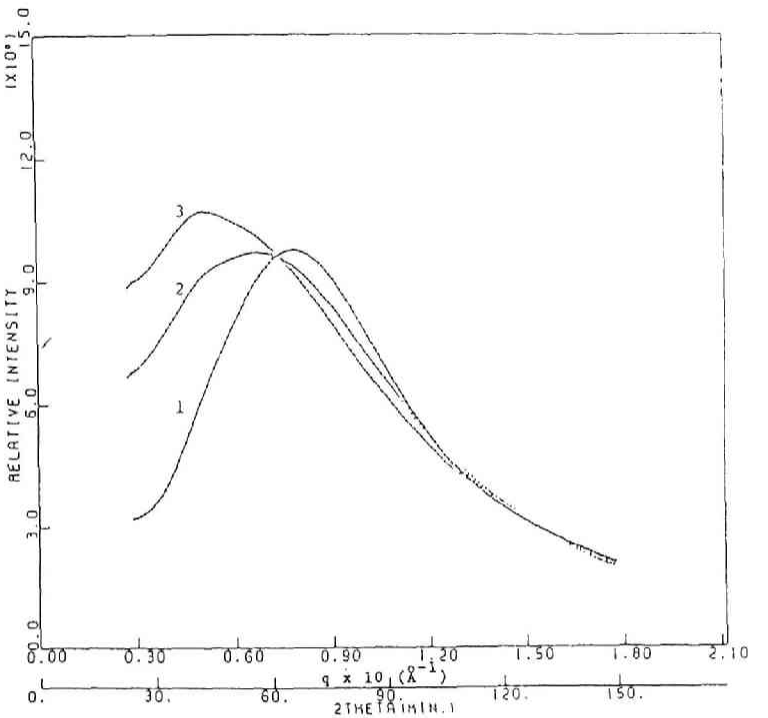

Fig.7 Salt concentration dependence of scattering curves for NaPSS. M_w=18000, polymer concentration: 0.0[illegible] g/ml, [NaCl]; curve 1:0 M, 2:0.05 M, 3:0.1M.

Figure 7 shows the scattering curves of NaPSS (M_w=18000) at various concentrations of added NaCl. Obviously, the q_m value shifted toward lower vectors with increasing NaCl concentrations, as observed for polyacrylate,[4] Poly-L-lysine[5] and t-RNA.[13]

Figure 8 demonstrates also the influence of various salts at a concentration of 0.1 equiv/l. In the case of NaCl, a shoulder was observed at a low angle, whereas the peak disappeared for $CaCl_2$ and $BaCl_2$.

III-4 Molecular weight dependence

Figure 9 gives the scattering curves of NaPSS samples with three different weight-average molecular weights (M_w). In accord with the previous results obtained for polyacrylate[4] and poly-L-lysine,[5] the q_m value became smaller with increasing M_w. Obviously the scattering behavior depends on the molecular weight in the range covered.[14]

The molecular weight dependence was demonstrated by some of the data shown in Table I. The experiments were designed so that two samples with different molecular weight had the same number concentration by adjustment of their weight concentration. (Compare Expt 1 and 7, Expt 2 and 8, Expt 3 and 9, or Expt 16 and 17). Obviously the higher the molecular weight of sample, the larger the q_m. The significance of this finding will be discussed below.

After finding that the scattering curves had a molecular weight dependence, the following mixing experiment was conducted. The two independent peaks for two fractions (M_w= 4600 and 74000) with a concentartion of 0.02 g/ml were first obtained. Then a

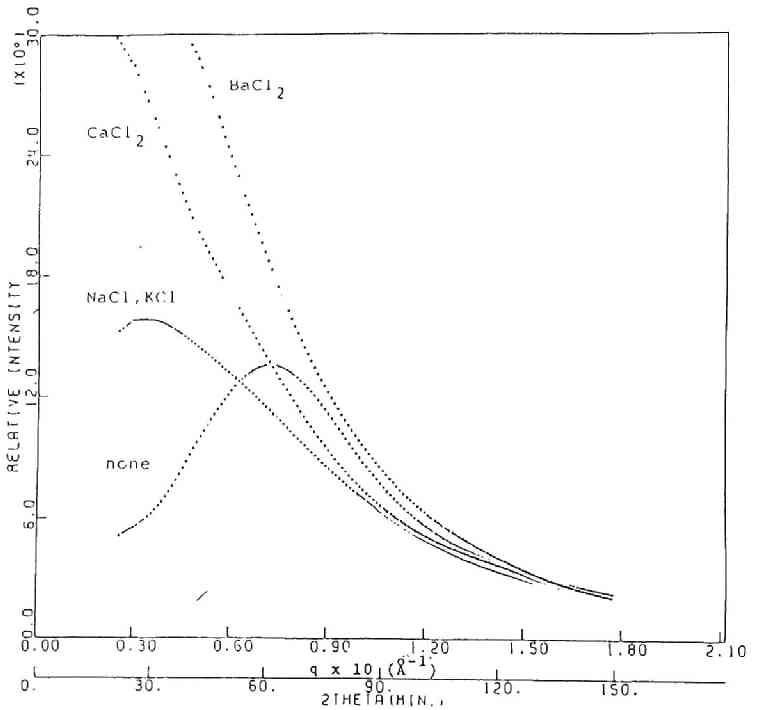

Fig.8 Scattering curves for NaPSS in the presence of NaCl, KCl, $CaCl_2$, and $BaCl_2$. M_w=74000, polymer concentration: 0.04 g/ml, [salt]=0.1M.

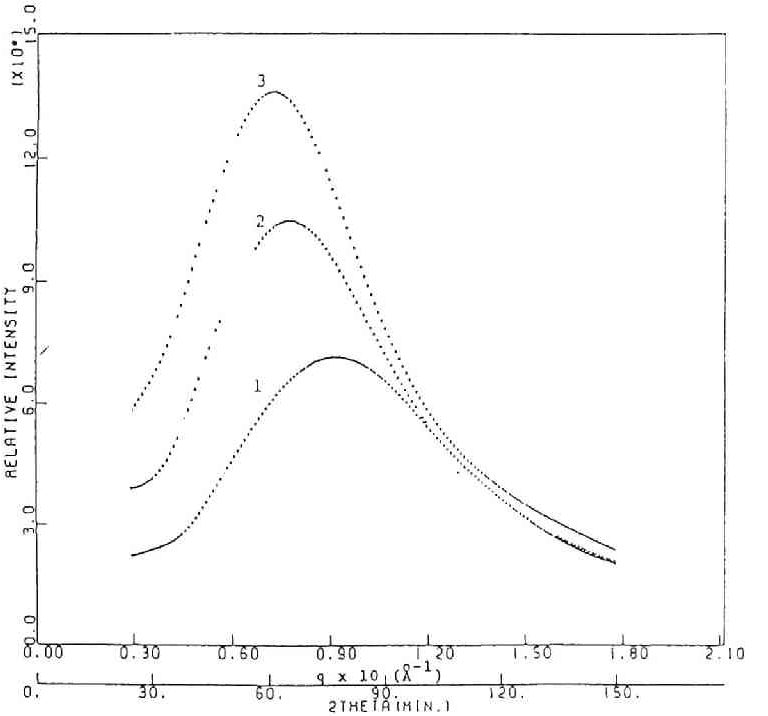

Fig.9 Molecular weight dependence of scattering of NaPSS. Polymer concentration: 0.04 g/ml, M_w; curve 1:4600, 2:18000, 3:74000. The scattering curve for M_w=780000 coincedes with curve 3.

binary solution containing the two fractions (0.02 g/ml for each component) was examined. As shown in Fig.10, a single peak was observed at a position different from that of the composite curve drawn by a summation of the two original curves obtained at 0.02 g/ml. The mixing experiment indicates that the observed scattering peak mainly is due to intermolecular ordering. If it orignates from intramolecular ordering, two independent peaks must be observed for the binary solution at the same posotion as the composite curve. However, in the experiment, this was not the case. Thus, the ordering is confirmed to be of an intermolecular nature, as was found for polyacrylate[4] and poly-L-lysine.[5]

III-5 Mixing with other polymers

Figure 11 shows the scattering curves for NaPSS, sodium polyacrylate (NaPAA) and their mixture. Only a single peak was observed for the binary mixture at a q_m value different from those of the mother peaks. It is noted that the q_m value for the mixture shifted toward larger values. This observation again confirms that the observed peak is due to intermolecular ordering.

Figure 12 gives the SAXS curves for NaPSS, polyvinylpyrrolidone (PVP) and their mixtures. It is clear that PVP itself has no peak. The mixture gave a single peak and the peak position did not change with the PVP addition.

III-6 Temperature dependence

The SAXS curves of an NaPSS solution are demonstrated at

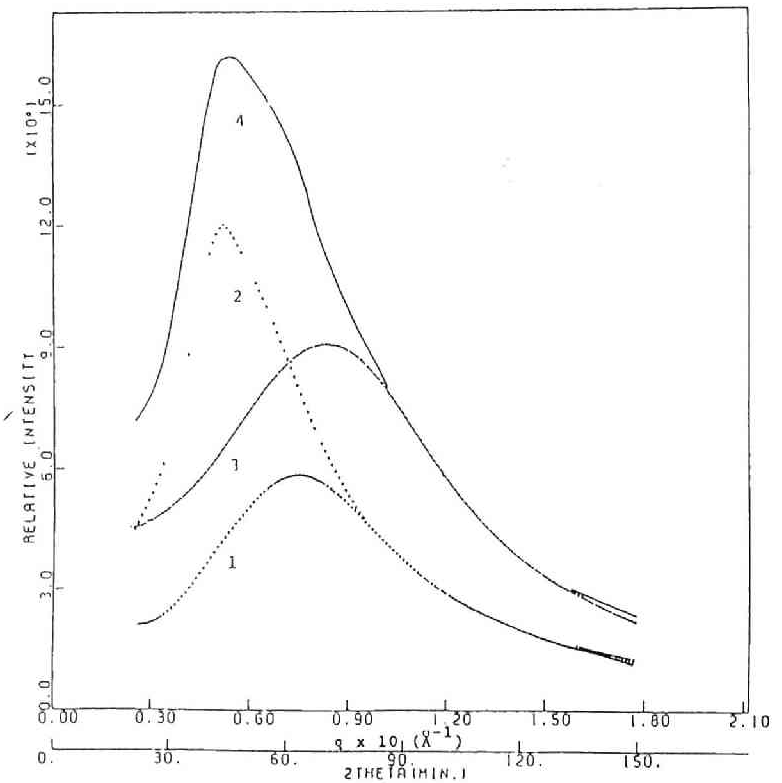

Fig.10 Mixing experiments of NaPSS with M_w=4600 and 74000. Polymer concentration: 0.02 g/ml before mixing and 0.04 g/ml (0.02 g/ml for each fraction) in the binary mixture. Curve 1:M_w=4600, 2:M_w=74000, 3:the mixture, 4:composite curve.

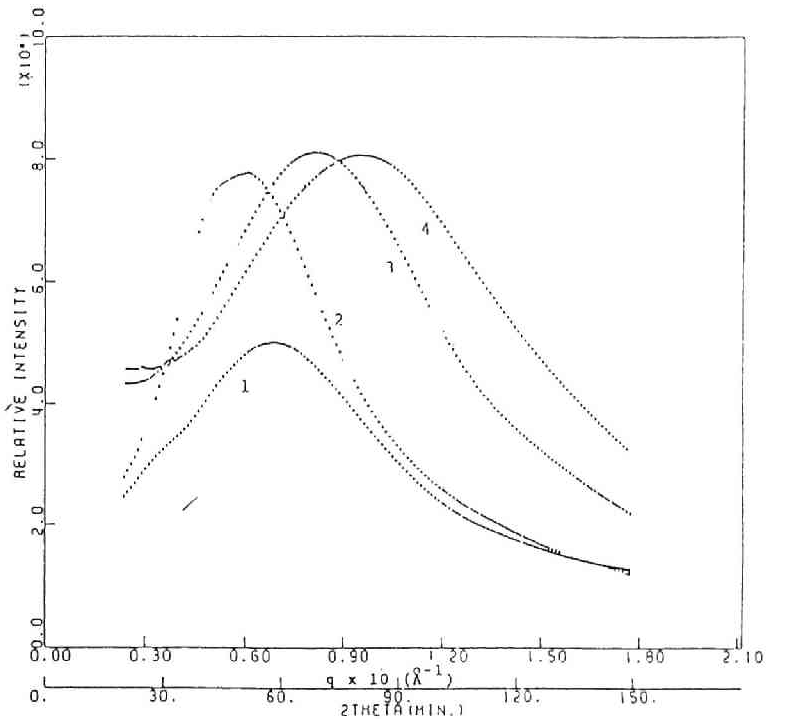

Fig.11 Scattering curves of NaPSS (M_w=18000), a sodium polyacrylate (NaPAA) (M_w=97000) and their mixtures. Curve 1:NaPAA, 0.02 g/ml, 2:NaPSS, 0.02 g/ml, 3:NaPAA (0.02g/ml) + NaPSS (0.02g/ml), 4:NaPAA (0.04g/ml) + NaPSS (0.02 g/ml).

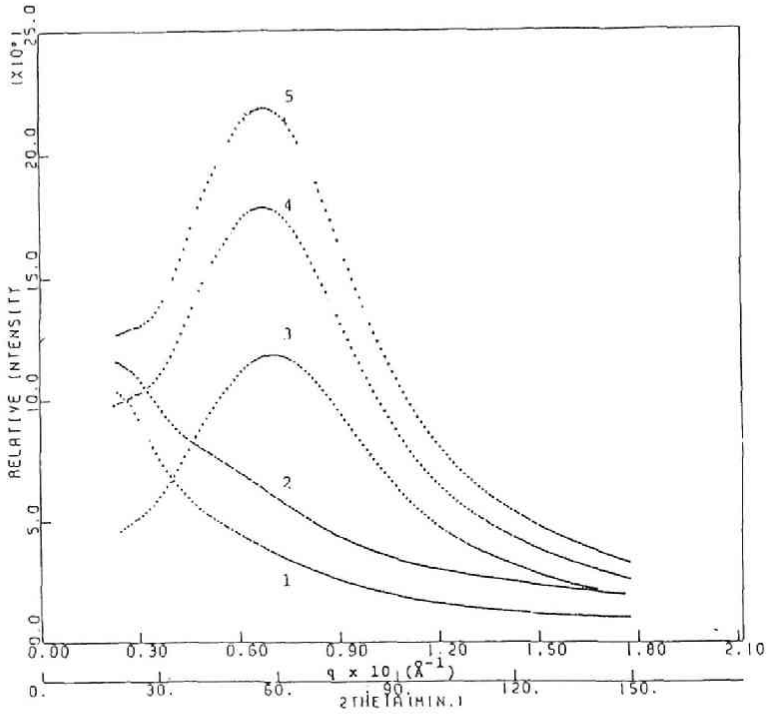

Fig.12 Scattering curves of polyvinylpyrrolidone (PVP) (M_w=40000), NaPSS (M_w=74000) and their mixtures. Curve 1 and 2: PVP, concentration: 0.04 and 0.08 g/ml, 3:NaPSS, 0.04 g/ml, 4: PVP (0.02 g/ml) + NaPSS (0.04 g/ml), 5: PVP (0.04 g/ml) + NaPSS (0.04 g/ml).

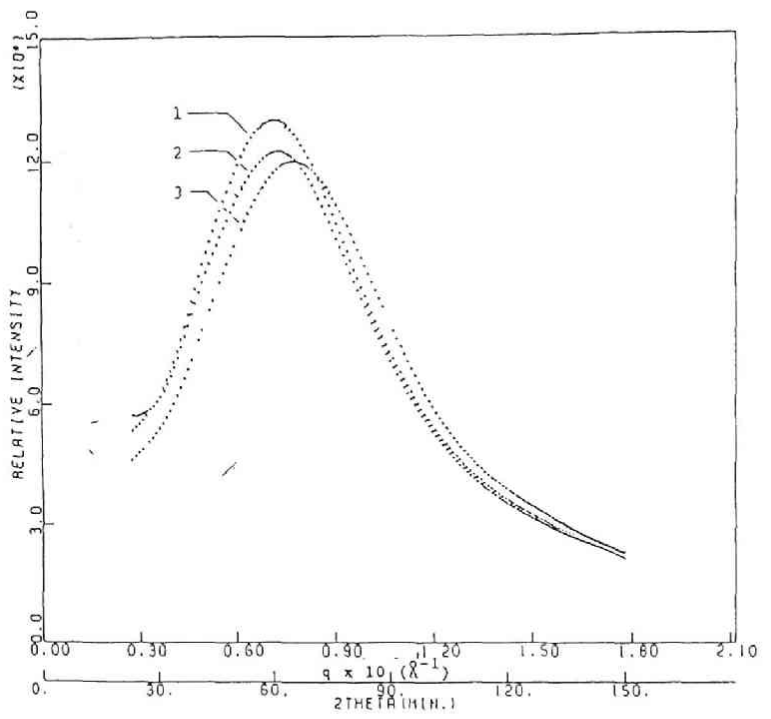

Fig.13 Temperature dependence of scattering curves for NaPSS. M_w=74000, polymer concentration: 0.04 g/ml, curve 1: 13°C, 2:25°C, 3:40°C.

three different temperatures in Fig.13. With increasing temperature, the peak was slightly lowered and the peak position shifted toward wider angles, though very slightly. It would be reasonable to suggest that the intermolecular ordering was disturbed by the kinetic energy.

IV. Discussion

IV-1 Comparison of $2D_{exp}$ (Bragg spacing) with $2D_0$

Table I gives the numerical data of the SAXS experiments for NaPSS. Evidently, the intermacroion distance ($2D_{exp}$) obtained from the peak position, based on the assumption that the Bragg equation holds, has the following features: (1) $2D_{exp}$ decreases with increasing polymer concentration (Expt.1-4, 5-9), (2) $2D_{exp}$ increases with addition of simple salt (Expt.3, 12, 13), and (3) $2D_{exp}$ is smaller than $2D_0$ (average intermacroion distance calculated by assuming the uniform simple cubic distribution throughout the solution) in the absence of the simple salt.

The third aspect is not clear for the low molecular weight sample, but is distinct for the sample of M_w=74000. All of these features are in agreement with previous observation for polyacrylate[4] and poly-L-lysine,[5] and confirm the interpretation proposed earlier by Ise et al. that there exists electrostatic attraction between the macroions, and that the ordered regions coexist with the disordered region, in other words, that the two-state structure is maintained.

IV-2 Molecular weight dependence of scattering behavior and $2D_{exp}$

As was observed before by Ise et al.,[4,5] the binary mixture

Table I Small-angle X-ray scattering data of sodium polystyrenesulfonates in aqueous solutions.

Expt.	M_w	conc. (g/ml)	[NaCl] (M)	q_m[a] (A^{-1})	$2D_{exp}$[b] (A)	$2D_0$[c] (A)	Temp. (^oC)
1	18000	0.01	0	0.046	136	144	25
2	18000	0.02	0	0.053	119	114	25
3	18000	0.04	0	0.078	81	91	25
4	18000	0.08	0	0.104	60	72	25
5	74000	0.01	0	0.040	157	231	25
6	74000	0.02	0	0.052	122	183	25
7	74000	0.04	0	0.073	87	145	25
8	74000	0.08	0	0.096	65	115	25
9	74000	0.16	0	0.134	47	92	25
10	4600	0.04	0	0.091	69	58	25
11	780000	0.04	0	0.073	87	319	25
12	18000	0.04	0.05	0.067	94	91	25
13	18000	0.04	0.1	0.051	(123)[d]	91	25
14	74000	0.04	0	0.071	88	145	13
15	74000	0.04	0	0.077	82	145	40
16	4600	0.02	0	0.074	85	73	25
17	18000	0.078	0	0.102	62	73	25
18	4600 + 780000	0.04	0	0.083	76	71	25

a q_m: scattering vector at the peak.

b $2D_{exp}$: intermacroion distance obtained from q_m on the assumption that the Bragg equation holds.

c $2D_0$: intermacroion distance calculated for a simple cubic distribution.

d This value is believed to be overestimated because the high salt concentration should weaken the intermolecular scattering so that a larger error might be associated with the q_m value than in other cases.

of two samples with different molecular weights gave a scattering curve independent of those observed before mixing, which was taken to indicate that the observed peak was not due to intramolecular ordering, but due to intermolecular ordering. This interpretation is now further reinforced by the data presented by Table I, which shows that the sample with a higher molecular weight has a $2D_{exp}$ different from that with a smaller M_w at a given number of macromolecules in the unit volume. (For example, compare Expt.16 and 17). If the scattering peak is due to intramolecular ordering, such a difference in the $2D_{exp}$ (and hence the scattering behavior) should not be observed. The data in Table I thus substantiates the presence of an intermolecular ordering.

IV-3 Intensification of intermacroion attraction with increasing valency

Table I shows another important aspect; $2D_{exp}$ of substances with higher molecular weights is smaller at the same number concentration. With polyelectrolytes such as NaPSS, the larger the molecular weight, the larger the number of charges (valency) of macroions. Thus, the experimental data imply that the intermacroion attraction becomes stronger as the macroion valency is increased. According to the widely "accepted" view, macroions should simply repel each other because of the charges on them. Thus, the more highly charged the macroions are, the more intensive the repulsion is, which is the reverse of what is observed. In this respect, the above-mentioned fact, that $2D_{exp}$ increases with increasing salt concentration, is also in

contradiction with the accepted view, according to which $2D_{exp}$ should decrease because it is the repulsion that must be weakened by the addition of salt if the above accepted view is ultimately correct. However, condensed system with free surface cannot exist without attractive interaction. It is suggested that the accepted view be checked carefully. In this respect, Sogami[15,16] developed an interionic interaction theory for macroionic solutions, in which, when the electrostatic interaction between macroion and counterions and that between macroions are duly considered, an electrostatic attraction between the macroions is demonstrated to exist. Furthermore, the conclusion brought by the DLVO theory on colloidal stability[17] that the electrostatic interparticle interaction in two-particle systems is repulsion, is shown in Ref.16 not to be generally correct. Although detailed discussion is to be found in Ref.16, careful consideration of the substantial infuluence of the counterion-macroion interaction suggests that there is a net attraction between the macroions, and that the attraction becomes more intense with increasing macroion charge.

Since this theoretical conclusion contradicts the theory of colloidal stability and the generally accepted view, although the former is in agreement with the experimental findings on the activity or activity coefficient,[10] X-ray and laser light scatterings,[3-6] and micrography,[8] some comments would be necessary. When the macroions are not highly charged, their counterions may exist even in regions far from the macroions as a concequence of relatively weak interaction between the

counterions and macroions. In other words, the electrostatic shielding of the macroion charges by the counterions would be weak so that one macroion would exert an almost purely "repulsive"[18] infuluence on other macroions. On the other hand, When the macroions are highly charged, the shielding is no longer weak. In other words, the counterions may now be confined to the vicinity of the macroions. The macroions attract the counterions, which in turn attract other macroions. When the number of the counterions is large enough (as is the case for highly charged macroions), this attraction overwhelms the repulsion between the macroions,[19] so that a net attraction would remain.

When the macroions are not highly charged, the net attraction is not noticeable, though they actually do exist. For example, the $2D_{exp}$ values for a polymer latex having a relativlely small number of charges were approximately equal to the $2D_0$ values, as have been found by Ise et al.[8] The relation $2D_{exp} \simeq 2D_0$ was also noticed for t-RNA,[13] which has a relatively low charge density. The relation can be found to hold for an NaPSS sample (e.g., Expt.10 of Table I.) with a small number of charges ($M_w=4.6\times10^3$). It is again to be emphasized that the inequality relation $2D_{exp}<2D_0$ and hence the contribution of the attraction can be clearly observed only for highly charged macroions.[20]

IV-4 Why do we observe only a single broad peak? -- The dynamic character and distortion of the ordered structure

It often has been claimed that the single peak reported for solutions of macroions by X-ray or neutron scattering is not the

Bragg diffraction. The reason for such an argument against our interpretation is that only a single, broad peak could be observed. This argument is, however, quite superficial. The scattering behavior influenced by the size and number of the ordered structures, and thermal motion and paracrystalline distortion of the diffracting components. In this respect, the microscopic study by Ise et al. on polymer latex solutions using a movie camera[21] clearly indicates that the latex particles display vigorous thermal motion around the equilibrium point even if they are in ordered regions. In the concentration range between 0.5% and 5%, the interparticle distance ($2D_{exp}$) was about 10^4 A, whereas its standard deviation $2D_{exp}$ amounted to 10^3 A. Theoretical details of the influence of the thermal vibration on the scattering curve will be described in chapter 7. and the exapmles of the scattering curve from the particles in ordered state with various amounts of the thermal vibration will be found in chapter 3, which will indicate the importance of this effect.

According to a theory on one-dimensional paracrystalline distortion by Hosemann and Wilke[22], the n-th peak of the scattering curve is not distinguishable when n x g is larger than 0.35, where g is the ratio of the standard deviation of the paracrystalline distortion and the nearest-neighbour interparicle distance. The paracrystal theory was extended to three-dimensional cubic lattice systems (simple cubic lattice, face-centered cubic lattice, and body-centered cubic lattice) as will be discussed in chapter 7, and the similar approximate criterion, i.e., the n-th number peak is not distingishable when n x g is

larger than about 0.2, was obtained as will be described fully in chapter 7.

The effect of the size of the ordered region will be also described fully in chapter 7. It will be recognized that the smaller the ordered region, the lower and the broader the scattering peak. Before claiming that the single broad peak is not the Bragg diffraction peak, due attention must be paid to the dynamic character and the distortions of the ordered structure.

IV-5 Mixing experiments with sodium polyacrylate (NaPAA) or with polyvinylpyrrolidone (PVP)

Figure 11 represents interesting aspects of the ordering of macroions. First, the curve 3 for the binary mixture of NaPSS and NAPAA (0.02 g/ml for each component) has a q_m value of 0.082 A^{-1}. For the single component solutions of NaPSS and NaPAA, the q_m values (for curve 2 and 1) were 0.062 and 0.070 A^{-1}, respectively. The fact, that the q_m value for the mixture is larger than that for the pure component solution definitely excludes the possibility that the scattering peak is due to intramolecular ordering. Instead, the observed fact implies that the peak results from an intermolecular ordering in the solution and, in the present case, that both polystyrenesulfonate ions and polyacrylate ions contribute to the formation of a mixed ordered structre. If the two macroionic species form their own ordered arrangements separately, or if a microscopic phase separation takes place, we should expect two independent peaks at q_m values of 0.062 and 0.070 (or a single peak between 0.062 and 0.070 A^{-1}). This is not the case however; the mixture gave a peak at

q_m=0.082.

The observed fact that the binary q_m increases beyond the higher of the two single macroion values invites some comment. From the M_w's and the monomer masses of NaPAA and NaPSS, the relative sizes of the macroions would approximately be 3:1 if a random coil model can be assumed. Since the mixing experiments were carried out in large excesses of NaPSS ions over NaPAA (the ration being about 12:1), the larger macroion (NaPAA) would be surrounded by a larger number of the smaller macroion(NaPSS) with a more closely packed arrangement. This appears to account for the observed fact, but a more quantitative argument will be given after the mixing experiment, which is being currently performed, has been completed.

Concerning Fig.12, it is to be recalled that neutral PVP showed no peak as was the case with unneutralized polyacrylate[4] and bovine serum albumin (an amphoteric protein) at the isoelectric pH.[23] Evidently, the ordering is due to electric charges on the solute particles. When PVP is mixed with NaPSS, the q_m values of the mixture stayed practically unchanged. This fact indicates that the ordered structure of NaPSS was not affected by the presence of PVP. It is not clear whether this result is specific to the PVP-PSS solution. Detailed discussion is postponed until more experimental data on other binary systems have accumlated.[24]

IV-6 Dependence on temperature

The lowering of the SAXS peak with increasing temperature

demonstrated in Fig.13 is reasonable, Because the ordering is progressively distorted by the kinetic energy. However, the small shift of the q_m toward larger vectors is rather surprising. While the temperature rise should cause widening of the intermacroion spacing, the decrease of the dielectric constant with temperature seems to be more important. The dielectric constant decreases from 83.8 at 10^{o}C to 73.15 at 40^{o}C.[26] This decrease supresses the dissociation of the counterions, causing a decrease in the net valency of the macroions and at the same time intensifies the attractive interaction between the macroions. These two factors exert counteracting influences on the interparticle distance, which probably explains the rather small change observed for q_m.

IV-7 Comparison with SANS data

A deurated sodium polystyrenesulfonate having a molecular weight of 72000 was studied by a small-angle neutron scattering (SANS) technique.[27] The results showed a single, broad peak in the intensity-scattering vector curves. In common with our SAXS data, the q_m shifted toward larger vectors with increasing polymer concentration. However, the q_m value did not change with addition of simple salt (NaBr) in the range between 0 and 0.03 M, on the contrary to our SAXS data and the previous observation, which showed systematic shifts toward lower vectors with increasing salt concentration for NaPAA,[4] poly-L-lysine,[5] and NaPSS (Fig.7). Nonetheless, rough agreement is seen between the SAXS and SANS data:e.g., at 0.01, 0.02, and 0.08 g/ml, the SANS measurements give $2D_{exp}$ values of 140, 108, and 52 A, whereas the SAXS experiments on a polystyrenesulfonate with M_w=74000 gave

$2D_{exp}$ values of 157, 122, and 65 A. Taking into account the difference in M_w, the $2D_{exp}$ values obtained by the two methods would become closer, though slightly. It is here to be stressed that above comparison is highly approximate, and that the two methods would give us a small but definite difference in the peak position and the change of the scattering intensity with charge density, as discussed earlier by Dusek et al.[28]

Although no remark was made in the paper on SANS,[27] the $2D_{exp} < 2D_0$ relation is seen to hold for the SANS measurements. For example, the $2D_0$ values at 0.01, 0.02, and 0.08 g/ml are calculated to be 228, 182, and 116 A, which are larger than the corresponding $2D_{exp}$ by factors of 1.6-2.3.

It is important to note that the SANS data are claimed to be explicable in terms of the isotropic model.[29] As was easily understood, the q_m value should not be dependent on the molecular weight, if this model is correct. In the present study, the scattering behavior was demonstrated to clearly depend on the molecular weight, especially when M_w is smaller than 100000. (See Fig.9, and Table I). Thus, the isotropic model does not appear to be generally valid.

IV-8 Further remarks on the two-state structure. States or phases ?

When the molecular weight is high, i.e., except for the sample of M_w=4600, the intermacroion distance ($2D_{exp}$) obtained from the peak position by using the Bragg equation is definitely smaller beyond the experimental uncertainty than the theoretical

distance ($2D_0$) calculated from the concentraion obtained on the assumption that the distribution of the solute ions is uniform throughout the solution. The $2D_0/2D_{exp}$ value appears to increase with increasing M_w and amounts to about two for a high molecular weight sample at high concentartions (Expt.7 - 9). At M_w=780000, the ratio reaches to 3.5 (Expt.11). This implies that the macroions are not uniformly distributed throughout the solution but form the two-state structure in which locally ordered dense regions coexist with disordered less dence regions. We note that the two-state structure model is consistent with the recent dynamic light scattering measurements by Schmitz[30] and Nemoto, Kurata et al.[31] and low frequency dispersion measurements by Schmitz,[32] as well as with some earlier work discussed in Refs.5 and 8.

It is further to be noted that there exists the close parallelism of these features with the two-state structure in solutions of highly charged latex particles, which has been observed by the naked eye. (See, e.g., Fig.1 in Ref.8.)

In order to avoid misunderstanding, it is emphasized that the ordered region of macroions should not be regarded as a phase. Although no information is deducible from the SAXS and SANS measurments, it seems highly plausible that the ordered regions undergo violent fluctuation with time and have no stable surface of discontinuity. This statement is based on the direct observation made with the naked eye on polymer latex solutions,[8] which shows that an ordered region at one place disintegrates into disordered arrangement and that at the next momont a new ordered region is created in another place. Thus the use of the

term "phase" in describing the ordered regions and the application of the phase rule in analyzing the ordering phenomena would have to be avoided. It probably would be pertinent to point out a similarity between the behavior of macroions and that of water molecules in liquid water which consists of one phase but contains (ordered) "iceberg" structures and (disordered) free water molecules.[33]

IV-9 Repulsion or attraction ?

The experimental facts mentioned above cannot be accounted for in terms of the widely accepted view; e.g., the inter-macroionic separation is usually thought to increase with increasing valency of the macroion. The experiments show that the separation decreases with valency. In this interpretation, the electrostatic repusion is present exclusively. The experimental data obtained here indicate the incorrectness of the accepted view. It is to be stressed again that <u>two macroions per se naturally repel each other when they can exist alone in solutions but that an attraction is generated between the two macroions as a consequence of the existence of their counterions in between the macroions</u>. This attraction becomes stronger with increasing number of counterions and hence with increasing valency. As has been claimed,[10] the attraction is possible through the inter-mediary of counterions. It is also important to note that there must exist a very strong repulsion between macroions at small separations. The attraction and repulsion create a "secondary" minimum. This situation can be accounted for, at least

qualitatively, by the new interionic theory,[15,16] which duly considers the role of counterions.

IV-10 Are macroions streched out or coiled up ?

A comment is necessary on the physical meaning of $2D_{exp}$ and the problems concerning the conformation of the macroion in solutions. In the calculation of $2D_{exp}$, no assumption is made on the geometry of the macroions. $2D_{exp}$ is thus an "approximate" distance between the centers of gravity of the periodically located space containg high electron density. It is not justified to assert that the macroion is fully streched or that it is a (dense) spherical coil in the concentration employed in the scattering experiments. Although a fully streched model is often assumed for macroions, we question whether this is the case at concentrations employed in the SAXS measurements. The justification for this assumption appears to be that α assumes a value close to two for salt-free polyelectrolyte solutions in the relation $[\eta]=KM^{\alpha}$. Even if η_{sp}/C could be measured accurately enough in salt-free water media, though this is not easy as is well recognized, it is recalled that $[\eta]$ refers to the infinite dilution. Thus, the justification is acceptable only for the extreme dilution, and the macroion may then be judged to be streched. This is probably correct, because the counterions can diffuse away from the macroion domain at such dilutions so that the ionized groups of the macroion would exert purely repulsive interaction upon each other. However the situation at higher concentrations is entirely unclear.[34]

However, we do not believe, either, that the macroions at

concentrations under consideration can be approximated by a model like a golf-ball. This model is to fail for high molecular weight samples and at high concentrations. For example, the $2D_{exp}$ value (87 A) derived from the SAXS peak for NaPSS of M_w=780000 at a concentration of 0.04 g/ml is not large enough to accomodate all styrenesulfonate units of one macromolecule, even if the largest possible density is the two extreme cases. Further detailed study is definitely necessary on this problem.

IV-11 A comment on Earnshaw's theorem

Finally, a comment is necessary on Earnshaw's theorem,[35] which claims that a charged body cannot be maintained in stable equilibrium under the influence of the electric field alone. We are not questioning this theorem, though the ordering under consideration is claimed to be due to purely electrostatic interactions. It must be reminded that, in addition to electrostatic interaction, we have an important second factor in real solutions, namely the kinetic energy contribution. Obviously, this factor exercises a counteracting influence against the electrostatic action. The ordering which we are observing results by the simultaneous contribution of the electrostatic interaction between ions and the kinetic energy. It is sometimes pointed out that our interpretation of the ordering of macroions in solutions in terms of the electrostatic interaction is not acceptable in light of Earnshaw's theorem. This is however the misuse of the theorem.

Referenes and notes

1 For a review of the topic, see (a) N.Ise and T.Okubo, Acc. Chem. Res., 13, 303 (1980); (b) N.Ise, Angew. Chem., 25, 323 (1986).

2 J.Plestil, J.Mikes and K.Dusek, Acta Polym., 30, 29 (1979).

3 N.Ise, T.Okubo, Y.Hiragi, H.Kawai, T.Hashimoto, M.Fujimura, A.Nakajima and H.Hayashi, J.Amer.Chem.Soc, 101, 5836 (1979).

4 N.Ise, T.Okubo, K.Yamamoto, H.Kawai, T.Hashimoto, M.Fujimura and Y.Hiragi, J.Amer.Chem.Soc., 102, 7901 (1980).

5 N.Ise, T.Okubo, K.Yamamoto, H.Matsuoka, H.Kawai, T.Hashimoto and M.Fujimura, J.Chem.Phys., 78, 541 (1983).

6 T.Kato, H.Masuda, and A.Takahashi, Polymer Prepr. Jpn., 31 2249 (1982).

7 P.Lagarde, A.Fontaine, D.Raoux, A.Sadoc, and P.Migliardo, J.Chem.Phys., 72, 3061 (1980); A.Sadoc, A.Fontaine, P.Lagardo and D.Raoux, J.Amer.Chem.Soc., 103, 6287 (1981).

8 N.Ise, T.Okubo, M.Sugimura, K.Ito, and H.J.Nolte, J.Chem.Phys., 78 536 (1983).

9 At high concentrations, the whole volume of the solution must be covered uniformly by ordered structures. On the other hand, at very low concentrations, the ordered structure would be completely destroyed. At intermediate, but still relatively low concentrations only, the two-state structure would be observable.

10 N.Ise and T.Okubo, J..Phys.Chem., 70, 536, 2400 (1966); 71, 1287, 1886, 4588 (1967); 72, 1370 (1968).

11 Langmuir, J.Chem.Phys., 6, 873 (1938).

12 J.A.Lake, Acta Crystallogr., 23 191 (1976).

13 A.Patrowski, E.Gulari, and B.Chu, J.Chem.Phys., 78, 4178 (1980)

14 One might claim that the molecular weight dependence is negligible. Hoewever, the tendency for q_m to shift toward lower angle beyond the experimental uncertainty is clear not only for PSS but also sodium polyarylate (Ref.4) and Poly-L-lysine (Ref.5) when M_w is smaller than about 100000.

15 I.Sogami, Phys. Lett., A96 199 (1983).

16 I.Sogami and N.Ise, J.Chem.Phys., 81, 6320 (1984).

17 See, e.g., E.J.W.Verwey and J.Th.G.Overbeek, Theory of the Stability of Lyophobic Colloids (Elsevier, amsterdam, 1948).

18 The reason why the quotation mark is put here is as follows: Sogami showed that the intermacroion interaction at short distances is repulsive, whereas that at large separation is attractive, creating a secondary minimum at relatively large distances. Thus, the interaction between macroions at equilibrium cannot be claimed to be purely repulsive or attractive. The exact description is that the attractive component is largely lowered as a result of depressed shielding.

19 The preponderance of the attraction is due to two facts, that the average distance between the likes is larger than between the unlikes, and the Coulombic potential is inversely proportional to the distance between ions.

20 The following preliminary comparison of the theory discussed in Ref.16 with the experimental data would be of interest.

For NaPSS sample of M_w=74000, the observed value of $2D_{exp}$ at 0.01 g/ml (157 A) can be reproduced by the theory if the net valency of macroion (Z), the dielectric constant of the Solvent (ϵ), and the radius of the macroion sphere (a) are assumed to be 200, 78.5, and 37 A, respectively. Since the analytical valency of this material is 74000/monomer mass (200)=370 and the counterion condensation takes place, the true net valency would not be far from 200: The assumed Z value would not be unreasonable. It is noted that the theory in the present form assumes spheres having charges on their surface, which would not be appropriate to the macroions. The extension of the theory to spheres having charges inside as well as on surface is in progress. Thus, the above comparison is to be taken as an approximate one.

21 N.Ise, T.Okubo, and K.Ito, Dosho and I.Sogami, J.Colloid Int. Sci., 103, 292 (1985).

22 R.Hosemann and R.Wilke, Makromol. Chem., 118, 230 (1968).

23 Chapter 3 of this thesis; H.Matsuoka, N.Ise, T.Okubo, S.Kunugi, H.Tomiyama, and Y.Yoshikawa, J.Chem.Phys., 83 378 (1985).

24 According to the recent SAXS study[25], the ordered structure of NaPSS was not so affected by the addition of the neutral polymers, such as polyethyrene glycol, polyvinylmethyl ether etc. However, the scattering curve from NaPAA in solution was anomarously affected by the addition of PVP, polyethylene glycol etc.; with increasing concentration of the neutral polymer, the scattering peak shifted to higher

angles and its intensity was lowered. This might be due to the change of the ordered structure of NaPAA. However, the reason is not clear, and the effect of the addition of neutral polymers is not yet fully understood. It seems useful to apply the so-called contrast variation method of SANS; by varying the contrast (the scattering density difference between the solvent and the solute) using the mixture of heavy and light water as solvent, it becomes possible to make either of polyelectrolyte or the neutral polymer "invisible" for X-rays. By this technique, we can get the scattering curve for the single component in the binary system.

25 M.Tsurumi, H.Matsuoka, and N.Ise, Polym. Prepr. Jpn., 35, 3006 (1986).

26 G.G.Malmberg and A.A.Maryott, J.Res.Nat.Bur.Stand., 56 1 (1956).

27 M.Nierlich, C.E.Williams, F.Bone, J.P.Cotton, M.Daoud, B.Farnoux, G.Jannink, C.Picot, M.Moan, C.Wolf, M.Rinaudo, and P.G.de Gennes, J.Phys. (Paris) 40, 701 (1979).

28 J.Plestil, J.Mikes, K.Dusek, Ju.M.Ostanevich, and A.B.Kunchenko, Polym. Bull., 4 225 (1981).

29 P.G. de Gennes, P.Pincus, R.M.Velasco, and M.Brochard, J.Phys. (Paris) 37, 1461 (1976).

30 K.Schmitz, M.Lu, and J.Gauntt, J.Chem.Phys., 78, 5059 (1983).

31 N.Nemoto, H.Matsuda, Y.Tsunashima, and M.Kurata, Macromolecules, 17, 1731 (1984).

32 K.S.Schmitz, J.Chem.Phys., 79 4029 (1983).

33 G.Nemethy and H.A.Scheraga, J.Chem.Phys., 36, 3382 (1961).

34 At concentrations employed in the scattering experiments, the counterions would not diffuse away so that a large portion of the counterions probably exist in the vicinity of the ionized groups. Then, the macroion domains would contain a large number of ionized groups and counterions, which correspond to highly concentrated solutions of simple electrolytes. For polystryrenesulfonate, the distance between two sulfonate groups is about 3 A for fully streched conformation. We note that the average interionic distance for symmetrical 1-1 type electrolytes at 10 M/l is about 4 A. Thus, various phenomena, which are found in the concentrated simple ion solutions, may and should be expected to occur in the macroion domain. One of such phenomena is ionic association such as the formation of ion pairs, triplet ions, quadruples, etc. A portion of counterions may therefore form ion-pair type aggregates with the ionized groups. Some of them might form triple-ion type aggregates; if one counterion is associated with two ionized groups of the same macroion, in other words, if intra-molecular triple ions are formed, the macroions can no longer take a streched conformation. Similarly, inter-molecular quadruples and high aggregates would diminish substantially the possibility for macroions to assume the fully streched conformation.

35 See, e.g., J.A.Stratton, Electromagnetic Theory, (McGraw-Hill, New York, 1941), Chap.2.

Chapter 3

"Ordered" Structure in Dilute Solutions of Biopolymers

I. Introduction[1,2]

Small-angle X-ray (SAXS) and neutron scattering (SANS) curves of dilute solutions of synthetic polyelectrolytes (polyacrylate[3-5], poly-L-lysine[6], polystyrenesulfonate[7]), proteins (bovine serum albumin[8]), virus particles (tabacco mosic virus[9]) and ionic micells[10,11], showed single, broad scattering peaks. The SAXS experiments on a mixture of samples containing two synthetic polyelectrolytes having different molecular weights demonstrated a new scattering curve different from the composite one drawn by a simple summation of the two parent curves for each component[5-7]. This fact indicates that the observed single, broad peak is not due to an intramolecular ordering but due to intermolecular ordering. Thus, this peak reflects an ordered arrangement of the charged solutes in solution. Such an ordered structure can clearly be seen for highly charged polymer latex solutions with the naked eye by microscopic methods[12,13]. Light scattering curves of latex solutions also showed a single, broad peak[14-15]. The formation of such an ordered structure, therefore, seems to be a generally observable basic phenomenon for charged solutes.

Previous systematic studies on synthetic polyelectrolyte

solutions by SAXS[3,5-7] and on polymer latex solution by the microscopic method have clarified the following two features:

1) In dilute solutions, highly charged solutes form a localized "two-state structure" in which ordered regions (with a relatively high solute density) and disordered regions of a relatively low solute density (see Fig.4 in Ref.2(a)) coexist. This was concluded to be true for ionic polymers based on the fact that the intermolecular distance estimated from the peak position (the Bragg spacing) was smaller than the theoretical value calculated from the concentration based on the assumption that distribution is uniform. The same inequality is also clear for the interparticle distance directly estimated on the micrograph (without the Bragg equation) for the polymer latex solutions.

2) The formation of such a localized ordered structure is possible as a result of an "attractive" electrostatic force between ionic solutes through the intermediary of counterions. This was concluded from the dependence of intermolecular distance on polymer concentration, salt concentration and molecular weight. Furthermore, we must note that a "two-state structure" or a localized ordered structure, cannot be maintained in a system in which only a repulsive interaction between solute particles exists.

In this chaper, the solutions of some biopolymers were studied by SAXS measurement. The samples were bovine serum albumin (BSA), lysozyme, chondroitin sulfate (a mucopoly-

succharide) and transfer ribonucleic acid (tRNA). BSA and lysozyme are ellipsoidal globular proteins. Chondoroitin sulfate and tRNA are claimed to have a rod-like[17] and "L"-letter-like shape,[18] respectively. For all materials used in this experiment, a single, broad peak was observed in their scattering curves. These biologically important macroions are also suggested to form an ordered structure in solutions.

The concentrations of BSA which we used here are much lower than those used in the famous study by Riley and Oster[8]. In the SAXS study performed by Chu et al.[19], a single broad peak was obtained for tRNA.

II. Experimental

II-1 Materials

Monomer Standard bovine serum albumin (BSA) purchased from Miles Laboratories Inc. (Elkhart, Indiana, USA) was used without further purification. Lysozyme (hen egg white, 6X crystalline) purchased from Seikagaku Kogyo (Tokyo, Japan) was used without further purification. Chondoroitin sulfate A and C (whale cartilage, ChS-A, shark cartilage,ChS-C) were purchased from Nakarai Chemicals Ltd. (Kyoto, Japan). The samples were carefully washed with purified water by using an ultrafiltration cell (Model 202, Amicon Co. , Lexington, Mass, USA) until the filtrate ceased to show UV absorbance at 200-300 nm. Then the samples were treated with cation- and anion- exchange resins (Amberlite IR-120B and IRA-400) and were freeze-dried.

The molecular weights of ChS-A and ChS-C were determined by

light scattering (Chromatix KMX-6, Mountain View, California, USA). The concentration dependence of the refractive index was measured by using an RM-2 difference refractometer (Union Giken, Osaka, Japan). The degrees of polymerization were determined to be 62 for ChS-A and 95 for ChS-C.

tRNA (baker's yeast) was purchased from Boeringer-Mannheim (Mannheim, West Germany) and was purified by the method of Lindahl and Fresco[20]. First, the sample was gel-filtrated with Sephadex G-100 gel using 1M NaCl + 0.01M Tris-HCl + 0.001M EDTA, pH 7.5 as eluent and main peak fractions were collected. Then the sample was dialyzed against 0.05M EDTA + 0.2M NaCl for 2 days. The sample was then washed with purified water by using an ultrafiltration cell and freeze-dried.

The water used for purification and preparation of solutions was purified by Milli-Q system (Type I, Millipore Ltd., Bedford, Mass.). The purification of ion-exchange resins is as previously described in chapter 2[7].

NaCl and KCl (analytical grade) were purchased from Merck. $CaCl_2$, $BaCl_2$ and $MgCl_2$ were of guaranteed grade.

For pH adjustment , 1N HCl or NaOH standard solution was used.

II-2 Small-angle X-ray scattering (SAXS) measurement

The SAXS apparatus used and data analysis were the same as previously described in chapter 2[7].

III. Results

III-1 Charge number dependence of SAXS curve

Figure 1 shows the typical scattering intensity curves of BSA at three different pH's as a function of scattering vector q ($q=4\pi \sin\theta/\lambda$, 2θ is the scattering angle and λ is the wave length of X-ray, 1.542 angstrom for copper target). At pH 3.44 and 10.94, a single broad scattering peak was observed. However, at pH 5.06 near the isoelectric point of BSA (pI=4.8-4.9), the peak disappeared. This feature clearly shows that the "ordered" structure is of electrostatic origin.

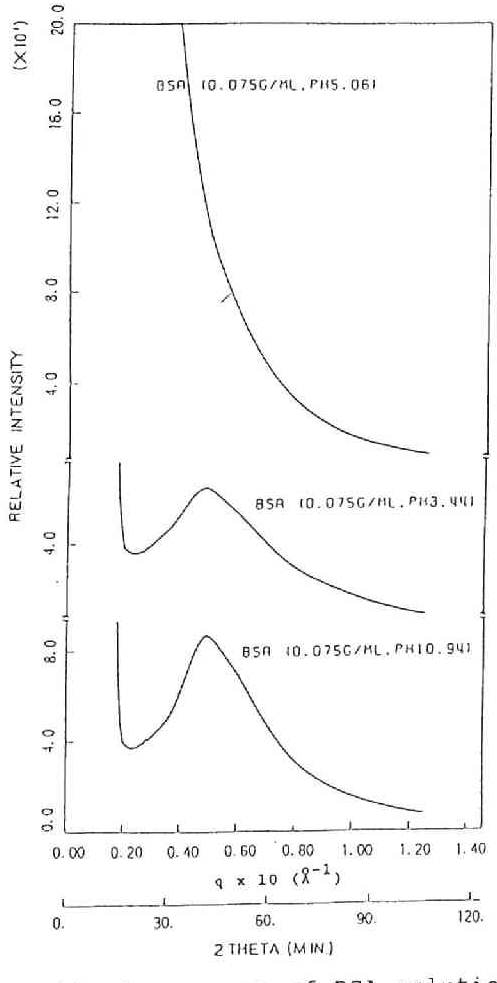

Fig.1 Scattering curves of BSA solutions at three different pHs.

III-2 Polymer concentration dependence

Figure 2 shows the typical scattering curves of lysozyme at various concentrations. In this concentration range, we could observed a single, broad peak. The peak position (q_m) shifted towards wider angles with increasing polymer concentration as observed for polyacryrate (PAA)[3,5], poly-L-lysine (PLL)[6] polystyrenesulfonate (PSS)[7] and tRNA[19].

A similar tendency was observed for tRNA (Fig.3), BSA, and Ch-S A. We note that the peak position observed for tRNA is in excellent quantitative agreement with previous data reported by Chu et al.[19], when experimental conditions are comparable.

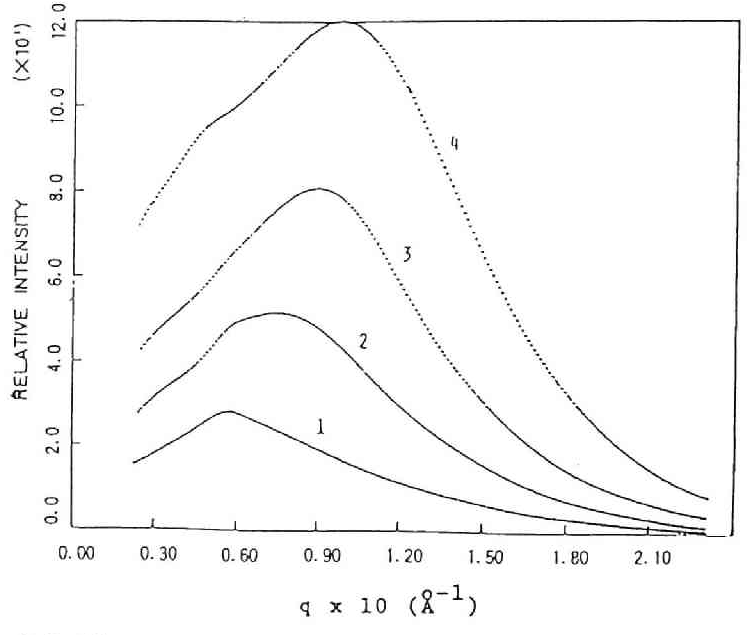

Fig.2 Influence of the concentration on the scattering curves of lysozyme at 25°C. 1:0.02g/ml, 2:0.05g/ml, 3:0.10g/ml, 4:0.25g/ml. pH3.70.

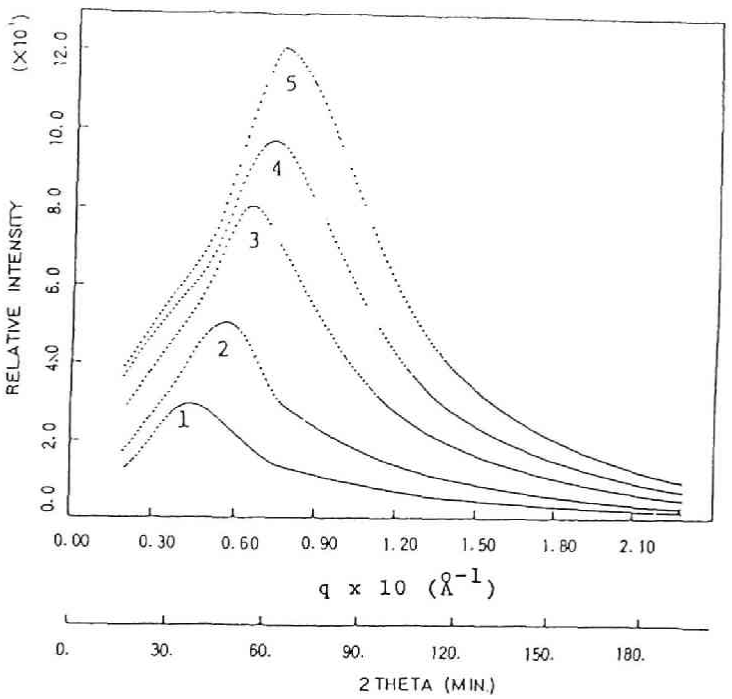

Fig.3 Influence of the concentration on the scattering curves of tRNA at 25°C. 1:0.01g/ml, 2:0.02g/ml, 3:0.04g/ml, 4:0.06g/ml, 5:0.08g/ml.

III-3 Salt concentration dependence

Figure 4 shows the typical scattering curves of tRNA at various NaCl concentrations. The peak position shifted towards lower angles (smaller q_m value) with increase in NaCl concentration. This tendency was also observed for PAA[3,5], PLL[6], PSS[7], BSA, lysozyme, and ChS-A.

Figure 5 demonstrates the influence of $MgCl_2$ added to the tRNA solution. The peak disappeared in 0.04M $MgCl_2$ (Fig.5, curve 4) although a peak was still observed in 0.08M NaCl (Fig.4, curve 4), indicating the higher efficiency of multi-valent cations in

destroying the ordered structure.

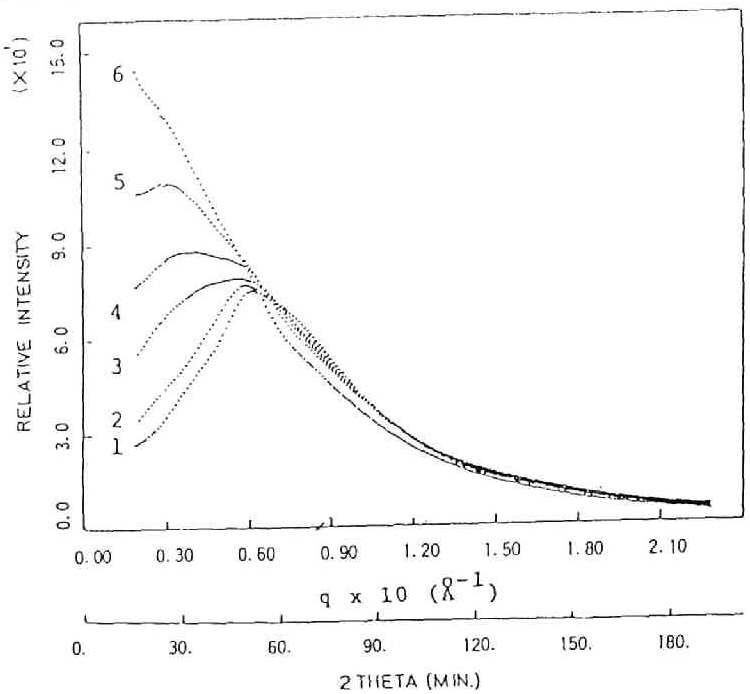

Fig.4 Influence of NaCl added on the scattering curves of tRNA at 25°C. [tRNA]=0.04g/ml. 1:0M, 2:0.01M, 3:0.04M, 4:0.08M, 5:0.15M, 6:0.30M.

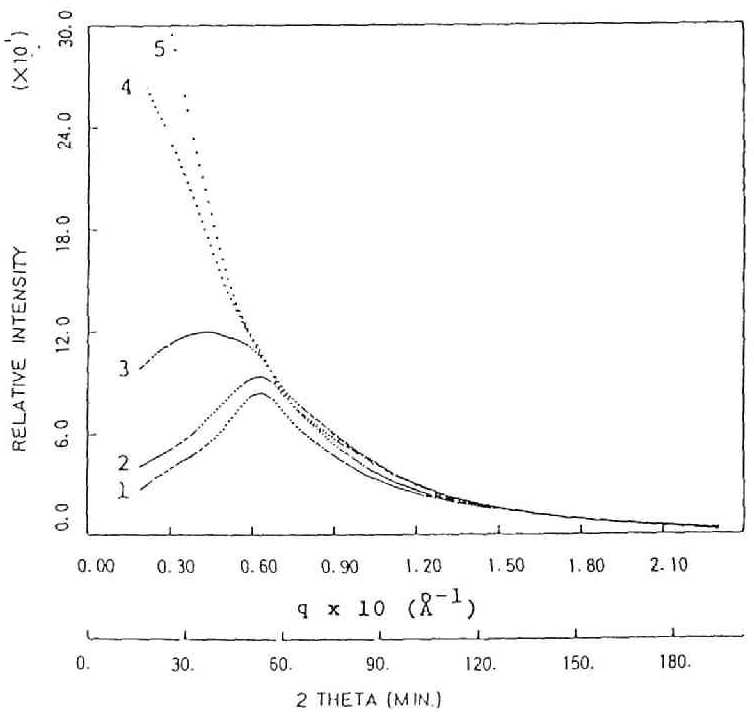

Fig.5 Influence of $MgCl_2$ added on the scattering curves of tRNA at 25°C. [tRNA]=0.04g/ml. 1:0 M, 2:0.005M, 3:0.02M, 4:0.04M, 5:0.

III-4 Temperature dependence

Figure 6 shows the SAXS curves of tRNA solution at three different temperatures. With increasing temperature, the peak was lowered and shifted slightly towards a wider angle, as was observed for PSS[7]. This peak shift was reversible. The scattering curves at 25°C observed after cooling from 40°C and after heating from 13°C, were almost identical to curve 2. No irreversible structural change of tRNA molecule probably occurred.

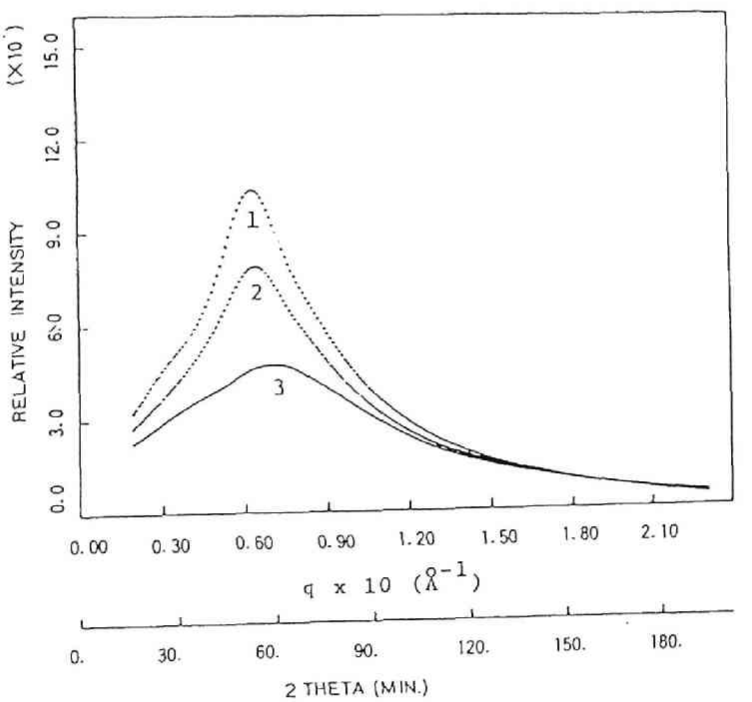

Fig.6 Scattering curves of tRNA at different temperatures. [tRNA]=0.04g/ml. 1:18.5°C, 2:25°C, 3:40°C.

IV. Discussion

IV-1 Charge number (pH) dependence of scattering curve

Figure 1 clearly shows that the formation of an ordered structure is due to electrostatic interaction. At pH 3.44 and 10.94, the net charge of BSA moleclues are inferred to be +40 and -40[21], respectively, and the scattering curves showed a clear single, broad peak. At pH 5.06 (near the isoelectric point), no peak was observed, when the net charge of BSA molecules was nearly zero.

Figure 1 shows an upturn of the scattered intensity at the smallest angles studied. Although this increase cannot be explained, it is believed to be not significant.

The importance of the electric charge was also observed for synthetic polymers. As mentioned previously, synthetic polyelectrolytes showed a scattering peak, while polyvinylpyrrolidone, a water soluble non-ionic polymer, did not[6,7]. Furthermore, unneutralized PAA showed no scattering peak[5].

IV-2 Evaluation of intermolecular distance ($2D_{exp}$) and its dependence for polymer and salt concentrations.

The peak shown in scattering curves reflects an ordered arrangement of charged solutes, as concluded from experiments in which samples of different molecular weights were mixed[5-7]. Then, the intermolecular distance ($2D_{exp}$) was evaluated based on the assumption that the Bragg equation holds. It should not be noted that the Bragg spacing thus obtained gives only approximate

information on a certain interparticle distance, as was carefully pointed out.[23] Keeping this in mind, only substantial systematic changes of, or deviation from $2D_0$ of, the $2D_{exp}$ values would be regarded as physically significant. For example, in the earlier work on the X-ray study in our laboratory,[5-7] when the $2D_{exp}$ values were smaller by a factor larger than 1.5 than the $2D_0$ value (a theoretical interparticle destance calculated from the macroion concentration by assuming a uniform distribution throughout the solution), the difference between $2D_{exp}$ and $2D_0$ was considered to be meaningful and was subsequently attributed to the localized (non-space-filling) two-state structure. This attitude will also be maintained in the present study (see below). As a counterexapmle, experimental data reported in one[24] of a series of contributions by Chen et al.[25,26] on intermicellar interaction shows that the Bragg spacing was 65 A, whereas the first maximum in the pair correlation function was at 70 A at a concentration of 0.294 M of lithium dodecyl sulfate in D_2O at 37°C. The difference between the two distances is judged to be physically not important.

The $2D_{exp}$ values are listed in Table I-IV. For all materials, the following tendencies are seen. First, the $2D_{exp}$ values decreased with increasing polymer concentration, and secondly, it increased with increasing salt concentration, which is in agreement with previous observations for PAA[3,5], PLL[6] and PSS[7]. The salt concentration dependence of $2D_{exp}$ is not in contradiction with the interpretation that the net electrostatic interaction between ionic solutes is "attractive", not

"repulsive". We note that the net electrostatic interaction between ionic solutes is "attraction" through the intermediary of counterions, as was earlier pointed out by Langmuir[27], and by Ise et al.[23]. Schmitz et al. proposed "attractive" interaction by counterion fluctuation[29].

IV-3 Charge number (pH) dependence of $2D_{exp}$

Figure 7 shows the charge number dependence of $2D_{exp}$ for BSA. The $2D_{exp}$ values decreased though only slightly, (did not increase) with charge number, both when the molecules were positively charged and when they were negatively charged, which depicts the interesting and unexpected nature of the electrostatic attraction acting between macroions that it becomes stronger with increasing number of charges. This result confirms our earlier observation for PSS[7] that the Bragg spacing becomes smaller with increasing molecular weight (and hence charge number) at a fixed number (not weight) concentration. (See Table I of chapter 2 Expt.16 and 17 or Expt.2 and 8)

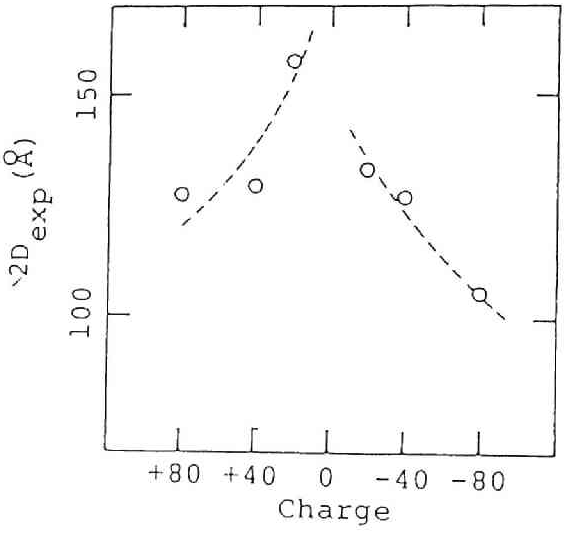

Fig.7 Charge number dependence of $2D_{exp}$ for BSA.

IV-4 Comparison of $2D_{exp}$ with calculated intermolecular distance ($2D_0$, or $2D_{th}$)

The $2D_0$ values in Tables I-IV are the intermolecular distance calculated based on the assumption that the solutes are distributed uniformly to form a simple cubic lattice throughout the solution. When we compare $2D_{exp}$ and $2D_0$, the $2D_{exp}$ values are seen to be nearly equal to or slightly larger than $2D_0$. For synthetic polyelectrolytes (PAA[3,5], PLL[6] and PSS[7]) of relatively high molecular weights, $2D_{exp}$ was smaller than $2D_0$ (by a factor of 2 or 3). For relatively low molecular weight samples (low charge number), for example, for PSS whose molecular weight was 4600, $2D_{exp}$ was nearly equal to $2D_0$[7].

From this fact, from the charge number dependence of $2D_{exp}$ for BSA (the previous section) and from the molecular weight dependence at a fixed number of macromolecules for PSS[7] as discussed above, the feature, that $2D_{exp}$ is equal to $2D_0$, can be said to be due to the low charge number of the biological macromolecules. As have already pointed out[2,5-7], attraction is possible through the intermediary of counterions. The more the counterions (and hence the more highly the macroions are charged), the stronger the attraction. This can be accepted if one realizes that counterions are attracted simultaneously by more than one macroions and the number of the counterions becomes larger with increasing charge number of the macroion. Thus the attraction would be relatively weak for the biopolymers whose charge number is only about 80 at highest, so that the macroions are situated at as distant a position as possible, namely at $2D_0$. Thus $2D_{exp}$ was close to $2D_0$. The observed fact, i.e. $2D_{exp}=2D_0$

Table I Small-angle X-ray scattering (SAXS) data of BSA at 25°C.

Conc. (g/ml)	pH	Added salt	[Salt] (M)	q_m[a] (A^{-1})	$2D_{exp}$[b] (A)	$2D_0$[c] (A)
0.049	3.46	---	0	0.046	136	131
0.094	3.62	---	0	0.049	128	105
0.220	3.44	---	0	0.063	101	79
0.069	2.65	---	0	0.049	128	117
0.072	3.44	---	0	0.049	129	115
0.073	4.07	---	0	0.040	157	114
0.075	5.06	---	0	none	---	114
0.073	8.08	---	0	0.047	133	114
0.072	10.9	---	0	0.049	127	115
0.069	12.2	---	0	0.060	105	117
0.072	3.62	NaCl	0.007	0.047	133	115
0.072	3.75	NaCl	0.08	0.028	223	115
0.072	3.62	$CaCl_2$	0.007	0.044	143	115
0.072	3.67	$CaCl_2$	0.08	0.028	221	115

a q_m : q value at peak position

b $2D_{exp}$: Intermolecular distance calculated from q_m value with assumption that Bragg equation holds.

c $2D_0$: Calculated intermolecular distance from concentration with assumption of uniform, simple cubic distribution of particles.

of lysozyme at 25 C.

Conc. (g/ml)	pH	[NaCl] (M)	q_m (A^{-1})	$2D_{exp}$ (A)	$2D_0$ (A)
0.02	3.25	0	0.058	108	106
0.05	3.56	0	0.074	85	78
0.10	3.67	0	0.090	70	62
0.25	3.87	0	0.098	64	46
0.10	3.86	0.05	0.061	103	62
0.10	3.66	0.10	0.045	140	62

Table III SAXS data of ChS-A and -C at 25°C.

Sample	Conc. (g/ml)	[NaCl] (M)	q_m (A^{-1})	$2D_{exp}$ (A)	$2D_{theor}$ [a,b] (A)	$2D_0$ [a] (A)
ChS-A	0.007	0	0.044	143	143	194
	0.01	0	0.051	124	120	173
	0.02	0	0.074	85	85	137
	0.04	0	0.099	64	60	109
	0.06	0	0.121	52	49	95
	0.04	0.034	0.082	77	63	109
	0.04	0.057	(0.072)	(87)	63	109
	0.04	0.17	none	--	65	109
	0.04	0.85	none	--	65	109
ChS-C	0.04	0	0.100	63	60	126
	0.04	0.05	0.077	81	63	126

a $2D_{theor}=(w/N_A lc\sin 60^o)^{1/2}$.

$2D_0=(MW/N_A c)^{1/3}$.

w: molecular weight of monomer.
MW: molecular weight of polymer.
N_A: Avogadro's number.

l: total length of helical rod divided by the degree of polymerization.
c: polymer concentration in g/ml.

b The salt concentration dependence of l was estimated on the basis of experimental data reported in Ref.17. At [NaCl]=0, 0.034, 0.05, 0.057, 0.17, and 0.85M, the l values were 6.7, 6.2, 6.0, 6.0, 5.8, and 5.6A, respectively.

Table IV SAXS data of tRNA.

Conc. (g/ml)	Added salt	[Salt] (M)	q_m ($Å^{-1}$)	$2D_{exp}$ (Å)	$2D_0$ (Å)	Temp. (^oC)
0.01	---	0	0.043	146	164	25
0.02	---	0	0.055	114	130	25
0.04	---	0	0.065	97	103	25
0.06	---	0	0.073	86	90	25
0.08	---	0	0.077	82	82	25
0.04	---	0	0.064	99	103	18.5
0.04	---	0	0.071	89	103	40
0.04	NaCl	0.01	0.059	106	103	25
0.04	NaCl	0.04	0.057	111	103	25
0.04	NaCl	0.08	0.039	160	103	25
0.04	NaCl	0.15	0.031	205	103	25
0.04	NaCl	0.3	none	---	103	25
0.04	$MgCl_2$	0.005	0.062	101	103	25
0.04	$MgCl_2$	0.02	0.043	146	103	25
0.04	$MgCl_2$	0.04	none	---	103	25
0.04	$MgCl_2$	0.05	none	---	103	25
0.04	$CaCl_2$	0.005	0.062	102	103	25
0.04	$CaCl_2$	0.01	0.060	105	103	25
0.04	$CaCl_2$	0.02	0.045	141	103	25
0.04	$CaCl_2$	0.03	0.018	344	103	25
0.04	$BaCl_2$	0.005	0.063	102	103	25
0.04	$BaCl_2$	0.01	0.060	105	103	25
0.04	$BaCl_2$	0.02	0.039	160	103	25

appears to have led many authors to the erroneous conclusion that the ordered distribution is caused by repulsions alone. This is completely wrong, because no condensed system with free boundary can exist without attractive interaction. If only repulsions are operating between macroions, they would not stay in solution, and their activity ($=f/f^{o}\simeq p/p^{o}$, where f and p are the fugacity and vapor pressure, respectively, and the superscript o refers to the reference state) must increase with increasing concentration with a rate much larger than we would expect from the Raoult law for an ideal solution. However, this is not true. Mesurements show that the activity of various macroions and polymer latex particles decreases (not increases) with increasing concentration[30,31]. On the other hand, if only attraction is present in solution, the macroions would coagulate. Thus, the true mechanism of the ordering is the potential minimum (or the secondary minimum according to the terminology in colloid science) created by the balance of the attraction (at the large distance) through the intermediary of counterions with the repulsion (at shorter distance) between the macroions.

The result showing that $2D_{exp}$ is larger than $2D_0$ is unreasonable (see Table I-IV). These results are due to estimation of $2D_{exp}$ directly from the observed SAXS curves. The SAXS curve is the sum of intramolecular scattering and intermolecular interference effect. The peak found in the interference function may be shifted to lower angles by the contribution of intramolecular scattering, and this effect is stronger at lower angles because the slope of the intraparticle scattering curve is

steeper. Strictly speaking, we must separate the intramolecular and intermolecular scatterings and read the peak position from the intermolecular interference function. Such an attempt will be described in chapter 5 for spherical ionic micelles and in chapter 6 for colloidal silica dispersion[32].

ChS has been reported to have the molecular structure of a rigid rod[17]. It is thus inappropriate to compare the $2D_{exp}$ of ChS with $2D_0$. Instead of $2D_0$, we must use $2D_{th}$ values calculated based on the assumption that rigid rods are distributed uniformly to form a two-dimensional hexagonal packing throughout the solution.

The $2D_{exp}$ values of ChS-A were always smaller than the $2D_{th}$ values. Thus it may be suspected that ordered regions having a relatively high solute density coexist with disordered regions having a relatively low solute density. In other words, a "two-state structure" is also maintained.

ChS-A and -C are more highly charged than the other materials studied here (BSA, lysozyme and tRNA). The analytical valency would be 130-200 from its molecular weights (there are two ionic groups, one sulfonic acid group and one carboxylic group in a monomer unit). Thus the "attractive" interaction is stronger; it is reasonable to form a "two-state structure".

IV-5 Temperature Dependence of SAXS Curve

The scattering peak was lowered when temperature was raised (Fig.6), as found for PSS[7] and micellar systems[33]. This is due to enhanced thermal motion of solutes in ordered regions. It is well known that an enhancement of thermal vibration lowers the

diffraction peaks of solid crystals[34].

The nature of thermal agitation of solute particles can be observed with the naked eye for latex particles by microscopic methods[35]. In ordered regions, the ratio of the standard deviation of the interparticle distance and the average interparticle distance was found to be about 0.1. This dynamic property may be one of the reasons why the scattering peak is single and broad. This aspect will be described in detail in the next section.

IV-6 Consideration on peak shape and number - Paracrystallinity and dynamic behavior of the ordered structure.

If ionic solutes form ordered structures in solution, we should obtain sharp scattering peak and/or higher order peak(s) as is widely claimed. This is a prevailing idea expressed by many. However, in this idea, an important aspect of the ordered structure is definitely overlooked, namely, the dynamic character of scattering elements in the ordered structure. First it should be reminded that the ordered structure under discussion is organized in the liquid state, not in the solid state. Thus the solute particles are subject to violent thermal agitation, which should cause substantial influence on the scattering behavior. Though details will be described in chapter 7, we like to show briefly that the observed, single broad peak can be accounted for by invoking the paracrystalline disorder and thermal motion of the scattering elements.

In general, there are four factors which affect the

scattering intensity from crystals; distortion of components, thermal vibration, paracrystalline distortion and size and shape of crystals. The first two factors, distortion of components and thermal vibration, are called "distortion of the first kind", and the paracrystalline distortion is called "distortion of the second kind".

When the crystal is assumed to be composed of uniform, spherically symmetric particles and to be large, the scattering intensity $I(\underset{\sim}{q})$ is expressed by Eq.(1),

$$I(\underset{\sim}{q})=N\overline{|f|^2}|D|^2Z(\underset{\sim}{q}) \qquad (1)$$

where N is the number of particles, f is the structure factor of particles, $|D|^2$ is the so-called temperature factor or Debye-Waller factor which corresponds to the thermal vibration, and $Z(\underset{\sim}{q})$ is the lattice statistics factor containing paracrystalline disorder.

First, let us consider only a distortion of the second kind. Then Eq.(1) reduces to

$$I(\underset{\sim}{q})=N\overline{|f|^2}Z(\underset{\sim}{q}) \qquad (2)$$

Hosemann showed that $Z(\underset{\sim}{q})$ can be expressed by Eq.(3) by his three-dimensional paracrystal theory[36],

$$Z(\underset{\sim}{q})=\prod_{k=1}^{3}\mathrm{Re}\frac{1+F_k(\underset{\sim}{q})}{1-F_k(\underset{\sim}{q})} \qquad (3)$$

When the distribution of the dislocation of lattice points from the ideal lattice points is Gaussian, whose standard deviation is Δa_k, and the lattice spacing is a_k, $F_k(q)$ in Eq.(3) is

given as follows:

$$F_k(\underset{\sim}{q}) = |F_k(\underset{\sim}{q})| \exp(-i\underset{\sim}{a}_k \cdot \underset{\sim}{q}) \qquad (4)$$

$$|F_k(\underset{\sim}{q})| = \exp[-(1/2)\Delta a_k{}^2 q^2] \qquad (5)$$

The g factor, a parameter which represents the degree of disorder, is given by Eq.(6),

$$g_k = \Delta a_k / a_k \qquad (6)$$

Cooper et al. calculated this three-dimensional Hosemann's paracrystal theory by Eq.(7)[37],

$$I(q) = N\overline{|f|^2}(2/\pi)\int_0^{\pi/2}\int_0^{\pi/2} Z(q,\theta,\psi)\sin\theta d\theta d\psi \qquad (7)$$

Using this method, the scattering intensity from a paracrystal was calculated and compared with the experimental curve.

Figure 8 gives the theoretical scattering curves at various g values from a paracrystal containing spheres (radius R). It is clearly seen that the peak becomes lower and broader with increasing g value, i.e., with increasing degree of disorder. Higher order (five) peaks are clearly seen in curve 1 (g=0.055), but in curve 4 (g=0.22), the higher order peaks disappear; only a single, broad peak is seen.

Figure 9 shows a comparison of theoretical and experimental curves. The experimental curve is that of lysozyme ([lysozyme]=0.08g/ml). In this theoretical calculation, it was

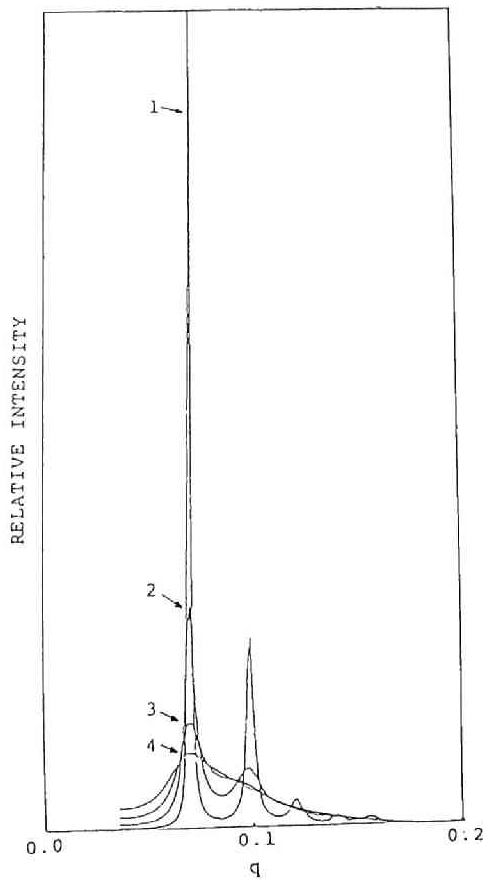

Fig.8 Scattering curves calculated by Hosemann's theory. Sphere model: Radius(R)=23A. Lattice spacing(a)=90A, g=0.056 (curve 1), 0.11(2), 0.17 (3), 0.22 (4).

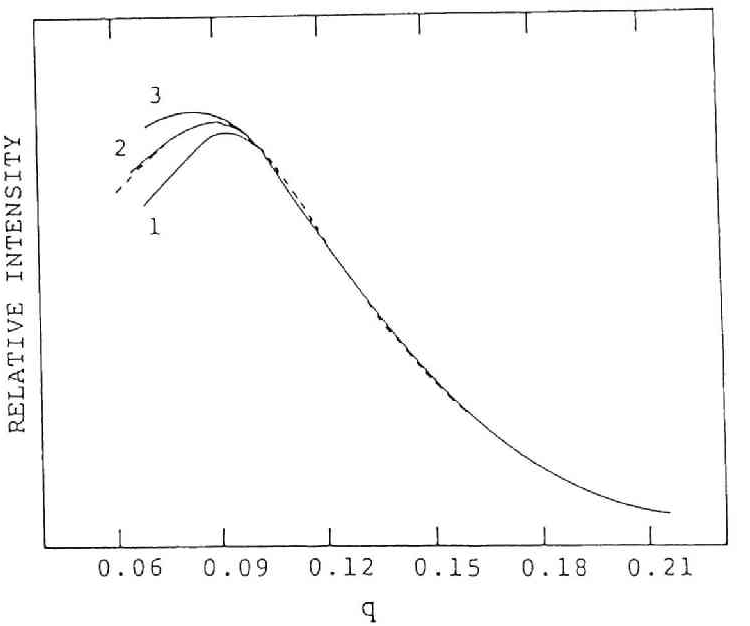

Fig.9 Comparison of the experimental scattering cu with theoretical ones. Broken line: experimental cur [lysozyme]= 0.08g/ml, solid line: calculated Hosemann's theory. Shoter radius(r_1)=15A, Lon radius(r_2)= 22.5A, Lattice spacing(a)=60A, g=0. (curve 1), 0.38 (2), 0.42 (3).

assumed that the lysozyme molecule could be approximated by an ellipsoid (shorter axis 30A, longer axis 45A)[38], and that the molecules form a simple cubic lattice with a lattice spacing of 60A. The fitting is fairly well when the g-factor is assumed to be 0.37, except for the lower angle region. Even when we consider only a distortion of the second kind, the fact, that only a single, broad peak is observed, is well explained if we admit that the ordered structure has a large paracrystallinity. We must bear in mind that the theory is based on the important assumption that three lattice vectors can change independently.

Next, let us consider thermal agitation which plays an important role and cannot be neglected, because the thermal vibration of particles in an ordered structure is expected to be larger than that in a solid crystal. When the vibration of a particle is isotropic and is a harmonic oscillation whose mean square of standard deviation is $\overline{u^2}$, the Debye-Waller factor is expressed as Eq.(8)[34],

$$|D|^2=\exp(-\overline{u^2}q^2) \qquad (8)$$

Figure 10 shows an example of theoretical scattering curves with various G values ($G=\sqrt{\overline{u^2}}/a$) and with a fixed g value (g=0.1). As the value of G becomes larger, the peak becomes lower and the higher order peaks disappear (curve 3). As is easily understood from Eq.(8), the effect of Debye-Waller factor is substantial for the higher q value, i.e. for higher order peaks. Even for solid crystals, the ratio of standard deviation, u, to lattice spacing, a, is about 0.06[34]. This value is too large to ignore. Needless to say, it cannot and should not be ignored for the ordered

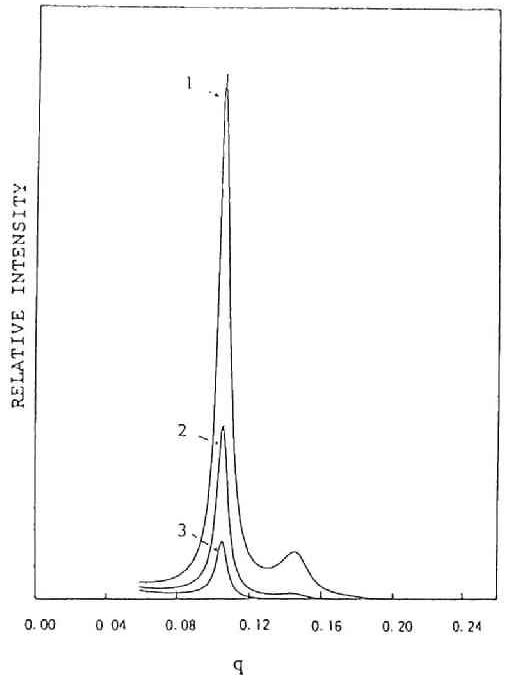

Fig.10 Calculated scattering curves at three different Debye-Waller factors. Sphere model: Radius(R)=20A. Lattice spacing(a)=60A, g=0.1, G=0.12 (curve 1), 0.20 (2), 0.26(3).

structure in solution under discussion. For example, the G value for polymer latex particle systems directly determined by the microscopic method was found to be about 0.1[35]. The scattering curves from such systems must be substantially influenced by this factor.

The effect of the size and shape of ordered region(s) would not be negligible, either. The diffraction peak becomes lower and broader as the crystal becomes smaller. This effect has been explained by using Laue's lattice factor[34]. Since it is believed strongly that there exists a "two-state structure" also in macroionic solution, as was clearly confirmed for polymer latex

solutions[12,13,35], this crystalline size effect may play an important role in the scattering behavior. As this factor also affects the broadness of the diffraction peak, if we can analyze the peak shape taking into account this crystalline size and shape effect, the g values, i.e., the degree of para-crystallinity, would have lower values than that we obtained above considering only the paracrystallinity (for lysozyme, g=0.38).

Reflecting the substantial contribution of these factors, the scattering structure factor experimentally found for polymer latex solutions had only one or two peaks.[16] It is furthermore quite reasonable that only a single, broad peak was observed in X-ray curves of solutions of various macroions, because the macroions are much lighter and smaller than the latex particles so that the former undergo much more violent motion than the latter. It is a grave mistake to imagine rigid and perfect lattice-like structures (such as found in solid crystal) for the ordered structure of macroions or latex particles in dilute solution. This problem will be fully discussed in chapter 7.

IV-7 Comments on the correlation hole theory

It has been claimed that a single, broad scattering peak observed is not due to the ordered arrangement of solute particles but due to a correlation hole[39] produced by the repulsive interaction between ionic solutes. Benmouma et al.[40] discussed the scattering behavior from solutions of charged spherical and rod-like macromolecules by considering only a Coulombic repulsive interaction. However, if only a repulsive

interaction exists and if an attractive component does not exist, two diffculties arises. One is that their theory fails to take into account the charge number dependence of experimentally obtained interparticle distance ($2D_{exp}$). As described in the previous section, the $2D_{exp}$ value for BSA decreased with increasing charge number. It must increase if the interaction is repulsive and if the correlation hole theory is correct. In addition, also in the case of the molecular weight dependence (hence charge number dependence) of PSS[7], the same argument can be made; the decreasing tendency (see Expt.16 and 18 or Expt.2 and 8 in Table I of Ref.7) of the $2D_{exp}$ for PSS with increasing molecular weight (and hence increasing number of charges) at a fixed number concentration is in a diametrical contradiction with the theory of Benmouma et al[40]. Secondly, we note that condensed systems in general cannot be maintained if the interaction between elements is repulsive. Furthermore, their theories are limited in very diluted and fairly low charge number systems. At relatively high concentrations or at a high charge number (larger than 8), the theoretical scattering intensity has negative values at the low angle region. This is physically impossible. The charge number limit, Z=8, is too small. The fact is that we observed SAXS peak for BSA whose charge number is 80. For synthetic polyelectrolytes, the analytical and even net charge is usually much higher than 8.[41] Under these circumstances, the correlation hole theory is not acceptable.

IV-8 Comparison of experimentally obtained intermolecular distance ($2D_{exp}$) with theoretical ones.

In colloidal science, the Derjaguin-Landau-Verwey-Overbeek theory (DLVO theory)[42], which is based on a direct electrostatic repulsion and van der Walls attraction, has been widely accepted. As it has been repeatedly emphasized[2,5-7], the experimental data accumulated on macroions and polymer latex particles indicate strongly the preponderance of intermacroion attraction and are in a complete contradiction with the DLVO theory. Recently, Sogami developed a new theory taking into account the difference between Gibbs free energy and Helmholz free energy (in short, the term PdV), and showed that there certainly exists an electrostatic attractive interaction between similarly charged ionic solutes through the intermediary of counterions[43,44]. This theory was used here in order to calculate the intermolecular distance in a preliminary manner. For example, in the case of tRNA, at 0.04g/ml (0.0466 volume fraction), the $2D_{exp}$ value from the SAXS peak was 95A, while 90A was obtained from the interference function. From Sogami's theory, the potential minimum position, Rm, was 91A when the charge number of tRNA particle, Z, is assumed to be 60. This value, Z=60, is reasonable, since the number of the phosphoric group is 75, if we take into account the counterion condensation.

V. Concluding remarks

In the present chapter, a single, broad peak is observed in the X-ray scattering curve for some biologically important polymers. The peak is ascribed to the ordering phenomenon of these ionic solute particles in dilute solutions, as was the case

for the other synthetic macroions previously studied. The scattering curves are furthermore theoretically calculated. Satisfactory agreements are obtained between theory and experiments, if crystalline distortion is assumed to be fairly substantial. The correlation hole, which was claimed to be responsible for the observed peak, is demonstrated not to be valid for the ionic polymers which we have been studying. Taking into account the present discussion and the previous argument against the isotropic model[40] on the basis of the observed dependence of the scattering behavior on the molecular weight, the present interpretation in terms of the translational ordering of the macroions is further reinforced.

References and Notes

1 For a review of this topic, see N.Ise and T.Okubo, Acc. Chem. Res. 13, 303 (1980).

2 N.Ise, Angew. Chem., 25, 323 (1986).

3 N.Ise, T.Okubo, Y.Hiragi, T.Hashimoto, M.Fujimura, A.Nakajima and H.Hayashi, J. Am. Chem. Soc. 101, 5836 (1979).

4 J.Plestil, J.Mikes and K.Dusek, Acta Polym. 30, 29 (1979).

5 N.Ise, T.Okubo, K.Yamamoto, H.Kawai, T.Hashimoto, M.Fujimura, and Y.Hiragi, J. Am. Chem. Soc. 102, 7901 (1980).

6 N.Ise, T.Okubo, K.Yamamoto, H.Matsuoka, H.Kawai, T.Hashimoto and M.Fujimura, J. Chem. Phys. 78, 541 (1983).

7 Chapter 2 of this thesis; N.Ise T.Okubo, S.Kunugi, H.Matsuoka, K.Yamamoto and Y.Ishii, J. Chem. Phys., 81, 3294 (1984).

8 D.P.Riley and G.Oster, Disc. Faraday Soc. 11, 107 (1951).

9 J.D.Bernal and I.Fankuchen, J. Gen. Physiol. 25, 111 (1941).

10 J.B.Hayter and J.Penfold, Coll. Polym. Sci. 261, 1022 (1983).

11 Chapter 5 of this thesis; Y.Ishii, H.Matsuoka, and N.Ise, Ber. Bunsenges. Phys. Chem., 90, 50 (1986).

12 (a) N.Ise, T.Okubo, M.Sugimura, K.Ito and H.J.Nolte, J. Chem. Phys. 78, 536 (1983); (b) N.Ise, T.Okubo, S.Dosho, and I.Sogami, Langmuir, 1, 176 (1985).

13 A.Kose, M.Ozaki, K.Takano, Y.Kobayashi and S.Hachisu, J. Coll. Int. Sci. 44, 330 (1973).

14 P.A.Hiltner and I.M.Krieger, J.Phys. Chem. 73, 2386 (1969).

15 T.Kato, H.Masuda and A.Takahashi, Polymer Preprints, Japan, 31, 2249 (1982).

16 W.Hartl, H.Versmold, U.Wittig and V.Marohn, Mol. Phys. 50, 815 (1983).

17 M.Nakagaki and K.Ikeda, Bull. Chem. Soc. Jpn. 41, 555 (1968).

18 I.Piltz, O.Kratky, F.Cramer, F.Haar, and E.Schlimme, Eur. J. Biochem., 15, 401 (1970).

19 A.Patrowski, E.Gulari and B.Chu, J. Chem. Phys. 78, 4187 (1980).

20 T.Lindahl and J.R.Fresco, Methods in Enzymology, 12, 78 (1967).

21 The charge number of BSA particle was calculated from the amount of added HCl or NaOH solution and pH change of the solution. The value obtained was checked with literature[22].

22 C.Tanford and G.L.Roberts.Jr, J. Am. Chem. Soc. 74, 2509 (1952).

23 A.Guinier and G.Fournet, Small-Angle Scattering of X-rays, (Wiley, New York, 1955), Chap. 4.

24 D.Bendedouch, S.-H. Chen, and W.C.Koeler, J.Phys.Chem., 97, 2621 (1983).

25 D.Bendedouch and S.-H. Chen, J.Phys.Chem., 87, 1652 (1983).

26 D.Bendedouch and S.-H. Chen, J.Phys.Chem., 88, 648 (1984).

27 I.Langmuir, J. Chem. Phys. 6, 873 (1938).

28 N.Ise and T.Okubo, J. Phys. Chem. 70, 536, 2400 (1966); 71, 1287, 1886, 4588 (1967); 72, 1370 (1968).

29 K.S.Schmitz, M.Lu and J.Gauntt, J. Chem. Phys. 78, 5059 (1983).

30 N.Ise and T.Okubo, J. Phys. Chem. 70, 2407 (1966).

31 M.Sugimura, T.Okubo, N.Ise and S.Yokoyama, J. Am. Chem. Soc., 106, 5069 (1984).

32 For spherically symmetric, monodisperse particles, the scattering intensity I(q) is represented simply by the product of the intraparticle scattering factor P(q) and the interparticle interference function S(q),

$$I(q)=n\,P(q)\,S(q) \qquad (a)$$

where n is the number of particles. If we can obtain P(q) by a theortical calculation (from size and shape of a particle) and/or by an experiment under other conditions (very dilute solution or solution with added salt where an interference effect can be neglected), S(q) can be determined by a division of I(q) by P(q) according to Eq.(a). For tRNA, at 0.04g/ml, we calculated S(q) using P(q) obtained at 0.001g/ml (the normalization of P(q) was of course effected for 0.04g/ml). The $2D_{exp}$ value from I(q) is 95A, whereas $2D_{exp}$ from S(q) was 90A, slightly smaller than that from I(q). This effect is due to the monotonical decrease of P(q) with increasing q values. Strictly speaking, the tRNA molecule is not spherical, but the result, that $2D_{exp}$ from S(q) was smaller than that for I(q). must be correct in qualitative terms. There is always the possibility of a small over-estimation in the $2D_{exp}$ values when evaluated from the total scattering curve.

33 D.Bendedouch, S-H. Chen, W.C. Koeler and J.S.Lin, J. Chem. Phys. 76, 5022 (1982).

34 See for example, a) R.W.James, "The Optical Principles of the Diffraction of X-rays" (Bell,London,1948),chap V. b) B.E.Warren, "X-ray Diffraction" (Addison-Weseley, 1969), chap 11.

35 N.Ise, T.Okubo, K.Ito, S.Dosho and I.Sogami, J. Coll. Int. Sci., 103, 292 (1985).

36 R.Hosemann and S.N.Bagchi, "Direct Analysis of Diffraction by Matter" (North Holland, Amsterdam,1962).

37 D.J.Yarusso and S.L.Cooper, Macromolecules 16, 1871 (1983).

38 O.Kratky, "Progress in Biophysics and Molecular Biology", J.A.Butler, H.E.Huxley, R.E.Zirkle (eds.), vol.13, chap.3 (1963).

39 P.-G. de Gennes, "Scaling Concepts in Polymer Physics", Cornell University Press, New York, (1979).

40 M.Benmouna, G.Weil, H.Benoit and A.Z.Akcasu, J. Phys. (Paris), 43, 1679 (1982).

41 In reference 40, the Debye-Hukel length was erroneously defined. If this mistake is corrected the charge number limit, Z=8, becomes about 60. However, this value is still small with respect to the real charge number.

42 See for example, E.J.W.Verwey and J.Th.G.Overveek, "Theory of the Stability of Lyophobic Colloids" (Elsevier,Amsterdam, 1948).

43 I.Sogami, Physics Lett. 96A, 199 (1983).

44 I.Sogami and N.Ise, J. Chem. Phys., 81, 6320 (1984).

Chapter 4

"Ordered" Structure of Polyallylamine Hydrochloride in Dilute Solutions

I. Introduction

The previous study on macroionic solutions showed that there exists a distorted ordering of macroions in dilute solutions.[1,2] Polymer latex particles, which are large enough to be seen by the ultramicroscope directly, were found to form an ordered arrangement and the colloidal crystal was concluded to have b.c.c. and f.c.c structures at low and high concentrations, respectively, by Kossel line analysis.[3] In the case of macroions, the situation was not so straightforward as was the case for the polymer latex systems, since small angle X-ray (SAXS) or neutron (SANS) scattering analysis had to be employed to obtain information on the distribution of "invisible" macroions. According to the previous investigation, a single broad peak was observed in the scattering curve when the polymer concentration and degree of polymerization were reasonably high, when the concentration of added salt was low, and when the macromolecular species were electrically charged. Although various counter-interpretations were proposed, the single broad peak was accounted for by us in terms of fairly largely distorted ordered arrangement of the macroions in solutions. This interpretation was reinforced by

successful comparison of the observed scattering curves with theoretical ones calculated with the Hosemann theory of paracrystalline distortion.[4,5] The reliabilty of the argument was further confirmed by comparison with light and neutron scattering data on polymer latex dispersions.[6] Thus, our current interpretation is that not only the polymer latex particles but also the macroions (including detergent ionic micelles, synthetic macroions, proteins, enzymes and polynucleotide) commonly form distorted ordered distribution of the macroions in dilute solutions. The recent EXAFS data indicated that there existed an ordered array of simple ions such as $ZnBr_2$ even at 0.1 M[7]. Thus the ordering appears to be a universal phenomenon in ionic solutions, whatever dimensions and geometry the solute particles have. In this chapter, SAXS study on aqueous solutions of polyallylamine hydrochloride is described, which has been recently synthesized by a free radical polymerization[8]. This cationic polymer has a very simple chemical structure, which was expected to make the situation simpler:

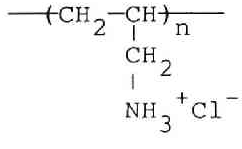

II. Experimental

II-1 Materials

Polyallylamine hydrochloride(PAA-HCl) was a fractionated product of the Nitto Spining Company, Tokyo, Japan. The received samples were purified by ultrafiltration as follows: 1 - 2 g of the fractionated sample were dissolved into 200 ml of purified water and the resultant solutions were placed into an ultradialy-

ser(200ml., Amicon Co., Lexington, Mass.) with a filter membrane (PM30 of Amicon Comp. for the fractions F1 to F6, PM10 for F7, and YM5 for F8). The solutions were condensed to about 60 ml by applying a nitrogen pressure of 2.0 kg/cm^2, and diluted with water. The condensation-dilution process was repeated three to four times. The extent of the purification was checked by the disappearance of UV absorbance at 230 nm from the filtrate. The filtrate condensed to 30 to 50 ml were passed through a glass filter (G3) and freeze dried for 24 hrs.

The molecular weight of the sample was determined by osmotic pressure and light scattering measurements. The membrane osmometer was a product of Wescan Co., model 231. The semipermeable membranes used were AS61 (acetyl cellulose, pore size $<0.005\ \mu m$) of Schleicher & Schuell Co. The measurements were done at $31^{\circ}C$ with an aqueous solution of 0.2 M or 0.5 M NaCl as solvent. A typical example of the osmotic measurements are shown in Fig.1. The plot showed a downward curvature. The molecular weight and the second virial coefficient were estimated from the intercept and linear slope at the low concentrations. The results are tabulated in Table 1. The light scattering measurements were done with KMX-6 of Chromatix, Mountain View, Cal., and the refractive index was determined by the differential refractometer RM102 of the Union Giken Manufacturing Company, Hirakata, Osaka, Japan. An NaCl solution of 0.04 M or 0.1 M was used as solvent, and the purification of the material was done by filtration with a filter of Millipore Millex -GS 0.22 μm. An example for F7 is shown in Fig.2. The weight-avarage molecular weight was estimated to be

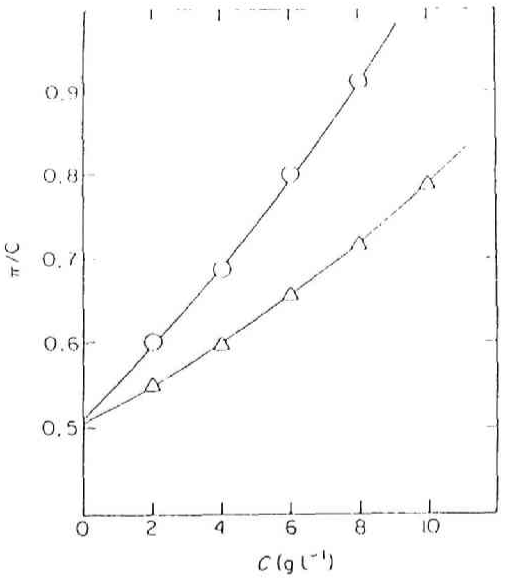

Fig.1 The osmotic pressure vs concentration plot for polyallylamine hydrochloride (F7) in NaCl solution at 31°C. [NaCl], O 0.2M, Δ ,0.5M.

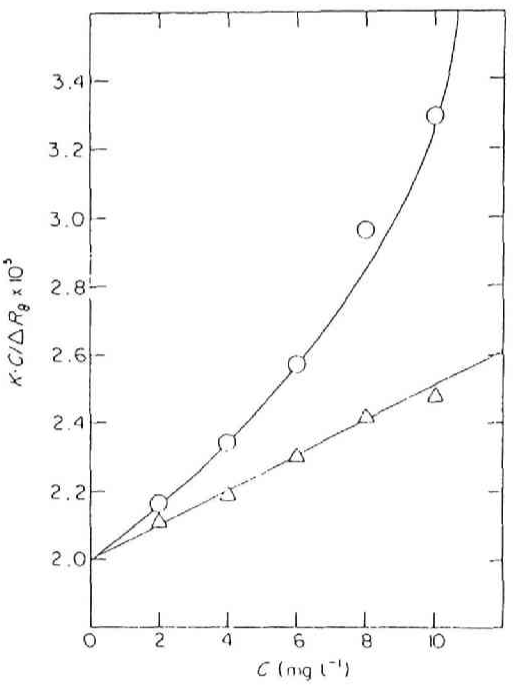

Fig.2 The light scattering data for polyallylamine hydrochloride (F7) in NaCl solutions at 25°C. [NaCl], O , 0.04M; Δ , 0.1M.

50,500 from the initial slope, which was fairly close to the value obtained from the osmometry(51,000). This fact indicates that the fractionated sample was fairly monodisperse, although a GPC study could not be carried out because of strong interaction of the polymer with the column beads.

Table I. The Molecular Weight of Polyallylamine Hydrochlorides and the Second Virial Coefficient of their NaCl Solutions

Fraction	M_n x10^{-3}	A_2x10^6 (l mol/g^2)	Solvent
F1	170	1.88	0.2M NaCl
F3	108	1.64	"
F4	92.7	1.28	"
F6	70.4	1.05	"
F7	50.5	1.39	"
"	51.0	0.81	0.5M NaCl

The *conductometric titration was conducted as follows*: A 1/10 N HCl solution (1 ml) was added to 0.047 g of F7, and the solution was titrated with an 1/10 N NaOH. The result is shown in Fig.3 together with the potentiometric titration curve. From this figure, it is clear that 0.047 g of F7 corresponds to 4.5 x 10^{-5} monomer mol. Furthermore the same amount of the polymer was titrated with a 1/100 N $AgNO_3$, which showed that 4.4 X 10^{-5} mol of chloride ions were contained. From these titration data, the degree of substitution by the chloride ions (or the degree of neutraliztion by HCl) of the polymer was found to be 0.98

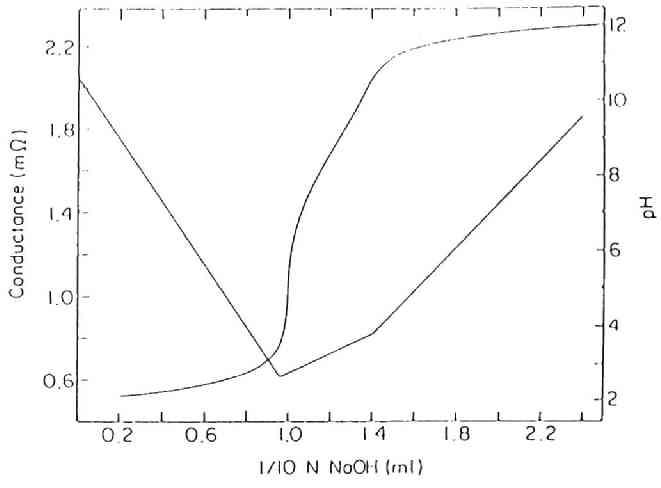

Fig.3 Conductometric and potentiometric titration curves of polyallylamine hydrochloride (F7).

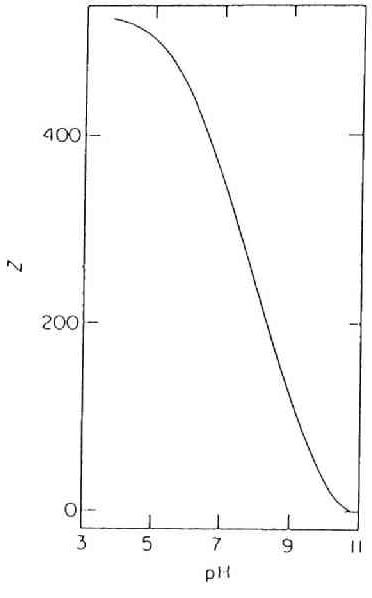

Fig.4 The apparent number of charges of polyallylamine hydrochloride (F7) as a function of pH.

(=4.4/4.5).

The polymers were found to be highly hygroscopic, as expected. Thus, the water content in the solid material was estimated from the elemental analysis with the assumption of the complete neutralization. It amounted to 9 % for F1, 6 % for F2, F3, F4, and F5,and 7% for F6, F7, and F8.

The potentiometric titration was carried out by using Radiometer pH meter under the same condition as for the conductometric titration. After the correction of the blanck experiment with water, the apparent number of the electric charges as a function of pH was determined for F7 and is given in Fig.4.

The water used was purified by Milli-Q system (type I, Millipore Ltd., Bedford, Mass.).

II-2 Small-angle X-ray scattering (SAXS) measurement

The SAXS apparatus used and data analysis were described in chapter 2[9]. Instead of glass capillary used in the previous study, a quartz capillary was employed as the sample cell. Because of the weakness of the scattered X-ray from this polymer, the intensity measurement was extended to 10,000 sec. The temperature of the SAXS measurement was 25^{o}C unless otherwise specified.

III. Results and Discussion

III-1 Polymer concentration dependence

The scattering curves at three different polymer concentrations of F7 are shown in Fig.5. As already found for other ionic polymers[9-12], a single, broad peak was observed and

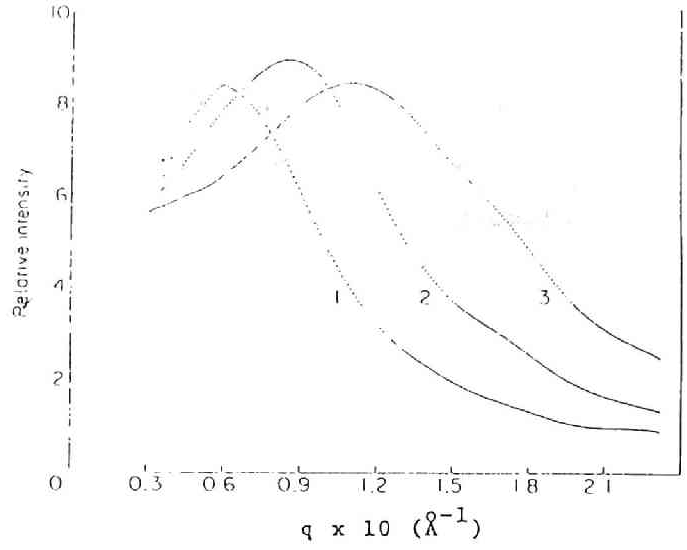

Fig.5 The concentration dependence of the small-angle X-ray scattering curves for solutions of polyallylamine hydrochloride (F7). The abscisa is the scattering vector q ($=4\pi \sin\theta / \lambda$). Polymer concentration: curve 1, 0.02; curve 2, 0.04; curve 3, 0.08 g/ml.

Table II The observed intermacroion spacing ($2D_{exp}$) and the average spacing ($2D_0$) of PAA-HCl(F7)

conc. (g/ml)	$2D_{exp}$ (A)	$2D_0$ (A)
0.02	106	161
0.04	73	128
0.08	57	101
0.12	45	88

the peak position shifted toward higher angles with increasing polymer concentration. Although detailed discussion has been given[1,2], it is strongly believed that this scattering peak is reminiscent of the existence of an intermolecular ordering of macroions in solutions. Accepting this interpretation, an approximate intermacroion distance ($2D_{exp}$) can be evaluated by assuming the Bragg equation, $n\lambda = 2(2D_{exp})\sin\theta$, where 2θ is the scattering angle, λ is the wavelength of X-ray, and n is the order of the peak. The values of $2D_{exp}$ thus obtained is tabulated in Table 2. Also in this table are given the values of $2D_0$, an average intermacroion distance calculated from the polymer concentration with the assumption of uniform distribution of macroions throughout the solution. It is seen that $2D_{exp}$ decreases with increasing polymer concentration, and that $2D_{exp}$ is smaller than $2D_0$ beyond the experimental error, namely $\pm$ 5%[10]. This implies that the two-state structure is maintained in the solution, namely there exist ordered regions of macroions and simultaneously disordered regions, as earlier suggested by Ise et al.[10,13] Although the presence of such a non-space filling ordered region might seem to be rather surprising, this kind of the situation could be confirmed by the naked eye for dilute solutions of electrically charged polymer latex particles, which are large enough so that the particle distribution in suspension can be studied by ultramicroscope.[14,15] Naturally, such a non-space-filling ordering is possible only when the net interaction between the similarly charged nacroions is attraction. As earlier pointed out by Ise et al.,[16] and as recently

theoretically elucidated by Sogami,[17] the electrostatic attractive interaction between the macroions is generated through the intermediary of oppositely charged counterions present in the space between the macroions.

III-2 Salt concentration dependence

Figure 6 demonstrates the dependence of the scattering curves of a PAA-HCl sample (F7) on the concentration of added salt. At no salt condition, a single peak was observed but addition of simple salt caused a shift of the peak toward lower angle. At the same time, the peak became more vague. In the presence of 0.4 M NaCl, the peak disappeared. These tendencies were earlier observed for other ionic polymers.[9-12] The observed salt concentration dependence implies that the forces, which are responsible for the ordering formation of the macroions, are of the electrostatic origin.

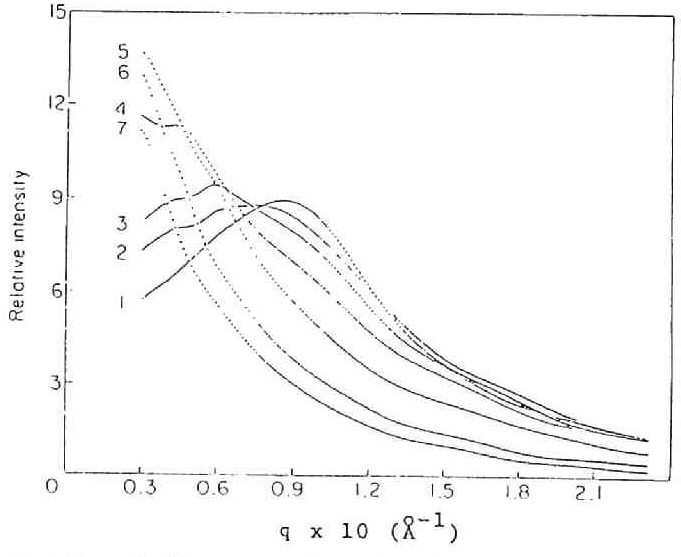

Fig.6 The influence of NaCl added on the scattering curves of polyallylamine hydrochloride (F7). [PAA-HCl]: 0.04 g/ml, [NaCl]: curve 1, 0; curve 2, 0.04; curve 3, 0.08; curve 4, 0.2; curve 5, 0.4; curve 6, 0.8; curve 7, 1.0M.

It is noteworthy that the height of the base line (or the scattering curve at high scattering vector) decreases with increasing salt concentration. This is a quite novel aspect with PAA-HCl.:the base line for other ionic polymers converged to the same curve at high angles. It was thought that the lowering of the base line was due to the absorption by the salt added but it turned out after the absorption correction that this was not the case. The reason for this base line shift is not clear.

III-3 Dependence on the degree of neutralization

The unneutralized sample was prepared by passing PAA-HCl F7 through a strongly basic ion-exchange resin (Amberlite IRA-402). The solution of the unneutralized material was purified by ultrafiltration and used for the SAXS experiment without freeze-drying. The concentration of the polymer was determined by the conductometric titration and by dry weight. The SAXS study was carried out after adjusting pH of the solution by adding a 1 N HCl solution. The results are shown in Fig.7. It is inferred from Fig.4 that the degrees of neutralization were about 0.1, 0.2 and 0.7 at pH 9.8, 9.0 and 7.1, respectively. Obviously, the peak position shifted toward higher angles and the peak became higher. This indicates that the intermacroionic distance becomes shorter with increasing degree of neutralization as a result of intensification of the electrostatic attractive interaction. This trend was also noted for other weak polyelectrolytes, indicating the incorrectness of the widely accepted view that the ordering is due to repulsive interaction, as was discussed by Ise.[2]

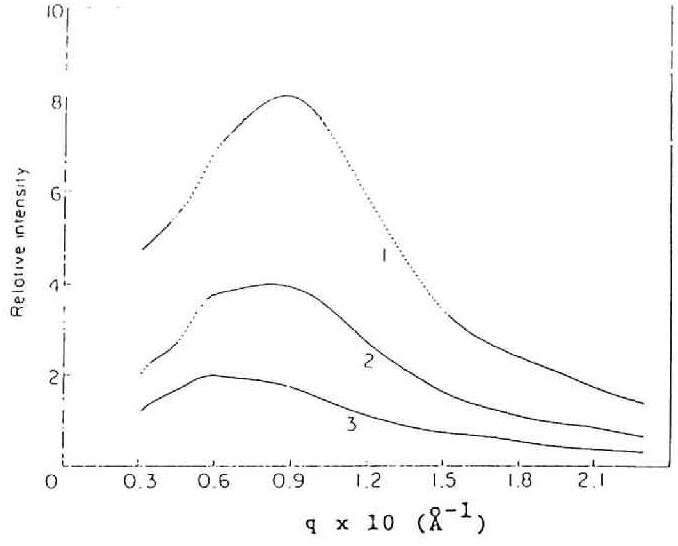

Fig.7 The influence of pH on the scattering curves of polyallylamine hydrochloride (F7) pH: curve 1, 7.1; curve 2, 9.0; curve 3, 9.8.

III-4 Temperature dependence

Figure 8 shows the scattering curves at three different temperatures. With increasing temperature, the peak was lowered, which can be accounted for in terms of the enhanced thermal motion of the macroions and hence of the enhanced thermal distortion of the ordering. The same tendency was also observed for some other polyelectrolytes.[9,12] We note that the peak position of PAA-HCl did not change with temperature whereas that of the other polyelectrolytes was slightly shifted toward higher angle with increasing temperature. It is true that the decrease of the dielectric constant of water with rising temperature is important, and cannot be ignored, but the difference in the position shifts of various polymers seems to be not large enough

to warrant quantitative discussion.

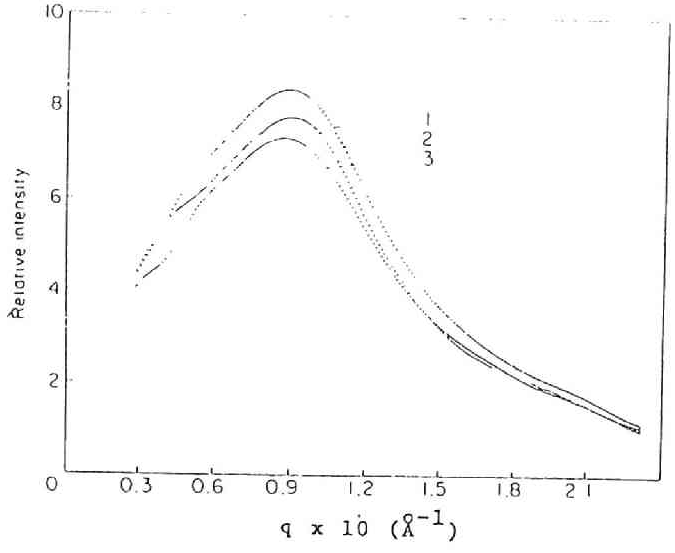

Fig.8 The scattering curves of polyallylamine hydrochloride (F7) at various temperatures. [PAA-HCl]: 0.04 g/ml; temperature: curve 1, 15; curve 2, 26; curve 3, 40°C.

III-5 Dependence on the molecular weight

The scattering experiments were carried out for all fractions of PAA-HCl. At a constant weight concentration, no molecular weight dependence was observed for the peak position. This is in contrast with the previously reported results for polystyrenesulphonates[9] and polyacrylates[10] but would be reasonable because the molecular weight range covered in the present experiment is much more limited than those in the previous ones.

III-6 Mixing experiments

In Fig.9 the scattering curves for F1 (M_n=170000) and for F7

(M_n=51000) are shown, which were obtained at a number concentration (of polymer) of 2.0 x 10^{-7} mol/ml. Obviously, the two fractions have different peak heights and positions. Then the equal volumes of the two fractions were mixed to give 1.0 x10^{-7} mol/ml for each component. The resultant solution having the total polymer concentration of 2.0 x10^{-7} mol/ml was studied and the scattering curve is shown in Fig.9 (curve 3). The curve 4 is the composite curve constructed from curves 1 and 2. The observed curve for the binary mixture is different from curve 4 and has a new peak in between the original peaks of curves 1 and 2. This fact strongly suggests that the scattering peak reflects an intermacroion ordering, but not intramacroion ordering. If the latter were responsible for the peak, the observed curve might be expected to coincide with the curve 4. The new peak reflects a new ordered arrangement containing two kinds of macroions of different sizes.

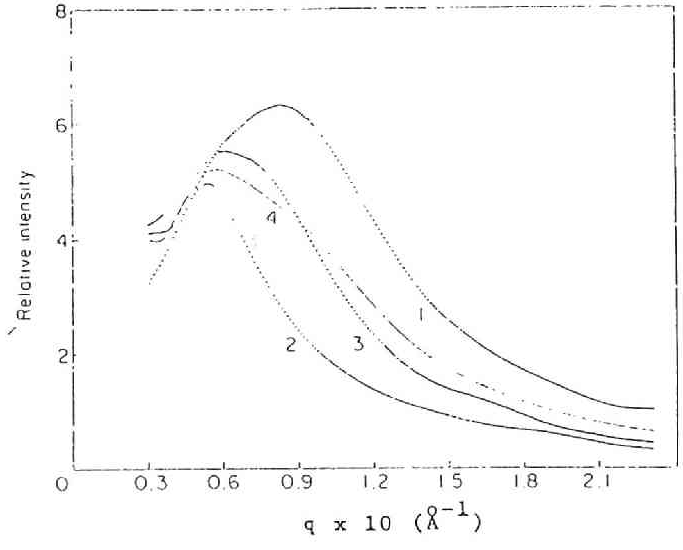

Fig.9 The influence of mixing of two samples of different molecular weights on the scattering curves of polyallylamine hydrochloride. Curve 1: F1 (M_n=170000), 2.0x10^{-7} mol/ml; curve 2: F7 (M_n=51000), 2.0x10^{-7} mol/ml; curve 3: F1+F7, [F1]=[F7]=1.0x10^{-7} mol/ml, curve 4: (curve 1 + curve 2)/2.

III-7 Variation of the scattering peak with time

The scattering experiments were repeated three times for an 0.04 g/ml solution of F7. The first measurement was done immediately after the solution preparation, the second one on the fifth day, and the third one on the 21st day. The solution was kept in the capillary in the meantime. The absolute intensity of the X-ray was determined by using Lupolen as standard before and after the scattering measurements, and the scattered intensity of the solution was corrected for the time change of the absolute intensity thus determined. The scattering intensity shown in Fig.10 is the "raw" data, which were not corrected for the sensitivity of the position-sensitive-proportional-counter, and for the slit width and height, nor corrected for solvent scattering. The three intensity curves almost completely overlap. This implies that the ordered structure is stable over such a prolonged period.

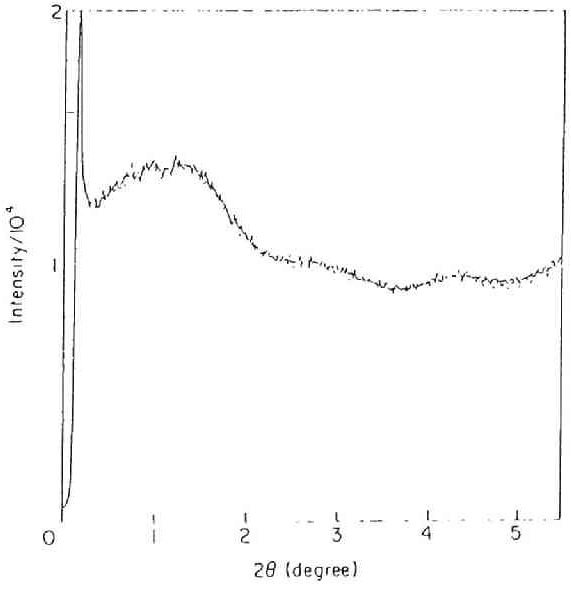

Fig.10 Three 'raw' scattering curves of polyallylamine hydrochloride (F7) observed immediately after the solution preparation, on the fifth day and on the 21st day.

IV. General Remark

Finally a few words appear to be necessary on the general character of the ordered structure of macroions. First, when we calculate the intermacroion spacing ($2D_{exp}$), any geometrical shape has not been assumed for the macroions. Thus $2D_{exp}$ simply refers to the distance between the centres of the gravity of the macroions. It is our position at the moment that even the vinylic macroions donot have a rod-like conformation in the cconcentration range covered in the scattering experiments, as discussed in the previous paper.[9] More exactly, we should state that the conformation is not yet known. For this reason, $2D_{exp}$ should not or cannot be given a very precise physical meaning. We have avoided to regard relatively small change of this quantity or small difference therefrom as physically significant. Secondly, for the same reason, we have not computed the radial distribution function, which is the standard and essential quantity in the discussion of the particle distribution. This kind of analysis would be meaningful when the conformation or the shape of the solute ions is well-established. As a matter of fact, a quantitative discussion on ordering phenomena of spherical micelles and likewise spherical polymer latex particles in solutions has been given in terms of the particle interference function (and hence the radial distribution funcion).[4,6]

Nevertheless, it is strongly believed that what is described in the present chapter is essentially and qualitatively correct. We note that the positive statement originates from the

qualitative coincidence of the X-ray observation on the macroions with the naked-eye observation on the polymer latex particles.[1,2] Third, the readers might be left with the impression that the ordered structure is static as far as the scattering method is concerned. This would not be correct;instead the ordered structure is belived to be quite dynamic and fluctuating. Here again, the positive interpretation is based on the naked-eye observation on dilute polymer latex solutions, in which localized, non-space-filling, ordered regions are seen to be formed in one place and disintegrate after some time.[18] Nonetheless the latex solutions give a "stable" scattering peak even in dilute solutions.[19] It is hoped that such a complicated but interesting phenomena of macroion solutions can be clarified before long.

V. Conclusion

The X-ray scattering experiments were performed for fractionated polyallylamine hydrochlorides with water as solvent. A sigle broad peak was observed, suggesting that the macroions are distributed in a fairly regular manner in solutions. The intermaroion distance (Bragg spacing) was found to be much smaller than the average spacing, which can be calculated from the concentration by assuming the uniform distribution. This indicates the presence of the two-state structure, in which non-space-filling ordered structure coexists with disordered structure. The scattering peak disappeared in the presence of a large amount of salt. With increasing temperature, the peak height was lowered while the peak position was practically

unaffcted. At a given number concentration of polymer, the peak position and height were molecular weight-dependent. When two samples of different molecular weights were mixed, a new scattering curve was observed with a peak at scattering vector different from the original positions. This mixing experiment strongly suggests that the scattering peak is reminiscent of an intermacroion ordering. The scattering curve was stable in a long period (upto 21 days).

Reference

1 N.Ise, Makromol. Chem. Suppl., 12, 215 (1985).

2 N.Ise, Angew. Chem., 25, 323 (1986).

3 T.Yoshiyama, I.Sogami, and N.Ise, Phys. Rev. Lett. ,513, 2153 (1984).

4 Chapter 5 of this thesis; Y.Ishii, H.Matsuoka, and N.Ise, Ber.Bunsenges.Phys.Chem., 90, 50 (1986).

5 R.Hosemann, and S.N.Bagchi, Direct Analysis of Diffraction by Matter, North-Holland, Amsterdam, 1962.

6 Chapter 7 of this thesis; H.Matsuoka, H.Tanaka, T.Hashimoto and N.Ise, Phys. Rev. B, in press.

7 P.Lagarde, A.Fontaine, D.Raoux, A.Sadoc, and P.Migliardo, Chem. Phys. 72, 3061 (1980); A.Sadoc, A.Fontaine, P.Lagardo, and D.Raoux, J.Amer. Chem. Soc., 103, 6287 (1981).

8 S.Harada, and S.Hasegawa, Makromol. Chem., Rapid Commun., 5, 27 (1984).

9 Chapter 2 of this thesis; N.Ise, T.Okubo, S.Kunugi, H.Matsuoka, K.Yamamoto, and Y.Ishii, J. Chem. Phys., 81, 3294 (1984).

10 N.Ise, T.Okubo, K.Yamamoto, H.Kawai, T.Hashimoto, M.Fujimura, and Y.Hiragi, J. Amer. Chem. Soc., 102, 7901 (1980).

11 N.Ise, T.Okubo, K.Yamamoto, H.Matsuoka, H.Kawai, T.Hashimoto, and M.Fujimura, J.Chem. Phys., 78, 541 (1983).

12 Chapter 3 of this thesis; H.Matsuoka, N.Ise, T.Okubo, S.Kunugi, H.Tomiyama, and Y.Yoshikawa, J. Chem. Phys., 83,

378 (1985).

13 N.Ise, and T.Okubo, Acc. Chem. Res., 13, 303 (1980).

14 N.Ise, T.Okubo, M.Sugimura, K.Ito, and H.J.Nolte, J. Chem. Phys., 1983, 78, 5536 (1983).

15 N.Ise, T.Okubo, K.Ito, S.Dosho, and I.Sogami, Langmuir, 1, 176 (1985).

16 N.Ise, and T.Okubo, J.Phys.Chem., 70, 1930 (1966).

17 I.Sogami, and N.Ise, J. Chem. Phys., 81, 6320 (1984).

18 K.Ito, and N.Ise, publication in preparation.

19 H.Hartl, and H.Versmold, Ber. Bunsenges. Phys. Chem., 88, 1063 (1984).

Chapter 5

"Ordered" Distribution of Ionic Micelles in Dilute Solutions of Alkyltrimethylammonium Chloride

I. Introduction[1]

In previous publications, aqueous solutions of macroions such as polyacrylate[2], poly-L-lysine[3] and polystyrenesulfonate[4] and polyallylamine hydrochloride[5] were studied by the small-angle X-ray scattering (SAXS) technique. The scattering curves of the macroion solutions showed a single, broad peak under suitable conditions. From this peak position, we estimated the approximate intermacroion distance ($2D_{exp}$) by assuming the Bragg equation. The $2D_{exp}$ value was revealed to be considerably smaller than the average intermacroion distance ($2D_0$), which was calculated by assuming a uniform distribution of the solutes throughout the solution.

This fact indicates the presence of non-space-filling ordering, in other words, a two-state structure in which some of the macroions are localized in ordered regions of a high density with an intermacroionic distance of $2D_{exp}$ whereas the rest are in disordered regions of a low density. Accordingly, it has been suggested that the macroion ordering is due to an intermacroion attraction through the intermediary of its counterions[1-4].

Recently, this intermacroion attraction was supported by a theoretical consideration[6,7].

The information obtained by the SAXS measurements on "invisible" macroions has been confirmed by independent microscopic observation on suspensions of polymer latex particles, which are large enough to be seen by the naked eye with an ultramicroscope[8-11]. The situation in this case is straightforward. The ordering of the particles in suspension is seen directly and the interparticle distance ($2D_{exp}$) can be determined from the pictures without assuming the Bragg equation. The inequality relation, $2D_{exp} < 2D_0$, and hence the coexistence of the ordered and disordered regions are almost unequivocally substantiated.

It is well known that surfactant molecules form micelles when the concentration is above the critical micelle concentration. When they are electrically charged, the micelles are expected to behave like macroions or latex particles, since the micelle charges are likewise localized in a small space in the solution. Thus it was thought quite interesting to carry out the SAXS measurements on micellar solutions and to compare the results with those obtained for macroions and latex particles. We should note that monodisperse and spherically symmetric micelles provide an advantage in the analysis of scattering data. For such systems, the SAXS intensity I(q) is proportional to the particle scattering function $[F(q)]^2$ and the interference function S(q)[12,13] where $q = 4\pi \sin\theta/\lambda$ is the scattering vector for radiation of wavelength λ scattered at an angle 2θ. In the cases of spherical ionic micelles, it is easier to estimate S(q) from

I(q) than in the case of linear polyelectrolytes, whose conformations are still ambiguous. A more exact intermicellar distance can then be evaluated from the S(q) curve[13] for the micelle cases than from the peak position of the I(q) peak. In this chapter, the solution structure of micellar solutions will be discussed on the basis of S(q) thus obtained.

II. Experimental

II-1 Materials

Dodecyltrimethylammonium chloride(DTAC) and tetradecyltrimethylammonium chloride (TTAC) were purchased from Tokyo Kasei Kogyo Co., Ltd., Tokyo and hexadecyltrimethylammonium chloride(HTAC) was obtained from Nakarai Chemical Co., Inc., Kyoto. The reagents were extracted with n-hexane for 24 hrs. on a Soxhlet extractor, and recrystallized three times from acetone.

The samples were analyzed for the distribution of hydrocarbon chain length by using the reaction gas chromatography method[14]. The chain length purities were 95.9-98.7 % (0.4 % C-10, 97.3% C-12 and 2.3 % C-14 for DTAC, 0.4% C-12, 95.9% C-14 and 3.7% C-16 for TTAC and 0.3% C-14, 98.7% C-16 and 1.1% C-18 for HTAC).

The critical micelle concentrations(cmc) for the samples were determined by surface tension, which was measured by the Wilhelmy method using a Shimadzu Surface Tensionmeter, ST-1, at 25^{o}C. The cmc values were 1.3×10^{-3} M for DTAC, 5.4×10^{-3} M for TTAC and 1.6×10^{-3} M for HTAC.

The water used was obtained by a Milli-Q System (Type I, Millipore Ltd., Bedford, Mass.).

II-2 SAXS measurement and data analysis

The SAXS apparatus and data analysis employed in this chapter were described in chapter 2.

The scattering data were corrected for contributions of absorption, sensitivity of the position-sensitive-proportional-counter(PSPC) and solvent (solution at the cmc). The corrected data were then smoothed and desmeared by Lake's method[15].

III. Results

The scattering curves of DTAC, TTAC and HTAC at various concentrations were characterized by a distinct, broad peak, as was the case with polyelectrolytes[1-4]. Experimental data for DTAC are shown in Fig.1.

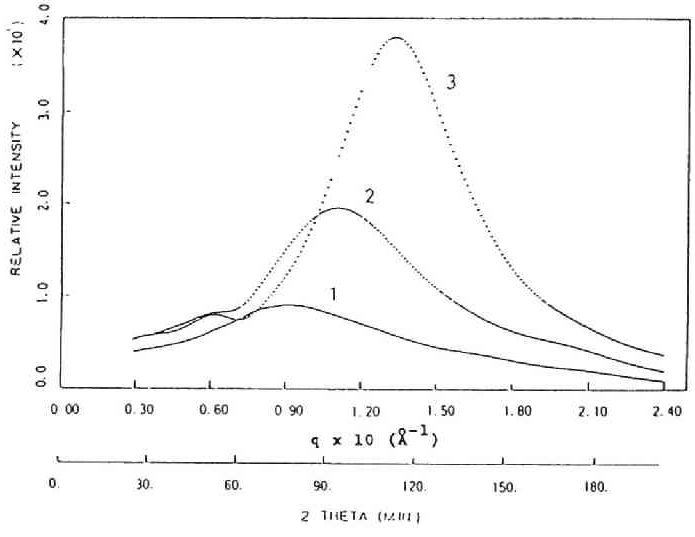

Fig.1 Scattering curves of DTAC in water at 28°C. [DTAC] ;1: 0.05 g / ml, 2: 0.10 g / ml, 3: 0.20 g / ml.

In order to evaluate the intermicelle distances, the interference function S(q) was evaluated from the scattering curves

as follows: When micelles in solution are spherically symmetric and monodisperse, the relative scattering intensity I(q) is given by

$$I(q) = k\, N\, [F(q)]^2\, S(q) \qquad (1)$$

where N is the number of micelles in the irradiated volume and k is a proportional constant which depends on experimental conditions[12]. It is assumed that the micelles are spherically symmetric and monodisperse at a low surfactant concentration ($N = N_o$) and that the relation

$$k\, N_o [F(q)]^2 = A \exp(-Bq^2) \qquad (2)$$

holds. At high q values, S(q) is nearly unity and I(q) is approximated by

$$I(q) = A \exp(-Bq^2) \qquad (3)$$

The constants A and B were determined in such a way to fit to the experimental curve.

At higher surfactant concentrations it was assumed that $[F(q)]^2$ did not change as long as the micelle size was constant. If the micelle sizes at surfactant concentrations c and c_o are the same, $kN[F(q)]^2$ is given by

$$kN[F(q)]^2 = (N/N_0)\ A \exp(-Bq^2)$$

$$= [(c-cmc)/(c_o-cmc)]A \exp(-Bq^2) \quad (4)$$

where N and N_o correspond to c and c_o, respectively.

The I(q) value in the high q-range is given by

$$I(q) = [(c-cmc)/(c_o-cmc)]A \exp(-Bq^2) \quad (5)$$

The interference function S(q) was obtained by

$$S(q) = I(q)/kN[F(q)]^2 \quad (6)$$

The number density of micelle n was estimated as follows.

It was assumed that the hydrocarbon core of the micelle is spherical and that the number of carbon atoms per alkyl chain imbedded in the core is $n_c - 1$, where n_c is the total number of carbon atoms per chain. Then the core radius l_{max} (in A)and the core volume per chain v (in A^3) are given by[16]

$$l_{max} = 1.5 + 1.265(n_c-1) \quad (7)$$

and

$$v = 27.4 + 26.9(n_c-1) \quad (8)$$

The micelle aggregation number m is obtained by

$$m = (4\pi/3)l_{max}^3/v \quad (9)$$

The calculated micelle aggregation number of DTAC, TTAC and HTAC

were 48, 64 and 84, respectively.

By using these aggregation numbers, the number density of the micelles was calculated.

The radial distribution function g(r) was obtained by[13]

$$g(r) = 1 + 1/(2\pi^2 nr)\int_0^\infty [S(q) - 1]q \sin qr \, dq \quad (10)$$

It should be remembered that this equation is strictly for spherically symmetric systems and is assumed to be valid for the solutions under consideration.

I(q), $kN_o[F(q)]^2$ and S(q) for a 0.05 g/ml DTAC solution are shown in Fig.2. In this case $kN_o[F(q)]^2$ is 11.5 exp (-40.7 q^2). The value of S(q) for the more concentrated DTAC solution was estimated by using Eqs. (4) and (6).

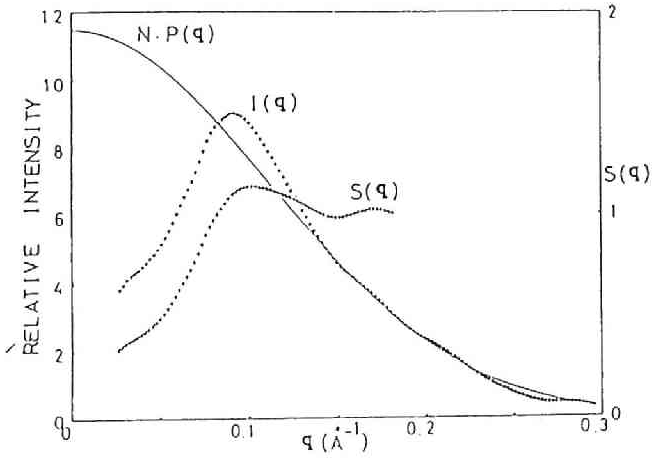

Fig.2 I(q), $kN_o[F(q)]^2$ and S(q) for 0.05 g / ml DTAC in water.

Figure 3 shows the S(q) values for 0.05, 0.10, and 0.20 g/ml DTAC. Then the corresponding g(r) values were calculated by using Eq.(10). Since we could experimentally obtain S(q) curves in the limited q-range ($q_{min} < q < q_{max}$), the integration was carried out by assuming that $S(q) = S(q_{min})$ for $q < q_{min}$ and $S(q) = 1$ for $q > q_{max}$. The function g(r) for DTAC is shown in Fig.4.

The functions S(q) and g(r) for TTAC and HTAC were obtained by the same procedure as DTAC and are shown in Figs.5 to 8.

The value of $kN_o [F(q)]^2$ for these surfactants was obtained by fitting $Aexp(-Bq^2)$ to the scattering curve for a 0.02 g/ml solution. The S(q) for 0.20 g/ml TTAC, 0.10 g/ml HTAC and 0.20 g/ml HTAC could not be evaluated, since Eq.(5) was found not to hold.

IV. Discussion

IV-1 Particle scattering function

Reiss-Husson and Luzzati have interpreted SAXS curves of various micelles by using a two-shell model of micelles[17]. In their model a micelle was divided into two regions, a region with a hydrocarbon core and a region of polar groups and hydrated counterions, and within each of the regions the electron density was assumed to be constant. The particle scattering function depended on the size and the shape of the micelle and the electron densities of the shells and the solvent[12].

Reiss-Husson and Luzzati concluded that HTAC micelle had a spherical shape and that the outer shell of HTAC micelle had the same electron density as the solvent had[17].

Recently, Hayter and Penfold analysed small-angle neutron

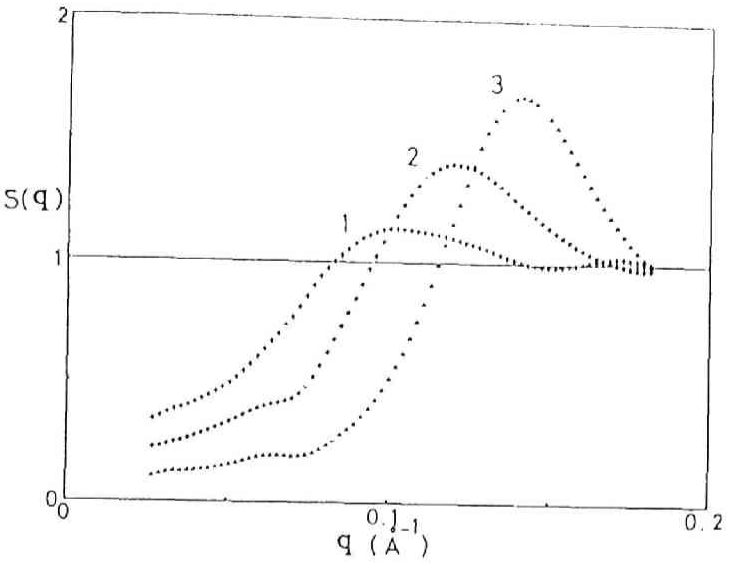

Fig.3 S(q) for DTAC in water. [DTAC] ; 1 : 0.05 g / ml, 2 : 0.10 g / ml, 3 : 0.20 g / ml.

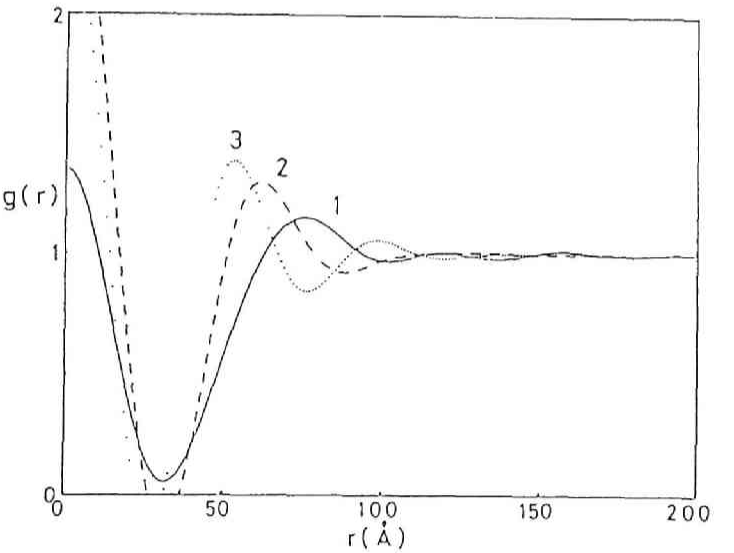

Fig.4 Radial distribution function for DTAC in water obtained from S(q). Surfactant conc.; 1:0.05 g/ml, 2:0.10, 3:0.20 g/ml.

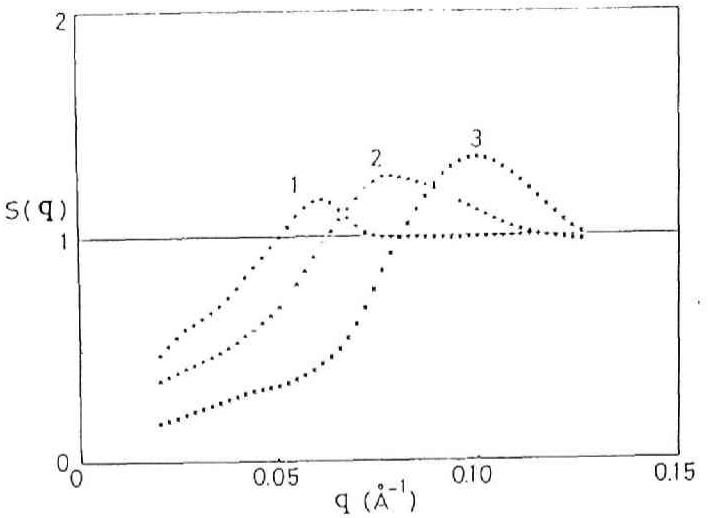

Fig.5 S(q) for TTAC in water. Surfactant conc.;1:0.02 g/ml, 2:0.05 g/ml, 3:0.10 g/ml.

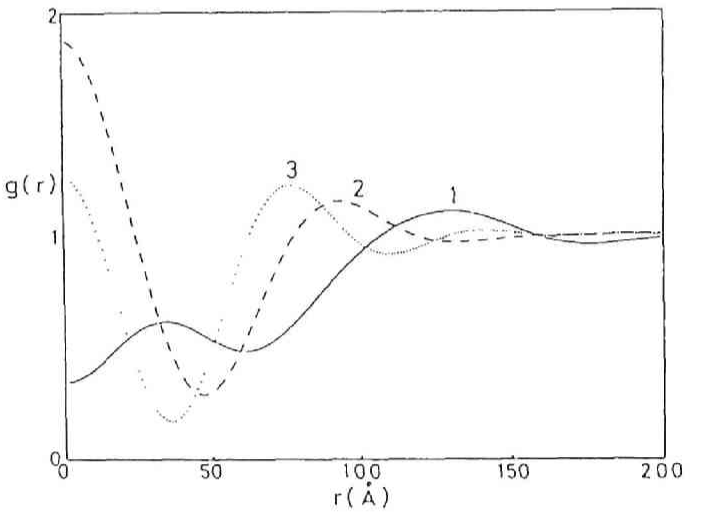

Fig.6 g(r) for TTAC in water from S(q) given in Fig.5. Surfactant conc.;1:0.02 g/ml, 2:0.05 g/ml, 3:0.10 g/ml.

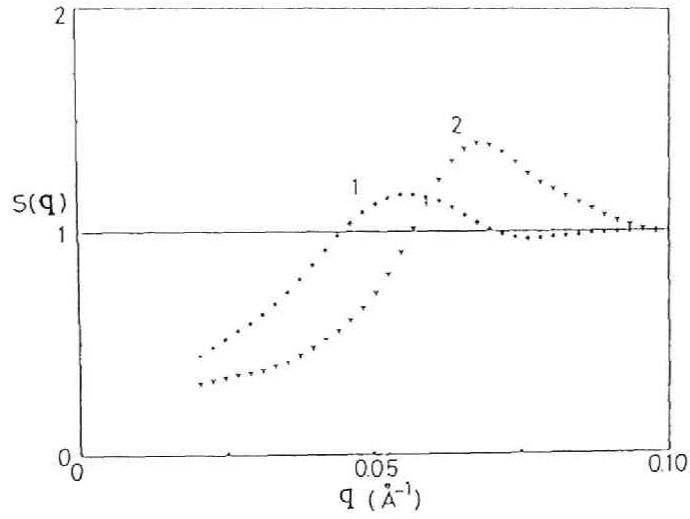

Fig.7 S(q) for HTAC in water. Surfactant conc.; 1:0.02 g/ml, 2:0.05 g/ml.

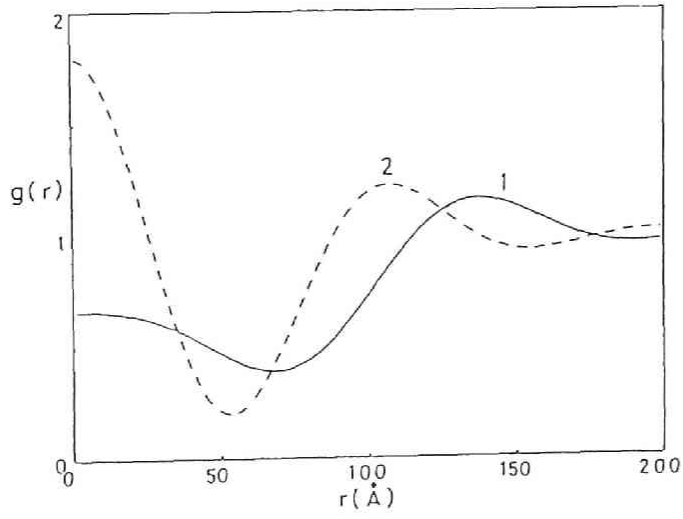

Fig.8 g(r) for HTAC in water from S(q) given in Fig.7. Surfactant conc.; 1:0.02 g/ml, 2:0.05 g/ml.

scattering (SANS) curves of HTAC by using a similar two-shell model[18]. In the SANS experiment the scattering function depended on the scattering length densities of the shells and the solvent instead of the electron densities. The electron densities and the particle scattering function of SAXS for HTAC micelle, which were calculated by using their model and parameters, were quite different from the results obtained by Reiss-Husson and Luzzati. This implies that it is very difficult to obtain a unique model of a micelle structure from small-angle scattering results.

The Guinier plot[19] of our own data for 0.02 g/ml HTAC gave a straight line from q = 0.07 to 0.15 A^{-1}. The slope of the straight line provided an apparent radius of gyration R_g = 15.2A, which is somewhat smaller than R_g = 16.8 A calculated from the core radius 21.7 A determined by Reiss-Husson and Luzzati.

Our apparent radius of gyration R_g can be explained by using a two-shell model, in which the electronic density of the outer shell is higher than that of the solvent. However, our data are not abundant enough to determine many parameters such as the core radius, the thickness of the outer shell and electron densities of the core and the outer shell.

Since the SAXS curves for the alkyltrimethylammonium chlorides become monotonic with dilution, it was concluded that Eq.(2) is correct. The apparent micelle radius R which is obtained by

$$R = (5/3)^{1/2} R_g = (5B)^{1/2} \qquad (11)$$

is supposed to be smaller than the real micelle radius, because the scattering from the core and the outer shell contribute oppositely to B[12]. In fact, the R values of DTAC, TTAC and HTAC were found to be 14.3, 16.7 and 19.6 A, respectively, whereas the corresponding core radii l_{max} calculated by Eq.(7) are 15.4, 17.9 and 20.5 A.

IV-2 Micelle aggregation number

It is difficult to obtain the micelle aggregation number under our experimental condition. However, Reiss-Husson and Luzzati showed that HTAC micelle had a spherical shape and a size from C_e = 0.05 to 0.40, where C_e is the electronic concentration (the number of electrons of micellized surfactant per electron of the solution[17]).

Since a micelle has the tendency to remain spherical with decreasing n_c[20], TTAC and DTAC are likewise thought to form spherical micelles. Thus the micelle aggregation number was evaluated by using Tanford's Eqs. (7)-(9) on the assumption that the number of carbon atoms per alkyl chain imbedded in the core is n_c-1.

Missel et al. showed that the mean aggregation numbers of alkylsulfates measured in pure water at cmc were in good agreement with Tanford's prediction[20]. The micelle aggregation number of DTAC at cmc has been measured by using the light scattering technique. The measured values were 37.5 in pure water, 41.71 in 0.04M NaCl[21] and 57 in 0.05M NaCl[22], and close to Tanford's value, 48. Recently, Ozeki and Ikeda have reported that only spherical micelles were formed by DTAC even in 4M NaCl[23]. It

was also assumed that the growth and the deformation of the micelles at higher surfactant concentration were negligible as long as Eq. (5) held in the high q-range.

IV-3 Intermicellar interaction

From the peak position of g(r) the distance between nearest neighboring micelles was estimated. The peak position r_m and the value of g(r) at $r = r_m$ together with the calculated average intermicelle distance $2D_0$ ($=n^{-1/3}$) for TTAC and HTAC are summarized in Table I. (See Table 2 for the corresponding data for DTAC.)

The $g(r_m)$ value became larger with increasing surfactant concentration. The large $g(r_m)$ indicates an enhanced ordering of the micelles. However, the micelle solutions seem to be rather isotropic than two-state structured as found for highly charged synthetic macroions[1-4] and latex particles[9,10], since the differences between r_m and $2D_0$ are relatively small.

A remark can be made on the difference between r_m and the Bragg spacing ($2D_{exp}$) obtained from I(q) by assuming the Bragg equation. For DTAC, the $2D_{exp}$ values at 0.05, 0.10 and 0.20 g/ml were found to be 69, 57 and 47 A, whereas the r_m values were 75, 62, and 53 A, respectively. Certainly these two spacings do not agree but the discrepancy is not large. Thus the arguments in previous papers[1-4] on the SAXS data of macroionic solutions, which were based exclusively on I(q) and the Bragg spacing, appear to be justified, although the Bragg spacing is an "approximate measure" of the distance of repeating regularity.

According to our interpretation such ordered structures are

Table I. SAXS data of tetra- and hexa-decyltrimethylammonium chlorides in water.

surfactants	conc. (g/ml)	r_m[a] (A)	$g(r_m)$[b]	$2D_0$[c] (A)
TTAC	0.02	130	1.11	119
	0.05	93	1.15	86
	0.10	76	1.23	66
HTAC	0.02	138	1.16	132
	0.05	107	1.22	97

[a] The peak position of the radial distribution function g(r) which corresponds to the distance between nearest neighboring micelles.

[b] g(r) at the peak position.

[c] The average intermicelle distance calculated for a simple cubic distribution.

formed owing to the intermacroion attractive force through the intermediary of the counterions. The number of charges on the micelle in this study are only 24 to 42, if we assume that half of the ionic groups are dissociated. Our interpretation is that the intermicellar attractive force is then not so strong as to cause a two-state structure because the number of charges on the micelle i.e. the number of intermediating counterions per micelle are not sufficiently large.

In this respect, it is to be noted that this unexpected trend was earlier suggested on the basis of the catastrophic decrease of the single-ion activities of the macroions and of the latex particles[24,25] with increasing concentration and was furthermore recently substantiated by Sogami's theory[6,7]. When the macroions or latex particles can exist without their counterions, only repulsive interaction must be present between the macroionic species. However, such a situation is not physically possible; the macroions and the equivalent amount of counterions must be in the solutions. Then, we have attraction between the macroionic species and counterions, in addition to the repulsion between the macroions and that between the counterions. Since the attraction makes the interionic spacing between the cation and anion shorter than that between the cations (or between the anions) and since the electrostatic interaction is inversely proportional to the interionic distance, the net interaction in the total system must be attraction. In other words, we have naturally repulsion between "bare" macroions or between "bare" counterions, but when the macroions

and counterions are mixed as is actually the case in the real solutions, the macroions attract each other through the intermediary of the counterions. The strength of the intermacroion attraction depends on the number of the counterions, which is in turn determined by the valency of macroions. When the macroion valency becomes larger, the number of free counterions increases, resulting in intensification of the attraction between the macroions[26]. Conversely, when the number of charges of the latex particles is lowered, the attraction is weaker. Then the particles may be in a position as distant as possible from each other, the largest possible separation being equal to $2D_0$. In other words, we may not have the two-state structure; instead, a space-filling, one-state structure is to be maintained. For this reason, the difference between r_m (or $2D_{exp}$) and $2D_0$ is small for the ionic micelles. Although a similar situation was encountered for t-RNA[27,28], which is a polyelectrolyte of relatively low charge density, the agreement between the observed and theoretical spacings does not justify the idea that the solution properties can be satisfactorily described by taking into account exclusively repulsive interaction between the macroionic species, which is claimed by so many authors (See Ref.27 -33 in Ref.7). It is believed that assuming only repulsions between macroions is a basic mistake, even though good agreement with experimental data is obtained, because condensed systems cannot exist without attraction[10].

One of the counterexamples often cited in refutation to our interpretation is the van der Waals condensation. It is to be

noted that, in addition to a repulsive (hard sphere) interaction, an attractive component (a/v^2) is explicitly involved in the equation of the state, $(p + a/v^2)(v - b) = kT$. The contribution of the attractive interaction is reminded to be aasociated with the pressure p in this equation and therefore does not play an important role at high pressures, or high concentrations, where the repulsive contribution becomes substantial. Thus ignoring the attraction is permissible and would probably provide quantitatively satisfactory agreement with experimental data, when the pressure or concentration is high. However this success should not be overemphasized. At low pressure regions, or at low concentrations, the a/v^2 term can no longer be overlooked. This consideration shows that conclusions derived from analysis of concentrated systems cannot generally be applied to dilute systems. Colloidal solutions are not exceptional. It is remembered that concentrated colloidal suspensions were extensively studied and their various properties were claimed to be explainable in terms of repulsive interaction only. It seems that this conclusion is not valid in dilute suspensions.

It is noteworthy that small-angle neutron scattering (SANS) experiments on micellar solutions[12,18,29-35] showed similar peak as the present X-ray analysis. The SANS peak have been analysed by many authors in terms of a mean spherical approximation[36] or a rescaled mean spherical approximation[37] by assuming an electrostatic repulsion based on a simplified DLVO potential and a hard sphere interaction[38]. The reason why an apparently good agreement with experimental data was obtained is inferred

to be that the ionic solutes under consideration, namely the ionic micelles, were not highly charged so that the attraction happened to be weak as was pointed out above[40].

IV-4 Distortion of ordered structure -- Comparison of observed and theoretical interference functions

In all of the SAXS and SANS experiments recently carried out on synthetic polyelectrolytes, proteins, polynucleotide and micelles, a single broad peak was observed. Even in the case of ionic micelles, in which the interference function can be separated from the particle scattering function in a less ambiguous, though not conclusive, way than linear macroions, the interference function showed a single broad peak, as is clear from Figs.3, 5, and 7. Even for solutions of polymer latex particles, the observed interference function showed only one or two peaks[41]. Because of the lack of higher peaks and of the broadness of the peak, a large number of authors claimed that there exists no ordered structure or only a liquid-like structure. In this section, it will be shown theoretically that the single broad peak experimentally observed can be obtained by the diffraction from a distorted ordered structure, the lattice structure will be discussed.

In chapter 3, the observed scattering curves were compared with the theoretical ones calculated by Hosemann's three dimensional paracrystalline theory[42]. In the present section, the experimental interference function, S(q), will be compared with Hosemann's paracrystalline lattice factor, Z(q), which will be

calculated for simple cubic lattice (s.c.), face-centered cubic lattic (f.c.c.) and body-centered cubic lattice (b.c.c.) with fairly large distortion. The method of the calculation used was that described by Cooper et al.[43] for simple cubic lattices. The assumptions in this calculation were, (1) the arrangements of the particles was isotropically distorted, (2) the lattice was infinitely large, (3) the thermal vibration was negligible and (4) each lattice vector could change independently. The present computation program could reproduce the theoretical curve reported in Cooper's original paper. Then the program was modified in order to calculate a lattice factor for f.c.c. and b.c.c. by axis transformation of unit vector for f.c.c. and b.c.c. to that of s.c. The detail of the theory will be described in chapter 7.[44]

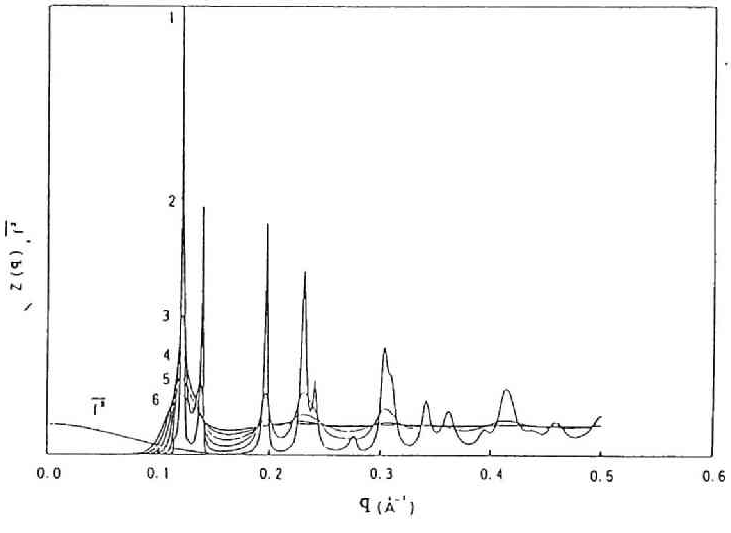

Fig.9 Paracrystalline lattice factors of an f.c.c. structure calculated by Hosemann's theory. $\overline{f^2}$:particle scattering function(sphere with radius =23A). a = 63.6 A

Curves	1	2	3	4	5	6
g	0.031	0.062	0.094	0.124	0.157	0.189

Figure 9 shows the results of a model calculation of Z(q) for f.c.c. at various degrees of distortion. It is clearly seen that the diffraction peak becomes lower and broader with increasing g-value (a parameter representing the degree of disorder, which is defined by $g = \Delta a/a$ where a is a length of unit vector and Δa is the standard deviation of the lattice points from the ideal lattice points), in other words, with increasing degree of disorder. Higher order peaks are observed in the curve 1 (g=0.031) but only a single, broad peak is seen for the curve 6 (g=0.189). It is evident that the broad peak is composed of the first and second order peaks.

According to Fig.9, even when we observe only a single, broad peak, we cannot and should not claim that there exists no ordered structure but only a liquid-like structure. From the height and broadness of the peak and from the lack of higher order peaks, it would be certain that the ordered structure is by no means perfect but it is still undeniable that there exists a highly distorted long-range order. This conclusion is also consistent with the fact that an ordered arrangement was observed for polymer latex particle solutions with the ultramicroscope by the naked eye[8-11] and nevertheless not so many diffraction peaks were observed.

Figure 10 shows a comparison of the experimental interference function, S(q), and calculated curves by the paracrystal theory for s.c., f.c.c., and b.c.c. in the case of a DTAC 0.20 g/ml solution. In all cases, the peak position and the peak height were fitted with the experimental ones. The peak width for

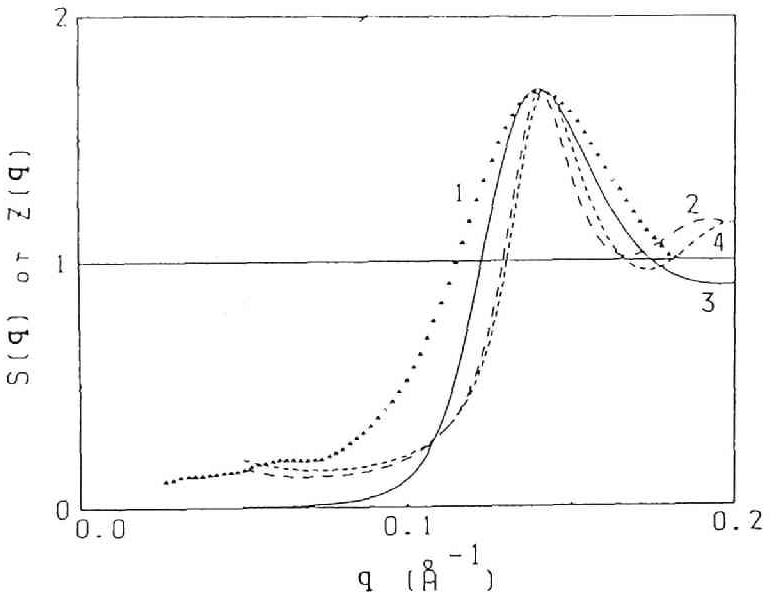

Fig.10 Comparison of the experimental interference function, S(q), with theoretical lattice factors for DTAC at 0.02 g/ml.

1: experimental. 2:lattice factor calcd. for an s.c. structure with a=45.0A, g=0.164. 3: lattice factor calcd. for an f.c.c. structure with a=53.4 A, g=0.214. 4: lattice factor calcd. for a b.c.c. structure with a=55.9A, g=0.125.

f.c.c. was the largest in these three lattices although the calculated peak was slightly narrower than the experimental ones, while the peak shape was similar to the one experimentally found. In the cases of s.c. and b.c.c. structures, there appeared a second order peak but in the case of f.c.c., we could not find higher order peaks in the q region under consideration. For these reasons it was thought that the f.c.c. structure was plausible for the micelle solution. In this respect, it would be of interest to point out that Sogami's theory predicts a higher

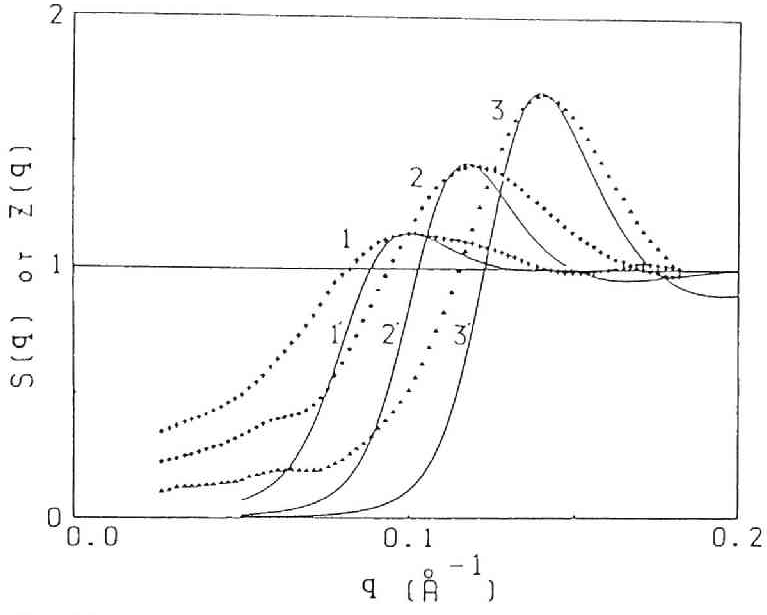

Fig.11 Comparison of the experimental interference functions with theoretical lattice factors of an f.c.c. structure for DTAC at three concentrations.

Experimental 1: [DTAC] =0.05g/ml
2: [DTAC] =0.10g/ml
3: [DTAC] =0.20g/ml

Theoretical 1': a=70.0 A, g=0.320
2': a=62.6 A, g=0.249
3': a=53.4 A, g=0.214

stability of an f.c.c. structure at higher concentrations[7] and furthermore a Kossel line analysis of polymer latex solutions demonstrated the preponderance of an f.c.c. structure at high concentrations and that of a b.c.c. structure at low concentrations[45]. Figure 11 shows comparison of S(q) and Z(q) for f.c.c. structures for DTAC at three different concentrations. Roughly speaking, the fittings were not unsatisfactory, except the narrowness of the Z(q) peak. It is believed that the

discrepancy is due to the assumption of infinitely large crystalline size. The smaller the crystal, the broader and the lower the diffraction peak. It has to be pointed out that the "real" g-values would be smaller than obtained in the present section if the crystalline size effect is duly taken into consideration. Recently it was pointed out that the g-factor was not fully independent of crystal size[46]. Further calculation with crystal size effect will be described in chapter 7.

Pertinent lattice parameters for DTAC are listed in Table II. Good agreement can be claimed among $2D_{exp}$ from the S(q) peak for an f.c.c. structure, r_m from the radial distribution function g(r) , and r_{fit} (the closest interparticle distance used for the fitting of Z(q) to S(q)). At the lowest concentration (0.05 g/ml) the r_{fit} value was slightly smaller than $2D_{exp}$ from S(q) for the f.c.c. structure, which indicates that for a very broad peak, the evaluation of the interparticle distance from the peak position using the Bragg equation becomes less accurate[19]. However, the difference amounts to only 7 % in this case, On the other hand, the $2D_{exp}$ value from I(q) was larger than the $2D_{exp}$ value from S(q) and the r_{fit} value. The $2D_{exp}$ values obtained from I(q) in previous papers[2-4] appear to render slightly overestimated interparticle spacing, paticularly at low polymer concentrations or high salt conditions. It should be mentioned that this remark does not affect our conclusion. On the contrary, the inequality relation $2D_{exp} < 2D_0$ and the conclusion therefrom, namely the two-state structure, are reinforced.

Table II Lattice parameters for DTAC solution

Conc.	$2D_{exp}$ from I(q) (Å)			$2D_{exp}$ from S(q) (Å)			r_m (Å)	r_{fit} (Å)			$2D_0$ (Å)		
(g/ml)	sc	fcc	bcc	sc	fcc	bcc		sc	fcc	bcc	sc	fcc	bcc
0.05	69	85	85	63	77	77	75	--	71	--	77	86	84
0.10	57	70	70	53	65	65	62	--	63	--	60	67	65
0.20	47	58	58	45	55	55	53	45	53	56	47	53	51

$2D_{exp}$: Interparticle distance evaluated from peak position in experimental scattering curve assuming Bragg equation.

r_m : Interparticle distance evaluated from peak position in radial distribution function.

r_{fit} : Interparticle distance used for the fitting of Z(q) to S(q).

$2D_0$: The average interparticle distance calculated by assuming a uniform distribution.

The r_m and r_{fit} values are slightly smaller or nearly equal to $2D_0$ values for the f.c.c. With increasing concentration, the r_m and r_{fit} values were close to $2D_0$ values. This tendency was observed for synthetic polyelectrolytes and latex particles.

It seems to us quite interesting to compare here the results obtained for ionic micellar solutions with those obtained for latex suspensions. For fairly concentrated latex suspensions, Cebula et al. compared the peak position of S(q) found by SANS measurements with the first Bragg peak of an f.c.c. lattice (diffraction from the (111) plane)[47]. They noticed a good agreement for suspension containing ion-exchange resins. At high salt

concentrations disagreement was observed and the transition point, at which the disagreement started to emerge, shifted to higher salt concentrations with increasing latex concentration. Cebula et al. classified the solution structure as "ordered-liquid lattice" when the agreement is satisfactory. They used the words "disordered liquid-like array" when this is not the case. Because the first Bragg peak position of an f.c.c. lattice is generally close to that of a b.c.c structure (diffraction from the (110) plane), as they pointed out, it would not be easy to identify conclusively the lattice structure on the basis of the first peak position only. However we note that their suggestion on the lattice structure, namely an f.c.c. structure, is in agreement with the present conclusion derived for ionic micelles by comparison of the experimental S(q) with the theoretical Z(q)'s calculated for various lattice types that an f.c.c. structure is more favorable than a b.c.c. structure. It might be possible that the latex particles and spherical micelles form a similar type of array in solutions. It is also to be noted that Sogami's theory predicts that an f.c.c. structure is favored over a b.c.c. at high concentrations[7].

The next remark would be useful in demonstrating the validity of the present method of analysis based on the para-crystalline theory. The method was applied to the light scattering data reported on polymer latex suspension by Versmold et al.[48] Their experimental S(q) values were satisfactorily reproduced by our calculation, when reasonable values of g (g=0.14-0.15) were assumed. Although the full account will be described in chapter 7[44], two points can be made here. First, as

described already, relatively distorted ordered arrangements of latex particles can be confirmed by the naked eye, although the latex concentrations were higher than those used in the light scattering experiments. The micrographic study revealed that the paracrystalline distortion and the vibrational motion of the latex particles were found to be so substantial but the displacements of the lattice points within considerable length of time (say, 30 sec) were practically zero. Based on this direct observation, it would not be unreasonable to anticipate more highly distorted ordered distribution of the latex particles in the more dilute suspensions studied by the light scattering experiments, and hence the agreement with the paracrystalline theory would not be surprising. Secondly it is to be recalled that the experimental S(q) values were claimed to be reproduced by the so-called RMSA method[48], which is an approach based on a liquid theory. The fact that the observed S(q) could be satisfactorily described both by the paracrystalline theory and the liquid theory might indicate the "intermediate" nature of the ordered structure of latex particles in suspensions, although reservation must be made with the use of purely repulsive interparticle interaction.

V. Conclusion

In the present chapter, the small-angle X-ray scattering experiment gave a single, broad peak for some ionic micelles, as was observed for other ionic polymeric materials. By taking advantage of the spherical shape of the micelles,

the observed intensity was divided into the interference function and particle factor. The radial distribution function was calculated by Fourier transform. In all cases, at most two peaks were observed. The distribution function was calculated and compared with the experimental values. The observed fact was accounted for by taking into consideration the fairly large distortion of the ordered structure of micelles in solutions. A face-centered cubic lattice structure with a fairly large distortion gave the best fit with the experiments. The present work indicates that, even when only a single broad peak is observed, it does not imply the absence of ordered structure.

References

1 For a convenient review of the topic see for example, N.Ise and T. Okubo, Acc. Chem. Res. 13, 303(1980), and N. Ise, Angew. Chem. 25, 323 (1986).

2 N.Ise, T. Okubo, K. Yamamoto, H. Kawai, T.Hashimoto, M. Fujimura and Y. Hiragi, J. Am. Chem. Soc.102,7901 (1980).

3 N. Ise, T. Okubo, K. Yamamoto, H. Matsuoka, H. Kawai, T. Hashimoto and M. Fujimura, J. Chem. Phys. 78, 541(1983).

4 Chapter 2 of this thesis; N. Ise, T. Okubo, S. Kunugi, H. Matsuoka, K. Yamamoto and Y. Ishii, J. Chem. Phys. 81, 3294 (1984).

5 Chapter 4 of this thesis; Y.Yoshikawa, H.Matsuoka and N.Ise, British Polym, J., 18, 242 (1986).

6 I. Sogami, Phys. Letter, A96, 199 (1983).

7 I. Sogami and N. Ise, J. Chem. Phys. 81,6320 (1984).

8 A. Kose, M. Ozaki, K. Takano, Y. Kobayashi and S. Hachisu, J. Coll. Interface Sci. 44, 330 (1973).

9 N. Ise, T. Okubo, M.Sugimura, K. Ito and H.J. Nolte, J. Chem. Phys. 78, 536 (1983).

10 N. Ise, T. Okubo, K. Ito, S. Dosho, and I. Sogami, Langmuir, 1, 176 (1985).

11 N. Ise, T. Okubo, K. Ito, S. Dosho and I.Sogami, J. Coll. Interface Sci.103, 292 (1985).

12 J. B. Hayter and J. Penfold, J. Chem. Soc., Faraday Trans. 1 77, 1851 (1981).

13 C. Cabos, P. Delord and J. C. Martin, J. Phys.40, L-407 (1979).

14 S. Takano, M. Kuzukawa and M. Yamanaka, J. Am. Oil. Chem.

Soc. 54, 484 (1977).

15 J. A. Lake, Acta Cryst. 23, 191 (1967).

16 C. Tanford, "The Hydrophobic Effect : Formation of Micelles and Biological Membranes", 2nd ed., Wiley, New York, 1980.

17 F. Reiss-Husson and V. Luzzati, J. Phys. Chem. 68, 3504 (1964).

18 J. B. Hayter and J. Penfold, Colloid Polym. Sci. 261, 1022 (1983).

19 A. Guinier and G. Fournet, "Small-angle Scattering of X-rays", Wiley, New York, 1955.

20 P.J. Missel, N. A. Mazer, G. B. Benedek and C. Carey, J. Phys. Chem. 87, 1264 (1983).

21 L. M. Kushner, W. D. Hubbard and R. A. Parker, J. Res. Natl. Bur. Stand. 59, 113 (1957).

22 M. F. Emerson and A. Holtzer, J. Phys. Chem. 71, 1898 (1967).

23 S. Ozeki and S. Ikeda, Bull. Chem. Soc. Jpn. 54, 552 (1981).

24 N. Ise and T. Okubo, J. Phys. Chem. 70, 2407 (1966).

25 M.Sugimura, T.Okubo, N.Ise and S. Yokoyama, J.Am. Chem. Soc. 106, 5069 (1984).

26 The same situation is of course possible for simple electrolyte solutions. According to the Debye-Huckel theory, the free energy of electrostatic interaction is given by $-(\Sigma N_i Z_i^2 e^2 \kappa / 3\epsilon)$ where N_i is the number of i-ions, Z_i their valency, $1/\kappa$ the Debye length, e the elementary charge, and ϵ the dielectric constant of the solvent. Because of its negative sign, the free energy shows that the solution is stabilized, in other words the net interaction is attraction,

in spite of the repulsive interaction between the ions of like-charges. Furthermore, the magnitude of the free energy becomes larger with increase in the valency Z_i, which should cause stronger repulsion with other ions of the same sign but nevertheless stronger stabilization of the total systems. This is exactly what was discussed for macroion systems in the text.

27 A. Patkowski, E. Gulari and B. Chu, J.Chem. Phys.78, 4187 (1980).

28 Chapter 3 of this thesis; H. Matsuoka, N. Ise, T. Okubo, S. Kunugi, H. Tomiyama and Y. Yoshikawa, J. Chem. Phys. 83, 378 (1985).

29 L. J. Magid, R. Triolo, J. S. Johnson, Jr. and W. C. Koehler, J. Phys. Chem. 86, 164 (1982).

30 R.Triolo, J. B. Hayter, L. J. Magid and J. S. Johnson, Jr., J. Chem. Phys. 29, 1977(1983).

31 J. B. Hayter and T. Zemb, Chem. Phys. Lett. 93, 91 (1982).

32 D. Bendedouch and S-H. Chen, J. Phys. Chem. 87, 1653 (1983).

33 D. Bendedouch, S-H. Chen and W. C. Koehler, J. Phys. Chem. 87, 2621 (1983).

34 J. Kalus, H. Hoffmann, K. Reizlein, W. Ulbricht and K. Ibel, Ber. Bunsenges. Phys. Chem. 86, 37 (1982)

35 H. Hoffmann, J. Kalus, H. Thurn and K. Ibel, Ber. Bunsenges. Phys. Chem. 87, 1120 (1983).

36 J. B. Hayter and J. Penfold, Mol. Phys. 42, 109 (1981).

37 J. P. Hansen and J. B. Hayter, Mol. Phys. 46, 651 (1982).

38 In the DLVO theory on colloidal stability (Ref.39), it is to be noted that, in addition to the electrostatic repulsion

between colloidal particles or plates, a van der Waals-type attraction was assumed.

39 See for example, E.J.W.Verwey and J.Th.G.Overbeek, Theory of the Stability of Lyophobic Colloids (Elsevier, Amsterdam, 1952).

40 Ref.7 should be referred to on the dependence of the inter-macroion attraction on the charge number.

41 W.Hartl, H.Versmold, U.Wittig and V.Marohn, Mol.Phys.50, 815 (1983).

42 R.Hosemann and S.N. Bagchi, Direct Analysis of Diffraction by Matter., North-Holland, Amsterdam, 1962.

43 D.J. Yarusso and S. L. Cooper, Macromolecules 16,1871 (1983).

44 Chapter 7 of this thesis; H.Mastuoka, H.Tanaka, T.Hashimoto and N. Ise, Phys. Rev. B, in press.

45 T. Yoshiyama, I. Sogami and N. Ise, Phys. Rev. Lett. 53, 2153 (1984).

46 a) R. Hosemann, W. Vogel and D. Weich, Acta Cryst. A37, 85 (1981); b) A. M. Hindeleh and R. Hosemann, Polymer 23, 1101 (1982).

47 J.Cebula, J. W. Goodwin, G.C. Jeffrey, R.H. Ottewill, A Parentich and R. A. Richardson, Faraday Dissc.76, 37 (1983).

48 W. Hartl, H. Versmold and U. Wittig, Ber. Bunsenges. Phys. Chem. 88, 1063 (1984).

Chapter 6

"Ordered" Structure in Colloidal Silica Suspensions.

I. Introduction[1]

In recent years, solutions of various synthetic and biological polyelectrolytes, such as polyacrylate,[2], poly-L-lysine,[3] sodium polystryrenesulfonate,[4] bovine serum albumin,[5] t-RNA[5,6] etc., were investigated by small-angle X-ray scattering (SAXS), and neutron scattering (SANS) techniques. The scattering curve showed a single broad peak and it has been concluded that the macroions were not distributed randomly, but in an ordered manner although its ordering is not perfect, contains distortions and is dynamic.[7] It has been also found that the light scattering curve from dilute polymer latex suspensions[8-10] and dilute solutions of sodium polystryrenesulfonate, whose molecular weight is fairly high, shows peak or peaks.[11] By the ultramicroscope technique, it was observed by the naked eye that polymer latex particles, whose diameter is about 3000 A, are distributed in an ordered manner.[12-14] Furthermore, the diffusion constant measured by quasi-elastic light scattering (QELS) technique on polyelectrolyte solutions showed an unusual salt concentration dependence[15-17]; with decreasing salt concentration, the appearent diffusion constant became dramatically small at a certain salt concentration. This observation may reflect the change of the structure of macroions in solution which is caused by the electrostatic interaction between the macroions.

In chapter 5, SAXS measurements were performed on spherical ionic micelles. The advantage of the system was the spherical nature of the macroion; one can easily obtain the interparticle interference function, S(q), from the observed scattering intensity, I(q), by considering the particle scattering factor, P(q). It became possible to discuss the interparticle distance ($2D_{exp}$) more exactly using the peak position of S(q). However, in micellar systems, the aggregation number might be changed with the surfactant concentration, or salt concentration. In this sense, the discussion in chapter 5 was associated with an unevitable vagueness.

In this chapter, SAXS investigation was performed on colloidal silica suspensions. Colloidal silica particles have some negative charges originated from silanol groups on the surface under high pH conditions. Colloidal silica particles are nearly spherical and its size and shape would not be affected by its concentraion and salt concentration. It is expected that this nature of colloidal silica particle permits us to get more detailed information on the distribution of macroions in suspension.

On the structure of colloidal silica suspensions, there are reported only some articles by Ramsay et al.[18-20], who tried to explain the scattering peak based on a liquid theory.

II. Experimental

II-1 Materials

Colloidal silica used in this investigation was Ludox SM

which was kindly provided from DuPont Japan (Tokyo). The original suspension (about 30 wt.%) was dialyzed against a 10^{-4}M NaOH solution for four days. After filtration by glass filter to remove some large aggregates, the concentration of the resultant suspension was determined to be 10.98 vol. % by dry weight method, and used as the stock suspension. The specific gravity of colloidal silica was assumed to be 1.576 g/ml.

The water used for preparation of suspension and the dialysis was obtained by Milli-Q system (Millipore, Bedford, Mass.). NaCl was of the analytical grade from Merk (Darmstat).

II-2 SAXS apparatus

The SAXS apparatus and the data processing system were described in detail in chapter 2. A Ni filter was used as a monochrometer.

II-3 Dynamic light scattering measurement

Dynamic light scatering apparatus which was used for the determination of the hydrodynamic radius of the silica particle is of Brookhaven Instruments Corp. (Ronkonkoma, NY.). The correlator is a Brookhaven BI-2030 degital correlator.

III. Results

III-1 Concentration dependence of the SAXS curve

Figure 1 shows the scattering curves of Ludox SM suspensions at various concentrations. The ordinate is the relative intensity of scattered X-rays and the abscissa is the scattering vector q

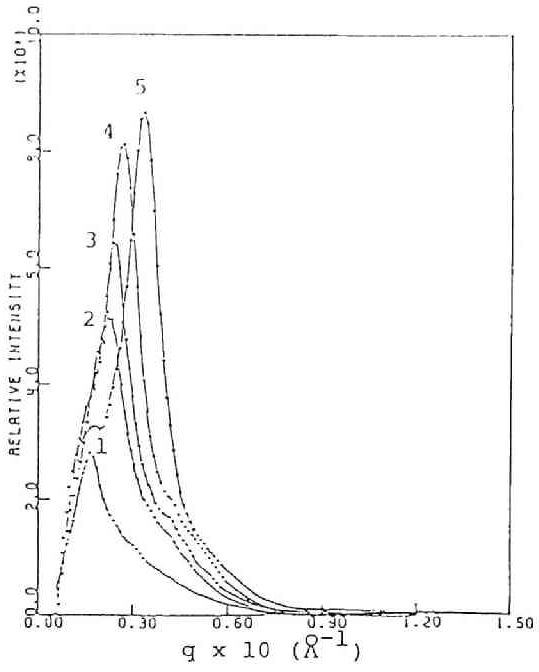

Fig.1 Concentration dependence of scattering curve of Ludox SM in water. 1:[Ludox]=1.10 vol.%, 2:2.75%, 3:3.66%, 4:5.49%, 5:10.98%.

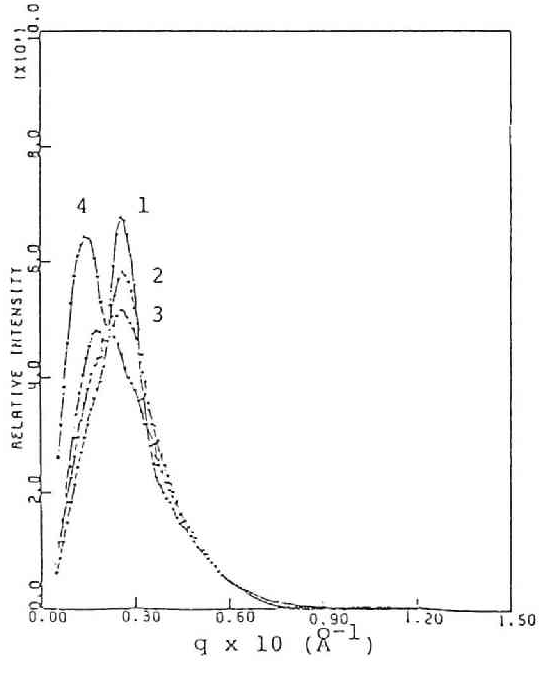

Fig.2 Salt concentration dependence of scattering curve of Ludox SM. [Ludox]=5.49%. 1:[NaCl]=0M, 2:0.005M, 3:0.01M, 4:0.1M.

($q=4\pi\sin\theta/\lambda$, where 2θ is the scattering angle and λ is the wave length of the X-ray.). In this concentration range (1.1 - 10.98 vol.%), a broad peak was observed, and a small "shoulder" could be seen at a higher angle. The peak position shifted to higher angles with increasing concentration.

III-2 Salt concentration dependence

Figure 2 shows the scattering curves of a Ludox SM 5.49 vol.% suspension at various NaCl concentrations. The scattering peak, which can be seen at $q \simeq 0.03$, became lower with increasing salt concentration, and disappeared at 0.1 M. In the curves 3 and 4, another peak could be observed at lower angle regions. However, it is believed that this peak is not due to interparticle interference, because there can be no lattice systems, which are expected to show a scattering peak at such a low angle region (i.e. a large interparticle distance, about 450 A) at the given concentration.

IV. Discussion

IV-1 Size and shape of colloidal silica particle

When there are no interparticle interaction in the system, the SAXS curve is proportional to the single particle scattering. In this case, the so-called Guinier law can be applied at small angle regions,[21]

$$I(q) = n \exp[\ (-1/3)\ R_g^2\ q^2] \qquad (1)$$

where n is a constant relating to the apparatus and proportional to the concentration, and R_g is the radius of gyration of the

particle. Thus, from the Guinier plot (ln I(q) vs. q^2), R_g of the particle can be obtained.

Figure 3 shows a Guinier plot of a Ludox SM suspension whose concentration is 5.49 vol.% at 0.1 M NaCl. In this q region, the plot shows an excellent linearity, which indicates the nearly spherical shape of the silica particle. The R_g value obtained from the slope is 47.4 A. For spherical particles, whose radius is R, the following relation between R and R_g holds,

$$R^2=(5/3)R_g^2 \qquad (2)$$

Using Eq.(2), the R value is found to be 61.1 A.

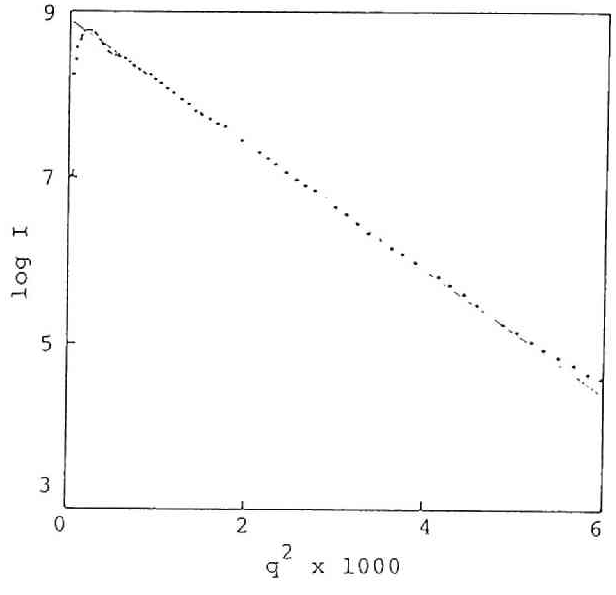

Fig.3 Guinier plot of Ludox SM. [Ludox]=5.49 vol.%, [NaCl]=0.1M.

The slope of the Guinier plot for a much diluted Ludox SM suspension (0.11 vol.%) without added salt gave R_g=47.1 A, which results in R=60.8 A. The R_g values at the two different conditions agreed to each other very well.

Dynamic light scattering measurements were performed on a 0.11 vol.% suspension to obtain the hydrodynamic radius (R_h) of silica particle. The obtained R_h values by the cumulant method was 65 A. This slightly larger R_h value than R obtained by SAXS is satisfactory in light of the physical nature of R_h, and supports the validity of the SAXS determination of R.

IV-2 Separation of the interparticle interference function S(q) from I(q).

In general, the scatterig intensity I(q) is related to both the intraparticle scattering and the interparticle interference. When the particles are spherically symmetric and not poly-disperse, the following relation holds,

$$I(q) = n\, P(q)\, S(q) \qquad (3)$$

where P(q) is the intraparticle scattering factor and S(q) the interparticle interference function. When the system has no interparticle interaction, S(q)=1, and thus I(q) is proportional to the scattering by the single particle. We can obtain S(q) by dividing I(q) by P(q) for spherical particles.

The I(q), P(q), and S(q) functions are shown in Fig.4. In this chapter, I(q) at a particle concentration of 5.49 vol.% and

at an NaCl concentration of 0.1M was equated to n P(q). The normalization was performed by fitting the P(q) to I(q) at higher angle regions where the interparticle interference might be negligible, i.e., S(q)=1. By this fitting, the factor n was obtained.

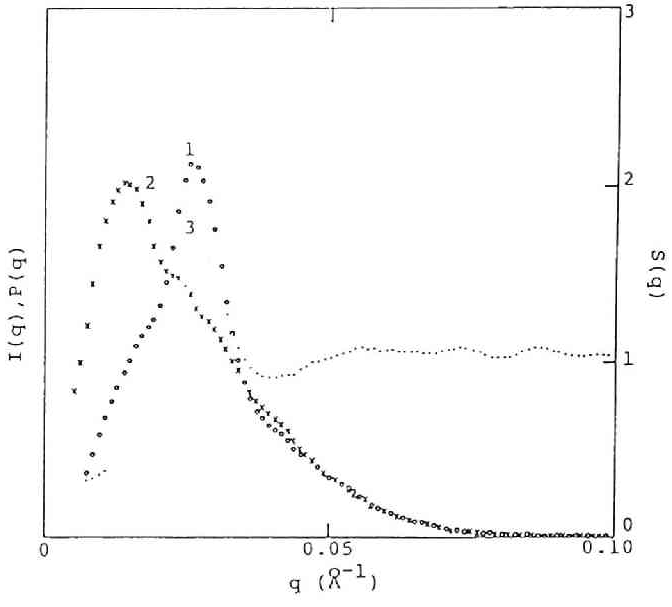

Fig.4 I(q), P(q), and S(q) for Ludox SM. [Ludox]= 5.49 vol.%. 1:I(q), 2:nP(q), 3:S(q).

IV-3 Concentration dependence of S(q)

The S(q)'s of Ludox SM suspension thus obtained were shown in Fig.5. For each S(q) curve, a peak and a small shoulder can be seen, which indicate that the silica particles are distributed in an ordered manner even in dilute suspensions. The first peak position shifts to higher angle regions with increasing concentration. This tendency is consistent with the earlier results for other synthetic and biological polyelectrolytes.[2-5]

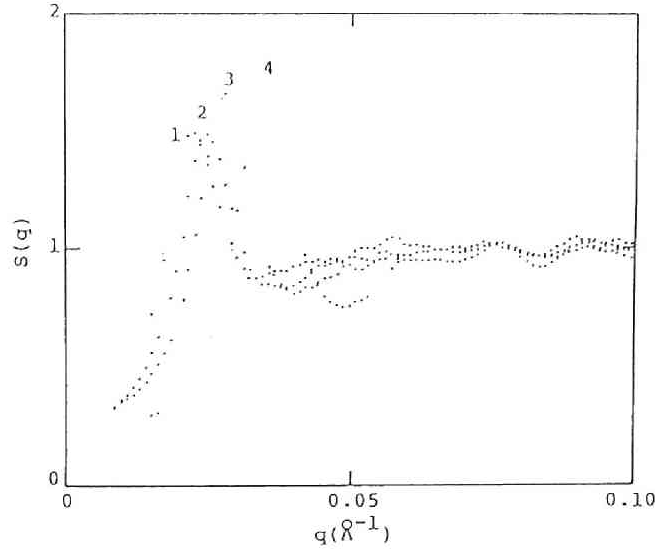

Fig.5 Concentration dependence of S(q) of Ludox SM. 1:[Ludox]=2.75 vol.%, 2: 3.66%, 3:5.49%, 4:10.98%.

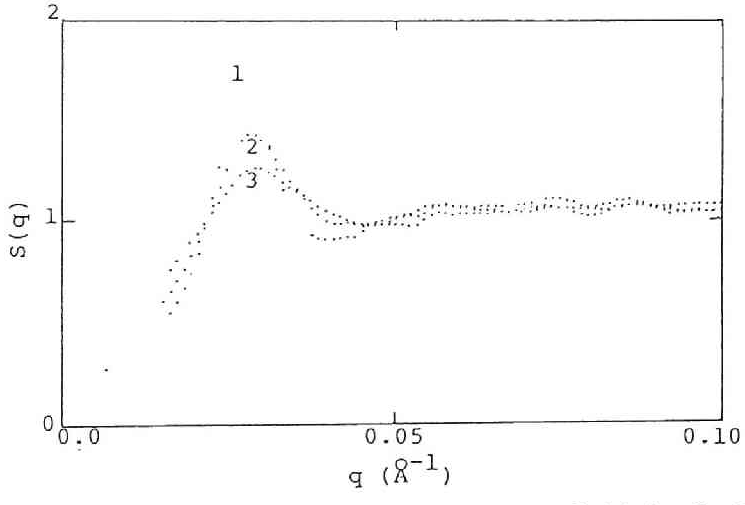

Fig.6 Salt concentration dependence of S(q) of Ludox SM. 1:[NaCl]=0M, 2:0.005M, 3:0.01M. [Ludox]=5.49 vol.%.

Table I SAXS Data of Ludox SM

Conc.	NaCl	pH	q_m of I(q)	$2D_{exp}$ from I(q) (Å)			q_m of S(q)	$2D_{exp}$ from S(q) (Å)			$2D_0$ (Å)		
(vol.%)	(M)		($Å^{-1}$)	sc	fcc	bcc	($Å^{-1}$)	sc	fcc	bcc	sc	fcc	bcc
1.10	0	9.3	0.0161	390	477	477	(0.0172)	(365)	(447)	(447)	442	497	483
2.75	0	9.2	0.0215	292	358	358	0.0226	278	341	341	326	366	356
3.66	0	9.2	0.0237	266	325	325	0.0247	254	311	311	296	332	323
5.49	0	9.1	0.0269	234	286	286	0.0279	225	275	275	259	290	282
10.98	0	8.8	0.0333	189	231	231	0.0343	183	224	224	205	231	224
5.49	0	9.1	0.0258	244	299	299	0.0279	225	275	275	259	290	282
5.49	0.005	9.0	0.0258	244	299	299	0.0290	217	266	266	259	290	282
5.49	0.01	8.9	0.0247	254	311	311	0.0279	225	275	275	259	290	282
5.49	0.1	8.2	(0.0140)	(450)	(511)	(511)	---	---	---	---	259	290	282

We can evaluate the interparticle distance ($2D_{exp}$) from the first peak position by using Bragg equation. Although the calculation method is different for the lattice system assumed, the $2D_{exp}$ values for typical cubic systems, namely simple cubic (sc), face-centered cubic (fcc), and body-centered cubic (bcc) lattices, were summarized in Table I.

IV-4 Salt concentration dependence of S(q)

Figure 6 shows the S(q) curves for a 5.49 vol.% Ludox SM suspension at various salt concentrations. The scattering peak becomes lower with increasing salt concentration which is consistent with earlier observations.[3-5] On the other hand, the peak position is not substantially affected by salt concentration, which does not agree with earlier observations. This may be due to the low charge density of silica particle; for highly charged solutes, the relation $2D_{exp} < 2D_0$ holds,[2-4] whereas $2D_{exp} \simeq 2D_0$ holds for low charge density macroions[5,20] due to the weakness of the electrostatic attractive interaction between macroions through the intermediary of counterions. In other words, the particles have already separated from each other as distant as possible, namely $2D_{exp} \simeq 2D_0$; the addition of salt can lower the degree of order (which results in a lowering of the peak intensity), but cannot affect the interparticle distance. Detailed discussion will be given later.

IV-5 Compaison of $2D_{exp}$ and $2D_0$

The $2D_{exp}$ values from I(q) and S(q), and the $2D_0$ values are

listed in Table I with experimental conditions. The $2D_{exp}$ value decreases with increasing concentration while it is not strongly affected by salt concentration. The slightly smaller (by 3 - 5%) $2D_{exp}$ values from S(q) than that from I(q) is due to the influence of the particle scattering factor (P(q)). Needless to say, the $2D_{exp}$ from S(q) are more correct values for the interparticle spacing. When we compare $2D_{exp}$ from S(q) and $2D_0$ for each lattice system, $2D_{exp}$ values are found to be very close to $2D_0$ for the case of fcc and bcc, while for the sc case $2D_{exp}$ is slightly smaller than $2D_0$ value. Although it is not easy to determine the charge density of the small particle such as Ludox SM, the present particle is not so highly charged,[19] so that $2D_{exp}$ is close to $2D_0$. On the basis of this fact and the higher packing efficiency of fcc and bcc with respect to sc, it can be suggested that colloidal silica particles are distributed almost uniformly throughout the suspension with an fcc or bcc symmetry, although the degree of the order is not so high.

IV-6 Evaluation of the lattice system of the distribution of colloidal silica particles by comparing with the theoretical scattering peak of the distorted crystal.

To determine the lattice system of the distribution of the colloidal silica particles, the information on the peak position is not enough, since the difference between the first peak positions of fcc and bcc is very small. However, it is possible to estimate the lattice system by using the whole profile of the scattering curve. Figure 7 shows the comparison of the S(q) is experimentaly obtained for a 10.98 vol.% suspension with the

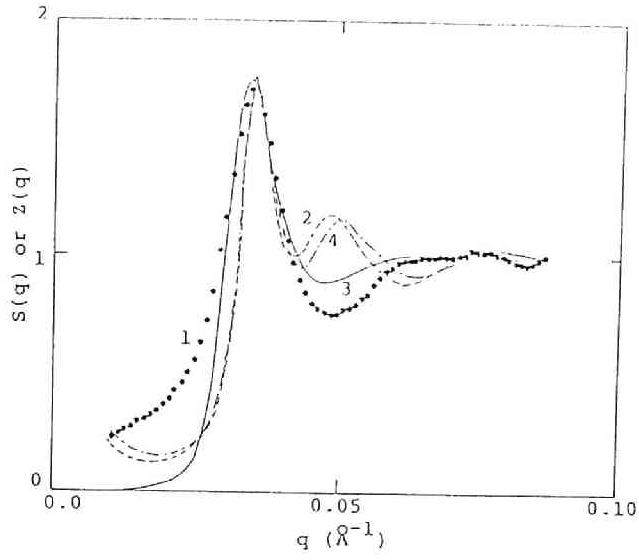

Fig.7 Comparison of the experimental interference function, S(q), with theoretical lattice factors, Z(q), for Ludox SM 10.98 vol.% suspension.

1: Experimental curve.

2: Theoretical lattice factor for sc, a=180A, g=0.16.

3: Lattice factor for fcc, a=310A, g=0.21.

4: Lattice factor for bcc, a=260A, g=0.124.

theoretical lattice factors, Z(q)'s for sc, fcc, and bcc with paracrystalline distortion. The theory of the scattering from cubic paracrystal will be discussed in chapter 7. In all cases, the height and the position of the first peak were fitted by varing the interparticle distance (a) and the g-value (the degree of distortion, the ratio of the standard deviation of the distortion of the lattice points and the interparticle distance). The shape and the width of the first peak is well reproduced by assuiming an fcc structure. Furthermore, the theoretical curve for the fcc can reproduce fairly well the position of the first

minimum though the agreement on the depth is not so satisfactory, while the theoretical curves for sc and bcc give the second peak at the position where the experimental curve showed the first minimum. Thus, it can be concluded that the distribution of the silica particle in a 10.98 vol.% suspension is fcc-like although it is fairly distorted. The g value used in the fitting is 0.21, indicating that the standard deviation of the distortion of lattice points is 21% of the interparticle distance. This g value cannot be claimed to be small. However, our interpretation, that the scattering peak observed for macroionic solutions can be explained by Bragg diffraction, is further strengthened.

IV-7 Comparison with the RMSA result

Ramsay et al. tried to reproduce the scattering curve by the RMSA theory, which was based on a liquid theory, and obtained a fairly good agreement.[19] The scattering peaks obtained for latex suspensions[9] by light scattering and for micellar solutions[23,24] by neutron scattering were also well reproduced by the RMSA method. However, the RMSA method is based on a repulsion-only assumption on the interaction between the macroions, which contradicts to the earlier experimental observation.[1] Although details will be described in chapter 7, no assumption on the interparticle interaction is involved in our three-dimensional paracrystal theory and nonetheless this theory can well reproduce the experimental curve as shown in Fig.7. This indicates that it is difficult to estimate the interparticle interaction only by fitting of the experimental curve with theoretical one. In this respect, Ramsay claimed that the RMSA method may have limitations

in providing absolute values.[19]

V. Concluding remarks

Dilute suspensions of colloidal silica particle (Ludox SM) were investigated by the small-angle X-ray scattering technique. A broad, but distinct peak and a small shoulder corresponding to the second order peak were observed in a concentration range from 1.1 to 10.98 vol.%. The silica particles were found to be nearly spherical and the interference function S(q) was obtained from the observed I(q). A distinct peak and a shoulder were also observed in S(q). These peak and shoulder are reminiscent of the ordered arrangement of the colloidal silica particles even in the suspension. The peak was lowered with increasing salt concentration, implying that the ordered structure of silica particles is due to an electrostatic interaction. The interparticle distance between particles ($2D_{exp}$) calculated by Bragg equation was very close to the $2D_0$ (the interparticle distance with the assumption of the uniform distribution) with the assumption that an fcc or bcc structure was maintained. The S(q) curve was well reproduced by the theoretical scattering curve of distorted fcc crystal, and its degree of distortion was found to be 0.21 for the 10.98 vol.% suspension.

References

1 For convenient reviews; (a) N.Ise and T.Okubo, Acc.Chem.Res., 13 303 (1980); N.Ise, Angew.Chem., 25, 323 (1986).

2 N.Ise, T.Okubo, K.Yamamoto, H.Kawai, T.Hashimoto, M.Fujimura, and Y.Hiragi, J.Am.Chem.Soc., 102, 7901 (1980).

3 N.Ise, T.Okubo, K.Yamamoto, H.Matsuoka, H.Kawai, T.Hashimoto, and M.Fujimura, J.Chem.Phys., 78, 541 (1983).

4 Chapter 2 of this thesis; N.Ise, T.Okubo, S.Kunugi, H.Matsuoka, K.Yamamoto, and Y.Ishii, J.Chem.Phys., 81 3294 (1984).

5 Chapter 3 of this thesis; H.Matsuoka, N.Ise, T.Okubo, S.Kunugi, H.Tomiyama, and Y.Yoshikawa, J.Chem.Phys., 83, 378 (1985).

6 A.Patrowski, E.Gulari, and B.Chu, J.Chem.Phys., 78, 4187 (1980).

7 Chapter 7 of this thesis; H.Matsuoka, H.Tanaka, T.Hashimoto, and N.Ise, Phys. Rev. B, in press.

8 R.H.Ottewill, Prog. Colloid & Polym. Sci., 67, 71 (1980).

9 D.J.Cebula, J.W.Goodwin, G.C.Jeffrey, R.H.Ottewill, A.Parentich and R.A.Richardson, Faraday Discuss.Chem. Soc., 76, 37 (1983).

10 W.Hartl, H.Versmold and U.Wittig, Ber. Bunsenges. Phys. Chem., 88, 1063 (1984).

11 M.Drifford and J.P.Dalbiez, J.Phys.Chem., 88, 5368 (1984).

12 A.Kose, M.Ozaki, K.Takano, Y.Kobayashi, and S.Hachisu, J.

Colloid Int. Sci., 44, 330 (1973).

13 N.Ise, T.Okubo, M.Sugimura, K.Ito and H.J.Nolte, J.Chem.Phys., 78, 536 (1983).

14 K.Ito, H.Nakamura, and N.Ise, J.Chem.Phys., 85, 6136 (1986).

15 S.-C.Lin, W.I.Lee, and J.M.Schurr, Biopolymers, 17, 1041 (1978).

16 K.Zero, and B.R.Ware, J.Chem.Phys., 80, 1610 (1984).

17 M.Drifford, and J.-P.Dalbiez, Biopolymers, 24, 1501 (1985).

18 J.D.F.Ramsay, R.G.Avery, and L.Benest, Faraday Discuss. Chem. Soc., 76, 53 (1983).

19 J.Penfold, and J.D.F.Ramsay, J.Chem.Soc., Faraday Trans. I, 81, 117 (1985).

20 J.Bunce, and J.D.F.Ramsay, J.Chem.Soc., Faraday Trans. I, 81, 2845 (1985).

21 A.Guinier and G.Fournet, Small angle scattering of X-rays, (Wiley, N.Y., 1955).

22 Chapter 5 of this thesis; Y.Ishii, H.Matsuoka, and N.Ise, Ber. Bunsenges. Phys. Chem., 90, 50 (1986).

23 J.B.Hayter, and J.P.Penfold, Coll. & Polym. Sci., 261, 1022 (1983).

24 D.Bendedouch, S.-H.Chen, and W.C.Koehler, J. Phys. Chem., 87, 2621 (1983).

Chapter 7

Elastic Scattering from Cubic Paracrystals

I. Introduction

The paracrystal theory of the diffraction pattern and the distribution function h(r) for one-dimensional crystals containing a distortion of the second kind was first proposed by Hosemann.[1] The theory was based on an operation of convolution polynomial, was extended later to two-dimensional cases and has been mainly applied to determination of the fiber structure[2]. For three-dimensional cases, Steffen and Hosemann calculated the function h(r) and compared it with experimental data for liquid lead[3]. Because of some uncertainties such as the termination effect[4] involved in the procedure for obtaining h(r) from an experimental scattering curve, direct comparison of theoretical and experimental scattering curves (not h(r)) seems more appropriate.

The lattice factor Z(q) is now calculated for randomly oriented three-dimensional cubic lattice systems with the paracrystalline distortion of the second kind, such as simple cubic (sc) lattice, face-centered cubic (fcc) lattice and body-centered cubic (bcc) lattice. It is believed that this three-dimensional theory is useful for the determination of the structure and the degree of distortion of the structure for three-dimensionally

ordered systems.

Colloidal particles such as polymer latex and synthetic and biological macroions form an ordered structure in solutions[5-7]. In the case of latex suspensions, scattering profiles have been analysed by Luck et al.[8] The ordering phenomena in such systems were almost unequivocally proven by ultramicroscopy.[9] Recently, the crystal structure was identified by the pseudo-[10] and intrinsic[11] Kossel line analyses: according to Yoshiyama et al.[11], bcc structures are stable at low concentrations whereas fcc structures are favored in concentrated regions. By using a cinematographic method, the particles forming the ordered structure were demonstrated to be differentiated from free particles, because the root-mean-square displacement of the free latex particles was very close to the prediction of the Einstein theory on Brownian motion[12-14] whereas that of the particles in the ordered state was practically zero for a reasonably long period of time (say 30 sec.). This observation convinced us of the existence of more or less distorted lattice-like distributions of the latex particles in dilute suspensions. These experimental facts on "visible" latex suspension appear to support our conclusion that synthetic and biological "invisible" macroions likewise form lattice-like ordered structures in dilute solutions, probably with a much larger degree of distortion than in the case of latex particles because of the difference in the geometrical size.

Recently spherical microdomains of block polymers in bulk and in solutions have been reported to be arranged in an ordered

manner with cubic symmetry[15-19]. The symmetry of ordered structures called "superlattices"[19] was in some cases discussed qualitatively on the basis of volumetric considerations, that is, from the peak positions of the scattering maxima observed in the small-angle X-ray scattering (SAXS) and neutron scattering (SANS) from the block polymers: it would be possible to estimate the nearest neighbor distance D between the spherical microdomains, e.g. A-spheres when A-block chains form A-spherical microdomains, and the radius R_A of the A-spheres. Comparison of the stoichiometric volume of an A block chain with a volume fraction of A-spheres estimated from the experimental values of D and R_A for a given symmetry made it possible to determine the symmetry of the cubic superlattice[16,18]. A relative peak position of the scattering maxima gave additional information on the lattice symmetry[15,16,18,19]. However no attempts[20] have been made so far to utilize whole scattering curves, such as peak heights and line widths of the scattering maxima and their positions, for quantitative determination of the symmetry, despite the fact that there is rich information associated with the scattering profiles. A quantitative determination of the symmetry and its distortion may be made possible by comparison of the experimental profiles with the theoretical profiles for paracrystals with the cubic symmetries.

Thus it would be interesting to analyse the nature of the ordered structures, particularly their distortion, and the diffraction patterns of scattered radiation from such distorted structures in terms of the three-dimensional paracrystal theory. We are fully aware of some adverse criticism of the

paracrystalline treatment in the three-dimensional cases,[21] but it is believed that the paracrystal theory is one of the most convenient methods for elucidating, though approximately, the symmetry of the cubic lattice and the distortion of the ordered structures in question. As an example of the applications, the ordered sructure in colloidal suspensions is discussed. An application to the ordering in block polymers will be found in elsewhere[22].

II. Theory

II-1 Review of General Paracrystal Theory.

Generally, the scattering intensity $I(\underset{\sim}{q})$ from a paracrystal with a given orientation to a reference axis is given by[1]

$$I(\underset{\sim}{q})=N[\langle|f_0|^2\rangle-|\langle f_0\rangle|^2]+N|\langle f_0\rangle|^2[1-D(\underset{\sim}{q})^2] +(1/v)|\langle f_0\rangle|^2 D(\underset{\sim}{q})^2 \widehat{Z(\underset{\sim}{q})\Sigma(\underset{\sim}{q})^2} \qquad (1)$$

where $\underset{\sim}{q}$ is the scattering vector, N the number of particles in the paracrystal, $f_0=f_0(q)$ the structure amplitude of the particle, v the volume available per particle, $Z(\underset{\sim}{q})$ the paracrystal lattice factor (associated with the distortion of the second kind[1]), and $\Sigma(\underset{\sim}{q})$ the shape amplitude of the paracrystal. The angular bracket $\langle\ \rangle$ designates an average with respect to distributions of particle size, density and orientation (in case when the particle is asymmtrical). The symbol $\widehat{f\ g}$ designates a convolution,

$$\widehat{f\ g}(\underset{\sim}{r})=\int du f(\underset{\sim}{u})g(\underset{\sim}{r}-\underset{\sim}{u}) \qquad (2)$$

The factor $D(\underset{\sim}{q})^2$ represents the thermal vibration of the particles (the distortion of the first kind[1]) about the paracrystalline lattice points.

When the particles are identical and spherical, the thermal vibrations not significant, and the size of the paracrystal infinitely large, then Eq.(1) is reduced to

$$I(\underset{\sim}{q})=N|f_0|^2 Z(\underset{\sim}{q}) \qquad (3)$$

We define here the three fundamental lattice vectors $\underset{\sim}{a}_k$ for the ideal perfect lattice. The distortion of the lattice points from the ideal lattice points is described by the displacement of the lattice vector $\Delta\underset{\sim}{a}_k$ from $\underset{\sim}{a}_k$. We assume that in a given direction of the lattice the nearest-neighbor distortions are independent and the distortions in three directions are also independent. Furthermore, in this investigation the distortion is assumed to be isotropic and given by a Gaussian distribution with a standard deviation Δa_k, although the distortion is generally anisotropic and $\Delta\underset{\sim}{a}_k$ a tensor quantity.

In this case, the lattice factor $Z(\underset{\sim}{q})$ for three dimensional paracrystals is generally given by[1],

$$Z(\underset{\sim}{q})=\prod_{k=1}^{3} Z_k(\underset{\sim}{q}) \qquad (4a)$$

$$Z_k(\underset{\sim}{q})=\mathrm{Re}\left\{\frac{1+F_k(\underset{\sim}{q})}{1-F_k(\underset{\sim}{q})}\right\}=\frac{1-|F_k|^2}{1-2|F_k|\cos(\underset{\sim}{a}_k\cdot\underset{\sim}{q})+F_k^{\,2}} \qquad (4b)$$

$$F_k(\underset{\sim}{q})=|F_k(\underset{\sim}{q})|\exp(-i\underset{\sim}{q}\cdot\underset{\sim}{a}_k) \qquad (5)$$

$$|F_k(\underset{\sim}{q})| = \exp[-(1/2)\Delta a_k^2 q^2] \quad (6)$$

When the paracrystals have an orientation distribution, the observed intensity distribution in one direction I_{obs} is obtained by averaging $I(\underset{\sim}{q})$ in Eq.(1) over all possible orientations.

$$I_{obs}(q) = \langle I(\underset{\sim}{q}) \rangle_{orient.} \quad (7)$$

where $\langle\ \rangle_{orient.}$ stands for the orientational average.

II-2 The Lattice Factor Z(q) for the Simple Cubic (sc) Lattice.

The lattice factor Z(q) for the sc lattice can be calculated by the method of Yarruso et al.[23] Their method is to calculate the diffraction pattern from the assembly of randomly oriented paracrystals by taking a rotational average of one infinitely large paracrystal.

Three unit vectors, $\underset{\sim}{a}_1$, $\underset{\sim}{a}_2$, $\underset{\sim}{a}_3$ for the ideal sc lattice, are taken as shown in Fig.1(a), and the length is represented by a.

$$|\underset{\sim}{a}_1| = |\underset{\sim}{a}_2| = |\underset{\sim}{a}_3| = a \quad (8)$$

Then,

$$\underset{\sim}{a}_1 \cdot \underset{\sim}{q} = -a\, q \sin\theta\cos\psi \quad (9)$$

$$\underset{\sim}{a}_2 \cdot \underset{\sim}{q} = a\, q \sin\theta\sin\psi \quad (10)$$

$$\underset{\sim}{a}_3 \cdot \underset{\sim}{q} = a\, q \cos\theta \quad (11)$$

Figure 2 shows the Eulerian angles (θ, η, φ) specifying the orientation of the coordinates Ouvw fixed to the unit cell with

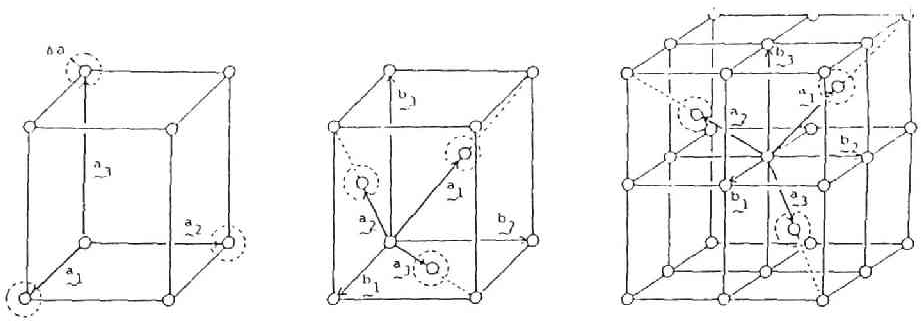

(a) (b) (c)

Figure 1(a): Three fundamental vectors $\underset{\sim}{a}_1$, $\underset{\sim}{a}_2$ and $\underset{\sim}{a}_3$ for simple cubic (sc) lattice. In Figs.1(a), (b) and (c), the isotropic lattice distortion is depicted by the spheres of radius Δa (broken circles).

Figure 1(b): The fundamental vectors $\underset{\sim}{a}_1$, $\underset{\sim}{a}_2$, $\underset{\sim}{a}_3$ and the orthogonal vectors $\underset{\sim}{b}_1$, $\underset{\sim}{b}_2$, $\underset{\sim}{b}_3$ for face-centered cubic (fcc) lattice.

Figure 1(c): The fundamental vectors $\underset{\sim}{a}_1$, $\underset{\sim}{a}_2$, $\underset{\sim}{a}_3$ and the orthogonal vectors $\underset{\sim}{b}_1$, $\underset{\sim}{b}_2$, $\underset{\sim}{b}_3$ for body-centered cubic (bcc) lattice.

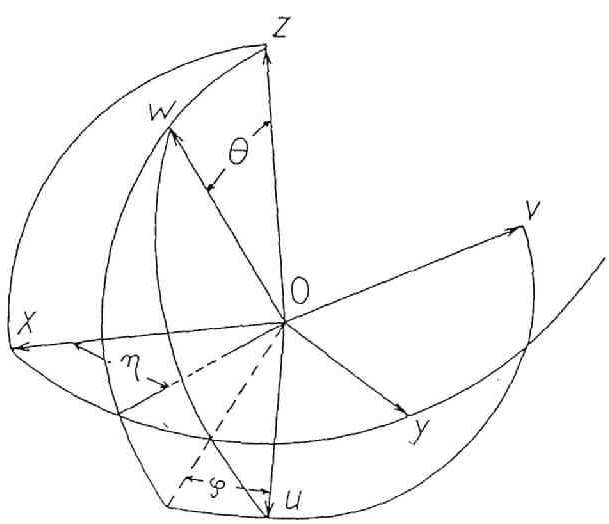

Figure 2 : Eulerian angles (θ,η,ψ) specifing the orientation of the coordinates Ouvw fixed to the unit cell with respect to the laboratory fixed coordinates Oxyz.

respect to the laboratory fixed coordinate Oxyz. The Oz axis is parallel to the vector $\underset{\sim}{q}$, θ and η are the polar and azimuthal angles specifying the orientation of the axis Ow and, φ is the angle specifying rotation of the the crystal around the Ow axis. In case of the sc lattice the axis Ow coincides with the vector $\underset{\sim}{a}_3$. By assuming the isotropic distortions of a real lattice point from an ideal lattice point designated by $\underset{\sim}{a}_1$,$\underset{\sim}{a}_2$ and $\underset{\sim}{a}_3$ (Fig.1(a))

$$\Delta a_1=\Delta a_2=\Delta a_3=\Delta a \tag{12}$$

We obtain from Eqs.(4) to (6) and (12),

$$Z_1(q,\theta,\psi)=\frac{[1-\exp(-q^2\Delta a^2)]}{1-2\exp[-(1/2)q^2\Delta a^2]\cos(q\ a\ \sin\theta\cos\psi)+\exp(-q^2\Delta a^2)} \tag{13}$$

$$Z_2(q,\theta,\psi)=\frac{[1-\exp(-q^2\Delta a^2)]}{1-2\exp[-(1/2)q^2\Delta a^2]\cos(q\ a\ \sin\theta\sin\psi)+\exp(-q^2\Delta a^2)} \tag{14}$$

$$Z_3(q,\theta,\psi)=\frac{[1-\exp(-q^2\Delta a^2)]}{1-2\exp[-(1/2)q^2\Delta a^2]\cos(q\ a\ \cos\theta)+\exp(-q^2\Delta a^2)} \tag{15}$$

Then we can calculate Z(q) for the randomly oriented paracrystals by

$$Z(q)=\frac{2}{\pi}\int_0^{\frac{\pi}{2}}\int_0^{\frac{\pi}{2}} Z_1(q,\theta,\psi)Z_2(q,\theta,\psi)Z_3(q,\theta,\psi)\sin\theta d\theta d\psi \tag{16}$$

II-3 Z(q) for the Face-Centered Cubic (fcc) Lattice.

We define the fundamental vectors, $\underset{\sim}{a}_1$, $\underset{\sim}{a}_2$, $\underset{\sim}{a}_3$, and the orthogonal vectors $\underset{\sim}{b}_1$, $\underset{\sim}{b}_2$, $\underset{\sim}{b}_3$, as in Fig.1(b) and take the Ow axis parallel to $\underset{\sim}{b}_3$. We obtain

$$\underset{\sim}{a}_1=(1/2)(\underset{\sim}{b}_2+\underset{\sim}{b}_3) \tag{17}$$

$$\underset{\sim}{a}_2=(1/2)(\underset{\sim}{b}_1+\underset{\sim}{b}_3) \tag{18}$$

$$\underset{\sim}{a}_3=(1/2)(\underset{\sim}{b}_1+\underset{\sim}{b}_2) \tag{19}$$

Therefore, using the relations of Eqs.(9) to (11), and noting that $|\underset{\sim}{b}_1|=|\underset{\sim}{b}_2|=|\underset{\sim}{b}_3|=a$, we obtain

$$\underset{\sim}{q}\cdot\underset{\sim}{a}_1=(1/2)q\ a\ (\sin\theta\sin\psi+\cos\theta) \tag{20}$$

$$\underset{\sim}{q}\cdot\underset{\sim}{a}_2=(1/2)q\ a\ (-\sin\theta\cos\psi+\cos\theta) \tag{21}$$

$$\underset{\sim}{q}\cdot\underset{\sim}{a}_3=(1/2)q\ a\ (-\sin\theta\cos\psi+\sin\theta\sin\psi) \tag{22}$$

Then, by assuming Eq.(12) again for the distortion of the lattice points from the ideal lattice designated by $\underset{\sim}{a}_1$, $\underset{\sim}{a}_2$, $\underset{\sim}{a}_3$ in Fig.1(b) and by using Eqs. (4) to (6) and (20) to (22), we obtain

$$Z_1(q,\theta,\psi)=\frac{[1-\exp(-q^2\Delta a^2)]}{1-2\exp[-(1/2)q^2\Delta a^2]\cos[(1/2)qa(-\sin\theta\sin\psi+\cos\theta)]+\exp(-q^2\Delta a^2)))} \tag{23}$$

$$Z_2(q,\theta,\psi)=\frac{[1-\exp(-q^2\Delta a^2)]}{1-2\exp[-(1/2)q^2\Delta a^2]\cos[(1/2)qa(-\sin\theta\cos\psi+\cos\theta)]+\exp(-q^2\Delta a^2)))} \tag{24}$$

$$Z_3(q,\theta,\psi)=\frac{[1-\exp(-q^2\Delta a^2)]}{1-2\exp[-(1/2)q^2\Delta a^2]\cos[(1/2)qa(-\sin\theta\cos\psi+\sin\theta\sin\psi)]+\exp(-q^2\Delta\ldots}$$

(25)

By substituting Eqs.(23) to (25) into Eq.(16), Z(q) for a randomly oriented fcc lattice can be calculated.

II-4 Z(q) for the Body-Centered Cubic (bcc) Lattice.

The three fundamental vectors $\underset{\sim}{a}_1$, $\underset{\sim}{a}_2$ and $\underset{\sim}{a}_3$, and the orthogonal vectors $\underset{\sim}{b}_1$, $\underset{\sim}{b}_2$ and $\underset{\sim}{b}_3$ are defined as shown in Fig.1(c). Then,

$$\underset{\sim}{a}_1=(1/2)(-\underset{\sim}{b}_1+\underset{\sim}{b}_2+\underset{\sim}{b}_3) \tag{26}$$

$$\underset{\sim}{a}_2=(1/2)(\underset{\sim}{b}_1-\underset{\sim}{b}_2+\underset{\sim}{b}_3) \tag{27}$$

$$\underset{\sim}{a}_3=(1/2)(\underset{\sim}{b}_1+\underset{\sim}{b}_2-\underset{\sim}{b}_3) \tag{28}$$

By taking the Ow axis parallel to $\underset{\sim}{b}_3$, noting that $|\underset{\sim}{b}_1|=|\underset{\sim}{b}_2|=|\underset{\sim}{b}_3|=a$, assuming isotropic lattice distortions as given by Eq.(12) from the perfect lattice defined by the vectors $\underset{\sim}{a}_1$, $\underset{\sim}{a}_2$ and $\underset{\sim}{a}_3$ in Fig.1(c) and by using Eqs. (4) to (6) and (26) to (28), we obtain

$$Z_1(q,\theta,\psi)=\frac{[1-\exp(-q^2\Delta a^2)]}{1-2\exp[-(1/2)q^2\Delta a^2]\cos[(1/2)qa(\sin\theta\cos\psi+\sin\theta\sin\psi+\cos\theta)]+\exp(-q^2\Delta a^2)} \tag{29}$$

$$Z_2(q,\theta,\psi)=\frac{[1-\exp(-q^2\Delta a^2)]}{1-2\exp[-(1/2)q^2\Delta a^2]\cos[(1/2)qa(-\sin\theta\cos\psi-\sin\theta\sin\psi+\cos\theta)]+\exp(-q^2\Delta a^2)} \tag{30}$$

$$Z_3(q,\theta,\psi)=\frac{[1-\exp(-q^2\Delta a^2)]}{1-\exp[-(1/2)q^2\Delta a^2]\cos[(1/2)qa(-\sin\theta\cos\psi+\sin\theta\sin\psi-\cos\theta)]+\exp(-q^2\Delta a^2)} \quad (31)$$

Z(q) for a randomly oriented bcc lattice can be calculated using Eqs.(16) and (29) to (31).

III. Results of Numerical Calculations.

We first define the paracrystalline distortion factor g as

$$g\equiv \Delta a/|\underset{\sim}{a}_1|=\Delta a/|\underset{\sim}{a}_2|=\Delta a/|\underset{\sim}{a}_3| \quad (32)$$

where $\underset{\sim}{a}_1$, $\underset{\sim}{a}_2$ and $\underset{\sim}{a}_3$ are the three fundamental vectors as shown in Fig.1 for sc, fcc and bcc lattices, and Δa is the distortion of the lattice point from the ideal lattice point as schematically drawn in Fig.1 with the spheres of radius Δa.

Figure 3 shows the results of numerical calculations of Z(q) for a randomly oriented sc lattice for various g values. At small g values (low degrees of distortion), many sharp peaks appear at the reduced scattering vectors $aq/(2\pi)=(h^2+k^2+l^2)^{1/2}$ characteristic for the sc lattice: the relative peak positions of the first and higher order peaks are at 1, $\sqrt{2}$, $\sqrt{3}$, $\sqrt{4}$, $\sqrt{5}$, ..., and these peaks correspond to diffractions from (100), (110), (111), (200), (210), and so on. As the g value increases, the peaks become lower and broader, and the higher order peaks disappear. According to Hosemann's prediction for the one-dimensional paracrystal lattice, the n-th peak disappears at the g value which satisfies the criterion $g\,n=0.35$[1]. The corresponding

criteria for the sc and bcc lattices will be discussed in section V-1.

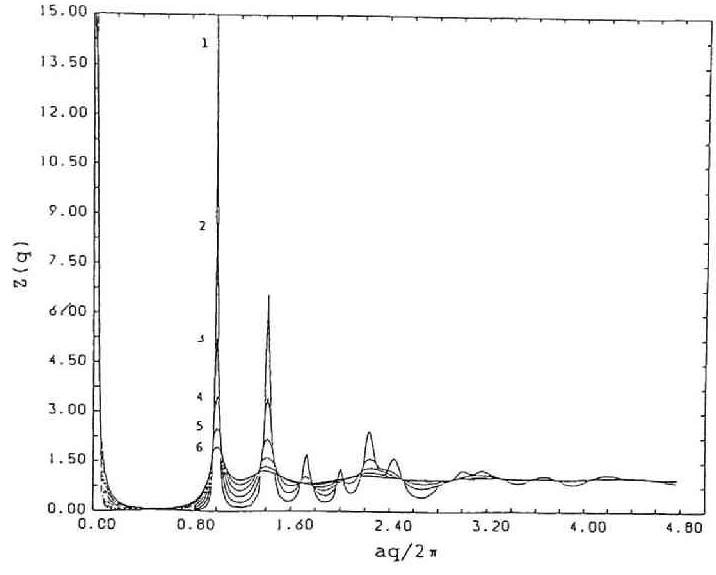

Figure 3 : Calculated paracrystalline lattice factors for sc structure. g=0.05 (curve 1), 0.07 (2), 0.09 (3), 0.11 (4), 0.13 (5), 0.15 (6).

Figures 4 and 5 show the Z(q) for randomly oriented fcc and bcc lattices, respectively. The relative peak positions of the first and higher order diffractions from (111), (200), (220), (311), (222) planes and so on for the fcc lattice are at 1, $(4/3)^{1/2}$, $(8/3)^{1/2}$, $(11/3)^{1/2}$, $(4)^{1/2}$, and so on, respectively. The relative peak positions from (110), (200), (211), (220), (310) planes and so on for the bcc lattice are at 1, $\sqrt{2}$, $\sqrt{3}$, $\sqrt{4}$, $\sqrt{5}$, and so on, respectively. As the g value increases, the peaks become lower and broader for these two cases, too. The criterion for the (hkl) diffraction peaks to be resolvable will be discussed also in section V-1.

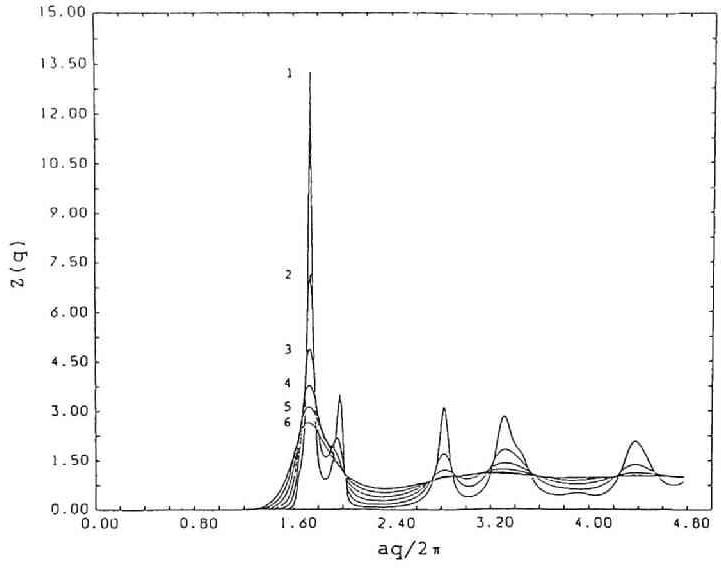

Figure 4 : Calculated paracrystalline lattice factors for fcc lattice. g=0.05 (curve 1), 0.07 (2), 0.09 (3), 0.11 (4), 0.13 (5), 0.15 (6).

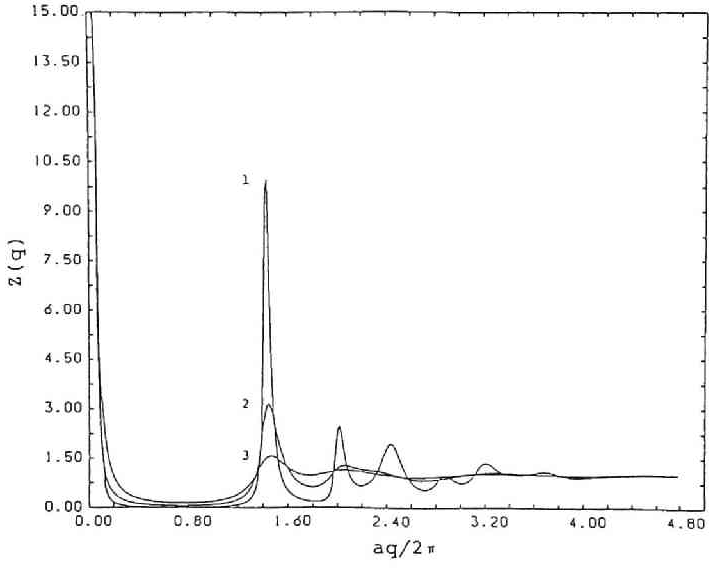

Figure 5 : Calculated paracrystalline lattice factors for bcc structure. g=0.05 (curve 1), 0.09 (2), 0.13 (3).

It should be noted that the strong zero-th order scattering exists for the three-dimensional paracrystal, and is especially marked for the sc and bcc. This peculiar effect which does exist even for the paracrystals with an infinite size does not exist for the one-dimensional paracrystal. Further details will be discussed in sec.V-2.

IV. Consideration of Other Distortions.

IV-1 Thermal Oscillation (distortion of the first kind) and the Effect of Interfacial Thickness.

The thermal vibration of the particles around the lattice points is one of the paracrystalline distortions called a distortion of the first kind, and the effect of an interfacial diffuse boundary is a problem associated with the variation of the scattering contrast between the particles and the medium at the interface. The two problems are inherent to the particle scattering function and hence these two effects can be treated mathematically in a similar way. The former effect is given by the exponential term, the so-called Debye-Waller factor, in Eq.(1) as follows,

$$D=\exp[-(1/2)\overline{u^2}q^2] \qquad (33)$$

where $\overline{u^2}$ is the mean-square displacement of the particles from the lattice points by thermal motion. Similarly the effect of the smooth diffuse-boundary is given by[24]

$$B=\exp[-(1/2)\sigma_s{}^2q^2] \qquad (34)$$

where B is the Fourier transform of the smoothing function $b(\underset{\sim}{r})$

characterizing the distribution of the scattering contrast $\rho(\underset{\sim}{r})$ at the interface

$$\rho(\underset{\sim}{r})=\widehat{\rho_i \; b(\underset{\sim}{r})} \qquad (35)$$

where $\rho_i(\underset{\sim}{r})$ is the scattering contrast profile for the sharp interface with $\sigma_s=0$ and

$$b(\underset{\sim}{r})=(2\pi\sigma^2)^{-3/2}\exp(-r^2/2\sigma^2) \qquad (36)$$

For the particles with the diffuse boundary f_0 in Eq.(1) should be replaced by $f_0B(q)$. Physically, these two effects can be recognized as the blur of the particle scattering. (See Ref.15 and Fig.10 in Ref.25 as examples of the influence of these factors on scattering behavior.) It must be noted that these effects influence the intensity of diffraction peak(s) and even more strongly those of the higher order peaks. However the influence on the width of the peaks is very small as is easily seen from Eqs.(1), (33) and (34).

IV-2 Effect of Size of the Paracrystals

The size of the crystal also affects the scattering behavior. The smaller the crystal, the lower the intensity of the diffraction and the broader the diffraction profile. Therefore, the scattering function I(q) must be calculated taking into consideration the effect of the finite crystal size especially for an assembly of microparacrystals, and even more so for greatly distorted microparacrystals because it is hardly feasible that a geatly distorted crystal can grow into a larger crystal. For an assembly of the microcrystals, the definition of the

crystal size is rather obvious. For greatly distorted continuous crystals, however, the situation is not simple. The "crystal size" implies now the limit of "correlation" of lattice points; if the crystal size is N by particle number in one direction, the lattice point of the (N+1)th particle is not affected by that of the particle at the origin. Generally the correlation is a statistical quantity and N is an ensemble-averaged quantity.

The effect of the finite size of the paracrystal is incorporated in Eq.(1) by the shape factor $\Sigma(\underset{\sim}{q})^2$. However from the technical point of view in the numerical calculation, it seems to be much easier to calculate directly the scattering of the paracrystal containing N particles in each direction specified by the fundamental vectors $\underset{\sim}{a}_1$, $\underset{\sim}{a}_2$, $\underset{\sim}{a}_3$, rather than taking a convolution of the lattice factor Z for infinitely large paracrystals and Σ^2 as in Eq.(1).

Hashimoto et al. previously presented full details of the equation for the lattice factor Z containing N unit cells for the one-dimensional paracrystal[26], the results of which can be extended to the three-dimensional paracrystals. With this approach instead of Eqs.(1) and (4), we obtain

$$I(\underset{\sim}{q})=N[\langle|f_0|^2\rangle-|\langle f_0\rangle|^2]+N|\langle f_0\rangle|^2[1-D^2(\underset{\sim}{q})] + |\langle f_0\rangle|^2 \prod_{k=1}^{3} N_k[Z_k+I_{ck}/N_k] \qquad (37)$$

where $N=N_1N_2N_3$ is the total number of unit cells in the paracrystal, N_k the number of the unit cell along the k-th direction, Z_k the lattice factor for infinitely large paracrystals along the k-th direction, and I_{ck} the zero-th order

scattering related to the finite-size effect of the paracrystal. The factor Z_k is given by Eq.(4b), and I_{ck} is given by

$$I_{ck}=-2\mathrm{Re}[F_k(1-F_k^{N_k})/(1-F_k)^2] \tag{38a}$$

$$=-2|F_k|\{(1+|F_k|^2)\cos(\underset{\sim}{q}\cdot\underset{\sim}{a}_k)-2|F_k|-|F_k|^{N_k}\cos[(N_k+1)\underset{\sim}{q}\cdot\underset{\sim}{a}_k] +2|F_k|^{N_k+1}\cos[N_k(\underset{\sim}{q}\cdot\underset{\sim}{a}_k)]-|F_k|^{N_k+2}\cos[(N_k-1)\underset{\sim}{q}\cdot\underset{\sim}{a}_k]\}/ [1-2|F_k|\cos(\underset{\sim}{q}\cdot\underset{\sim}{a}_k)+|F_k|^2]^2 \tag{38b}$$

Again the assumptions of the independent distance statistics in each direction and between the three directions were employed in the calculation. The intensity I(q) is subjected to the orientational average as in Eq.(7) when the paracrystals have an orientation distribution with respect to the laboratory coordinate. For example $Z(q,N_c)$ is defined as a lattice factor per unit size, i.e., normalized by $N_1N_2N_3=N_c^3$ for the randomly oriented paracrystal with $N_1=N_2=N_3=N_c$.

$$Z(q,N_c)=<\prod_{k=1}^{3}[Z_k+(I_{ck}/N_k)]>_{\text{random orient.}} \tag{39}$$

Figure 6 shows results of the numerical calculations of $Z(q,N_c)$ for three different N_c values and at a fixed g-value for the fcc lattice. The intensity level of each profile was shifted vertically to avoid overlapping. It obviously approaches unity at a large q, regardless of the value of N_c. With decreasing N_c value, the diffraction peak(s) clearly become lower and broader, and the higher order peaks tend to be smeared. The up-turn of a scattering curve at low angle regions which is observed for a

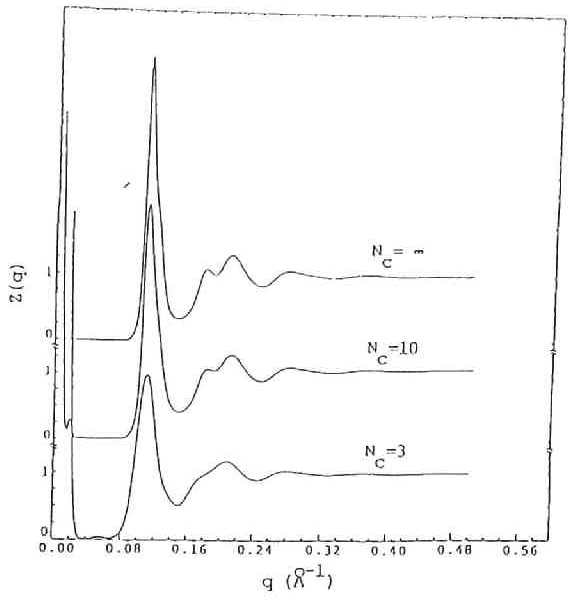

Figure 6 : Effects of the crystal size on the para-crystalline lattice factor for fcc with the nearest neighbour distance a_n=70.7A. Each curve was vertically shifted to avoid an overlap. g was 0.10.

small value of N_c corresponds to the contribution of the zero-th order scattering I_{ck} from a finite size of the paracrystal. In this calculation, outside the paracrystal is assumed to be a vacuum. Therefore, this up-turn appears. If the difference in the electron densities or the scattering length inside and outside of the paracrystal is zero, this up-turn would disappear.

As both of the parameters g and N simultaneously affect the height and the width of the diffraction peak, it is fairly difficult to determine unique values of g and N from a single diffraction maximum[27]. Hosemann and his coworkers found experimentally that the values of g and N should not be

independent. They proposed the so-called α^* -law[28],

$$g\sqrt{N} = \alpha^* \qquad (40)$$

$$0.1 < \alpha^* < 0.2$$

This α^*-law may be used for the approximate determination of g and N. It is a very interesting problem to examine whether the α^*-law holds in such systems as latex dispersion and block copolymers which have not been tested so far.

V. Discussions on Criterion for the (hkl) Diffraction Maximum to be Resolved and on Z(q→0) for the Three-Dimensional Paracrystals

V-1 Criterion for the (hkl) Diffraction Maximum to be Resolved for the Three-Dimensional Paracrystals.

Hosemann predicted the following equation as the criterion for the n-th peak to be resolved for the one-dimensional paracrystal,

$$g\,n=0.35 \qquad (41)$$

This relation was obtained analytically on the assumption that the relation

$$Z_{max}/Z_{min}=1.5 \qquad (42)$$

was a limit for the n-th peak to be resolved, where Z_{max} was a value of Z(q) at the n-th peak position and Z_{min} was a corresponding minimum value.

We reexamined this relation in our numerical calculations for a one-dimensional paracrystal. Figure 7 shows the g_ℓ vs. n^{-1}

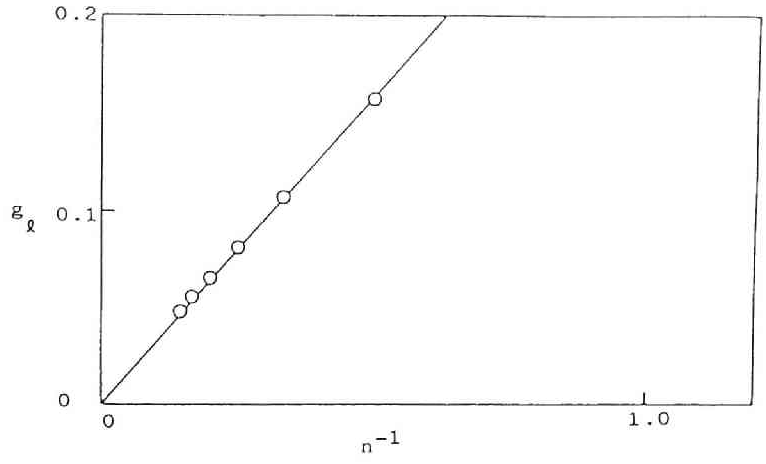

Figure 7 : g_ℓ vs. n^{-1} plot for a one-dimensional paracrystal. The straight line is a result of the first-order least-square fitting, $g_\ell=0.319\ n^{-1}$.

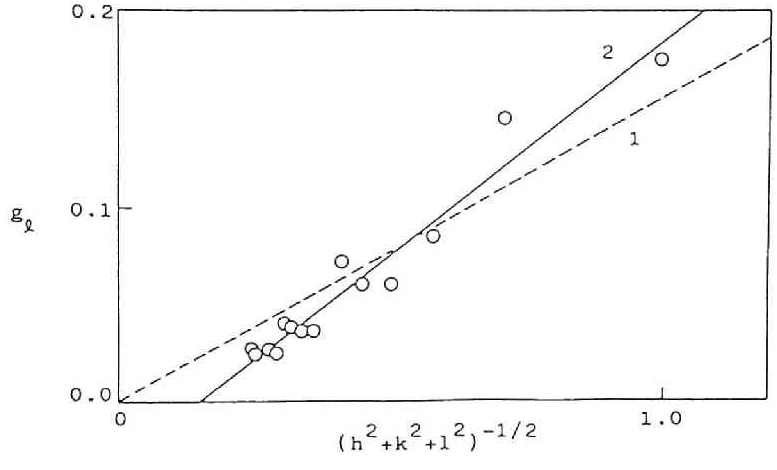

Figure 8 : g_ℓ vs. $(h^2+k^2+l^2)^{-1/2}$ plot for sc lattice. The straight lines are the results of the first-order least-square fitting.

1 : $g_\ell=0.155x(h^2+k^2+l^2)^{-1/2}$

2 : $g_\ell=0.215x(h^2+k^2+l^2)^{-1/2}-0.0313$

plot for a one-dimensional paracrystal, where g_ℓ is the value g which satisfies Eq.(42). The straight line is the result of the first-order least-square fitting of the data points, which predicts the following relation,

$$g_\ell \, n = 0.319 \qquad (43)$$

The slight discrepancy between Eqs.(41) and (43) may be due to the approximations involved in the procedure of obtaining Eq.(41) analytically.

For three-dimensional paracrystals, the situation becomes much more complicated, because each scattering peak corresponds not only to a different order but also to a different reflection plane which has different multiplicity. Furthermore, the extinction rule has to be taken into account. Thus it seems to be impossible to obtain analytically a criterion for the three-dimensional paracrystal. Therefore we tried to obtain the criterion by the numerical calculations of the lattice factor with an infinite size.

Figure 8 shows the g_ℓ vs. $(h^2+k^2+l^2)^{-1/2}$ plot for a simple cubic paracrystal. It is obvious that the linearity is not as good as for the case of the one-dimensional paracrystal, as we expected. The straight lines are obtained by the first-order least-square fitting by two functions, y=ax and y=ax+b. These fittings give us the following relations,

$$g_\ell \, (h^2+k^2+l^2)^{1/2} = 0.155 \qquad (44)$$

$$g_\ell = 0.215 \, (h^2+k^2+l^2)^{-1/2} - 0.031 \qquad (45)$$

which may be used as criteria for the simple cubic paracrystal lattice. As is clearly seen from Fig.8, Eq.(45) gives a better fit. However, this equation predicts that the higher order peaks, whose $(h^2+k^2+l^2)$ values are larger than 48, cannot appear even if the g-value is zero (i.e. for ideal crystal). This is physically unreasonable. Actually in the three-dimensional paracrystal the relation between g_ℓ and $(h^2+k^2+l^2)$ may not be a simple linear relation. Hence Eq.(45) is an approximate criterion. The value specifying the criterion for the three dimensional paracrystal appears to be close to that for the one-dimensional paracrystal divided by $\sqrt{3}$ (viz. $0.35/\sqrt{3}=0.202$).

For the bcc lattice, the following approximate criteria were obtained using reflections from (110), (200), (211), (220), (310), and (321) planes,

$$g_\ell (h^2+k^2+l^2)^{1/2}=0.170 \qquad (46)$$

$$g_\ell =0.215(h^2+k^2+l^2)^{-1/2}-0.024 \qquad (47)$$

As was the case for the sc lattice, Eq.(47) is a better criterion. It is interesting to note that we obtain similar criteria for sc and bcc lattice.

It was impossible to obtain a criterion for the fcc lattice because the fusion of the peaks hindered the estimation of the characteristic Z_{max} and Z_{min} values for each peak.

V-2 Behavior of the Lattice Factor Z at $q \to 0$ for the Cubic Paracrystals.

In this section, we discuss the origin of the intensity upturn for Z in the limit of $q \to 0$ which was found clearly for sc (Fig.3) and bcc (Fig.5) lattices. This intensity upturn may be thought peculiar in light of the behavior of Z for the one-dimensional paracrystal as reported by Hosemann and Wilke[29]. For the one-dimensional paracrystal it was found that

$$\lim_{q \to 0} Z(q) = g^2 \qquad (48)$$

As q approaches zero, the intensity Z(q) continuously decreases to the limiting value of g^2 and the intensity upturn is not found.

For a three-dimensional paracrystal, we should study Eq.(4) to understand this upturn.

For example, $Z_3(q)$ can be calculated as follows

$$1-|F_3|^2 = q^2 \Delta a_3^2 + O(q^4) \qquad (49)$$

$$\begin{aligned} 1-2|F_3|\cos(\underset{\sim}{q}\cdot\underset{\sim}{a}_3)+|F_3|^2 &= [4\sin^2[(1/2)a_3 q\cos\theta)][1-(1/2)q^2\Delta a_3^2]+O(q^4) \\ &= a_3^2 q^2 \cos^2\theta + O(q^4) \end{aligned} \qquad (50)$$

Thus it follows that

$$\lim_{q \to 0} Z_3(q) = \frac{\Delta a_3^2}{a_3^2 \cos^2\theta} \equiv \frac{\Delta a_3^2}{a_{3,\mathrm{eff}}^2} \equiv g_{3,\mathrm{eff}}^2 \qquad (51)$$

for a one-dimensional paracrystal with periodicity along the $\underset{\sim}{a}_3$ direction and observation of the scattering with $\underset{\sim}{q}$ vector along $\underset{\sim}{a}_3$ direction, $\cos\theta = 1$ and hence

$$\lim_{q\to 0} Z_3=\Delta a_3^{\,2}/a_3^{\,2}=g_3^{\,2} \qquad (52)$$

which was obtained by Hosemann and Wilke. However for a three-dimensional crystals, the effective unit cell size $a_{3,eff}\equiv a_3\cos\theta$ which is a projection of $\underset{\sim}{a}_3$ onto $\underset{\sim}{q}$, depends on the orientation of the vector $\underset{\sim}{a}_3$ with respect to $\underset{\sim}{q}$. Thus the limiting value of Z at $q\to 0$ is equal to the effective g-value (g_{eff}) as defined in Eq.(51), which goes to infinity as θ approaches $\pi/2$. This divergence, which causes the upturn of Z(q) as q goes to zero, occurs as a consequence of a random orientation of the paracrystal and of a spherically symmetric distortion of the lattice points, e.g. $\Delta a_{31}=\Delta a_{32}=\Delta a_{33}\equiv\Delta a_3$. Similarly to Eq.(51), we obtain

$$\lim_{q\to 0} Z_1(q)= \frac{\Delta a_1^{\,2}}{a_1^{\,2}\sin^2\theta\cos^2\psi} \equiv \frac{\Delta a_1^{\,2}}{a_{1,eff}^{\,2}} \equiv g_{1,eff}^{\,2} \qquad (53)$$

$$\lim_{q\to 0} Z_2(q)= \frac{\Delta a_2^{\,2}}{a_2^{\,2}\sin^2\theta\sin^2\psi} \equiv \frac{\Delta a_2^{\,2}}{a_{2,eff}^{\,2}} \equiv g_{2,eff}^{\,2} \qquad (54)$$

Therefore

$$\lim_{q\to 0} Z(q)= \prod_{k=1}^{3} g_{k,eff}^{\,2} \qquad (55)$$

We may extend similar arguments for fcc and bcc.

VI. Comparison with Experimental Scattering Profiles.

In recent years, scattering techniques have been employed for the investigation of the ordering phenomena[5-7] of macroions (including synthetic macroions,[30] biopolymers,[25] and ionic surfactant micelles[31]) in solutions. Laser light and neutron scattering techniques have also been used for solutions of monodisperse polymer latex particles.[32-34] The ordering of larger latex particles with a diameter of about 3000 A in solution has been almost unequivocally proven by observation through ultramicroscopy.[9] SAXS and SANS techniques have been used to study the microdomain structure of block copolymers in the solid state [15-17] and in solutions[18,19]. In this section, the applications of the three-dimensional paracrystal theory is applied to aqueous suspensions of ordered latex particles. An application to the ordered spherical microdomains of block polymers will be dicussed in elsewhere[22].

VI-1 Small-angle Neutron and Laser Light Scattering of Polymer Latex Suspensions.

In the colloid science, the lattice factor (Z(q)) is often called the interparticle interference function, and represented by S(q). All the S(q) functions to be discussed in this section are obtained from the scattering curve with the assumption of $\sigma_r=\sigma_s=0$, i.e., the latex particles are homogeneous spheres and monodisperse. The scattering intensity in Eq.(3) is rewritten by

$$I(q)=N\ P(q)S(q) \qquad (56)$$

$$P(q)=|f_0|^2, \quad S(q)=Z(q) \qquad (57)$$

where $P(q)$ is the intraparticle scattering function. All the interference functions $Z(q)$ are obtained for $N_c \rightarrow \infty$ unless otherwise stated.

In Fig.9 are given the interference function for a polymer latex dispersion obtained by laser light scattering[32] (filled circles) and $Z(q)$ calculated by the present theoretical treatment (full curve). The concentration of latex particles is much lower than those employed in microscopic observation to avoid some experimental difficulties such as multiple scattering. We cannot observe directly the spatial distribution of the particles by microscopy for this system. However, it is expected that the spatial arrangement of the particles will be highly distorted due to the low concentrations. The first peak position and height were fitted with a g value of 0.19 for fcc, though the observed height of the secondary peak could not be reproduced well by the theory.

In Fig.10 the interference functions obtained by neutron scattering for latex solutions[33] are compared with the theoretical curves which were obtained for fcc structures. Investigations on the more concentrated dispersions were possible for small latex particles by employing the SANS technique. Here again the first peak position and height were fitted. Although the disagreement at low scattering vectors and for the secondary peak are obvious, the agreement between theory and experiment is satisfactory. The g values are again about 0.2. With decreasing

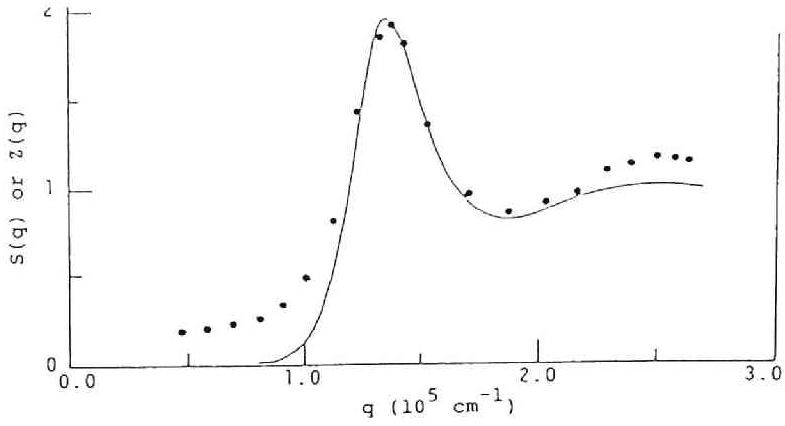

Figure 9 Comparison of the experimental interference function, S(q), with theoretical paracrystalline lattice factor, Z(q).

Circles : S(q) for latex solution by Ottewill, vol. fraction (ϕ):10^{-3}, Particle radius:256A.

Line : Z(q) for an fcc structure, a_n=5597A, g=0.19.

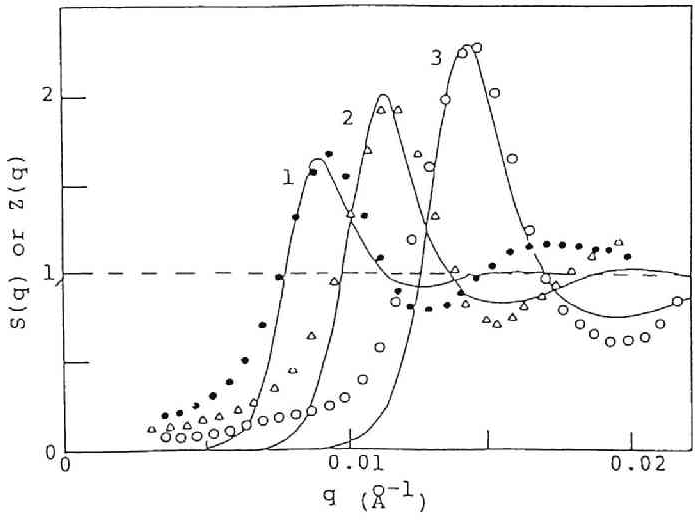

Figure 10 Comparison of the experimental interference function, S(q), obtained by neutron scattering for latex solutions by Cebula et al. and theoretical lattice factors, Z(q).

● , Δ , and ○ : S(q) observed for a latex of R=157 A at ϕ=0.04, 0.08, and 0.13, respectively.

Curves 1, 2 and 3: Z(q) for fcc structures with a_n=830 A, g=0.22, a_n=679 A, g=0.19, and a_n=539 A, g=0.17, respectively.

concentration, the g value becomes larger. This trend is quite understandable and is consistent with the microscopic observation.[35] Also the tendency of the interparticle spacing to decrease with increasing concentration (volume fraction : ϕ) is readily acceptable and is in accordance with earlier microscopic observations.[36]

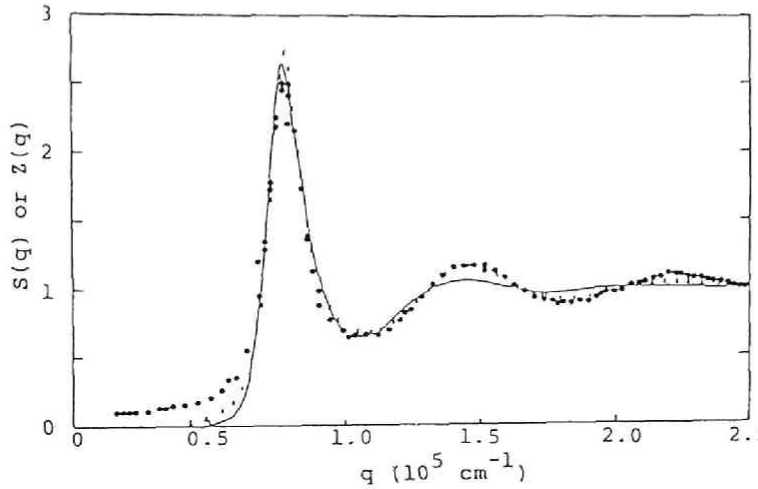

Figure 11 : Comparison of the experimental interference function, S(q), and theoretical paracrystalline lattice factor, Z(q).

Circles : S(q) obtained by light scattering for latex solution by Versmold et al. 1.34×10^{18} particles $/m^3$.

Line : Z(q) for fcc structure. a_n=9824A, g=0.15.

x : RMSA result.

Figure 11 shows the experimentally obtained interference function for polymer latex dispersion from light scattering[34] and the theoretical curve obtained for an fcc structure with a g value of 0.15. The agreement is fairly satisfactory, though the

agreement for the second peak is not so good. The disagreement in the low angle regions is also clear, but it may be at least partially due to the inaccuracy in the experimental data caused by multiple scattering, dust scattering, etc.

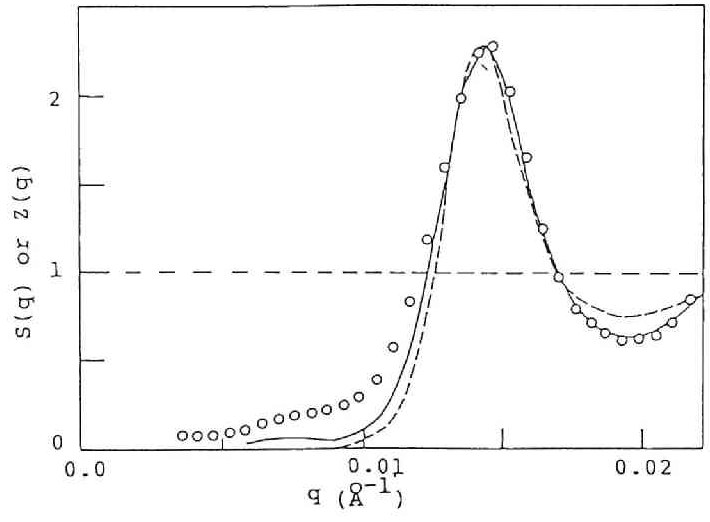

Figure 12 : Comparison of the experimental interference function, S(q), and theoretical lattice factors Z(q).

Circles : S(q) obtained by neutron scattering for a latex solution. (Ottewill et al.) ϕ=0.13 , R=157A.

Broken curve : Z(q) for an fcc structure.

a_n=539A, g=0.17, N_c= ∞ .

Full curve : Z(q) for an fcc structure.

a_n=539A, g=0.12, N_c=3.

Figure 12 shows the experimental data given in Fig.10 for a volume fraction (ϕ) of 0.13, together with theoretical curves, which were obtained for two different sets of N_c and g. The profile for the smaller N_c and g values gives a better fit with the experimental data. Though it cannot be claimed that this pair of g and N_c values (g=0.12,N_c=3) is the only one which can reproduce this S(q) curve because both g and N_c simultaneously

affect the peak height and the peak width as was discussed in Sec.IV-2. It might be interesting to note the rough agreement of these values with the α^*-law ($\alpha^*=0.12 \times 3^{1/2}=0.207$). As will be discussed in detail later, the interparticle distance obtained from the S(q) peak position is very close to the one calculated assuming a uniform distribution. Thus, it is believed that the crystal size, in this case, must be recognized as the region which has correlated particles for the directions of the three axes as described in Sec.IV-2.

Note that the interparticle distances, a_n, used in the calculation of Z(q) in Figs.9-12 are all fairly close to the average interparticle spacing ($2D_0$) which can be calculated from the concentration by assuming a uniform distribution of the particles throughout the space and fcc symmetry.[37] In the case of Fig.9, the a_n value was 5600 A whereas the $2D_0$ value was 4633 A for fcc. For Fig.10 the agreement is even much better: the values a_n were 830, 679 and 539A at the volume fractions of 0.04, 0.08 and 0.13, respectively, whereas the $2D_0$ values were 831, 659 and 561A. In Fig.11, the value a_n was 9824 A and the $2D_0$ value was 10180 A. Except for a case in Fig.9, the two interparticle spacings are fairly close to each other. This agreement and the fact that the experimental scattering profiles were well reproduced by the theoretical profile for the fcc lattice, support the validity of the present extension of the paracrystal theory.

Another interesting point is the similarity between the interference functions calculated by the so-called RMSA (rescaled

mean spherical approximation) method and those calculated by the present treatment. The RMSA results are shown by crosses in Fig.11, which were taken from the work by Versmold.[34] Our values, calculated on the basis of the paracrystal theory, are in fairly good agreement not only with the observed S(q) but also with the RMSA results. The RMSA method is based on a liquid theory whereas the paracrystal theory has its foundation in ideal lattices. Thus the agreement shown by the two methods might indicate that the nature of the ordered structure under consideration is intermediate between a liquid and a solid. The RMSA method is based on a purely repulsive interaction whereas in our approach the type of the interaction does not explicitly come into question. Thus, it is not warranted to claim that the interparticle interaction is purely repulsive on the basis of the agreement of the RMSA calculation with the observed S(q). In order to clarify the nature of the interparticle interaction, the analysis of the structure factor in terms of the RMSA method is not adequate: a much more thorough study is required of the scattering behavior and of other fundamental physico-chemical properties of the systems as well.

VII. Conclusion

In the present chapter, a three-dimensional paracrystal theory has been developed for cubic lattices. The lattice factors were calculated by taking the paracrystalline distortion into account. Also disscussed were the thermal oscillation of the scattering elements around the lattice point, the interfacial thickness and the size of the paracrystals. The theory was

compared with scattering profiles obtained for polymer latex suspensions. From the comparison, the lattice symmetry and the degree of paracrystalline distortion were evaluated. The fcc structures with fairly large distortions gave the best fit with the latex suspensions studied.

References

1 R.Hosemann and S.N.Bagchi, "Direct Analysis of Diffraction by Matter", (North-Holland, Amsterdam, 1962).

2 W.Frank and W.Wilke, Coll. Polym. Sci., 261, 1010 (1983).

3 R.Steffen and R.Hosemann, Phys. Rev. B, 13, 3232 (1976).

4 O.Glatter and O.Kratky, "Small-Angle X-ray Scattering", (Academic Press, London, 1982), Chap.4.

5 N.Ise and T.Okubo, Acc. Chem. Res., 13, 303 (1980).

6 N. Ise, Makromol. Chem.,12,215 (1985).

7 N. Ise, Angew. Chem. Int.Ed., 25, 323 (1986).

8 W.Luck, M.Klier and H.Wesslau, Ber. Bunsenges. Phys. Chem., 67, 75 (1963).

9 A.Kose, M.Ozaki, K.Takano, Y.Kobayashi and S.Hachisu, J. Colloid Interface Sci., 44, 330 (1973).

10 N.A.Clark, A.Hard and B.J.Ackerson, Nature, 281, 57 (1979); Ackerson and N.A.Clark, Phys. Rev. Lett., 46, 123 (1981).

11 T.Yoshiyama, I.Sogami and N.Ise, Phys. Rev. Lett., 513, 2153 (1984).

12 R. M. Cornell, J. W. Goodwin and R. H. Ottewill, J. Coll. Interface Sci.,71, 254 (1979).

13 N. Ise, T. Okubo, K. Ito, S. Dosho and I. Sogami, Langmuir, 1,176 (1985).

14 N. Ise, K. Ito, T. Okubo, S. Dosho and I. Sogami, J. Amer. Chem. Soc., 107, 8074 (1985).

15 T.Hashimoto, M.Fujimura and H.Kawai, Macromolecules, 13,

1660 (1980).

16 F.S.Bates , R.E.Cohen and C.V.Berney, Macromolecules, 15, 589 (1982).

17 D.J.Kinning and E.L.Thomas, Macromolecules, 17, 1712 (1984).

18 M.Shibayama, T.Hashimoto and H.Kawai, Macromolecules, 16, 16 (1983).

19 T.Hashimoto, M.Shibayama, H.Kawai, H.Watanabe and T.Kotaka, Macromolecules, 16, 361 (1983).

20 Thomas et al.[17] attempted to compare the experimental profiles with the profiles calculated based upon a Percus-Yevick type potential function between the spherical domains. However this approach to the block polymer systems is phenomenological and best applied to the systems with a large distortion so that the higher order maxima due to the cubic lattice symmetry do not exist.

21 R.Bramer and W.Ruland, Makromol. Chem., 177, 3601 (1976).

22 H.Matsuoka, H.Tanaka, T.Hashimoto, and N.Ise, Phys. Rev. B, in press.

23 D.J.Yarusso and S.L.Cooper, Macromolecules, 16, 1871 (1983).

24 W.Ruland, J.Appl.Crystallogr., 4, 70 (1971).

25 Chapter 3 of this thesis; H.Matsuoka, N.Ise, T.Okubo, S.Kunugi, H.Tomiyama and Y.Yoshikawa, J. Chem. Phys., 83, 378 (1985).

26 T.Hashimoto, A.Todo and H.Kawai, Polym. J., 10, 521 (1978).

27 It is well known that, if the scattering profile contains

more than two diffraction maxima from the lattice, we can separate the effects of g and N by analyzing the peak breadth as a function of the order of the diffractions.[1]

28 F.J. Balta-Calleja and R.Hosemann, J. Appl. Crystallogr., 13, 521 (1980).

29 R.Hosemann and W.Wilke, Makromol. Chem., 118, 230 (1968).

30 Chapter 2 of this thesis; N. Ise, T. Okubo, S. Kunugi, H. Matsuoka, K.Yamamoto and Y.Ishii, J.Chem.Phys.,81, 3294 (1984)

31 Chapter 5 of this thesis; Y. Ishii, H. Matsuoka and N. Ise, Ber. Bunsenges. Phys. Chem., 90, 50 (1986).

32 R. H. Ottewill, Progr. Colloid & Polymer Sci.,67,71 (1980).

33 D. J. Cebula, J. W. Goodwin, G. C. Jeffrey, R. H. Ottewill, A. Parentich and R. A. Richardson, Faraday Discuss. Chem. Soc. 76, 37 (1983).

34 W. Hartl, H. Versmold and U. Wittig, Ber. Bunsenges. Phys. Chem., 88, 1063 (1984).

35 K.Ito and N. Ise, J.Chem.Phys., in press.

36 N. Ise, T Okubo, M. Sugimura, K. Ito and H. J. Nolte, J. Chem. Phys.,78,536 (1983).

37 When the interparticle distance was measured by the microscopic method, it was found to be smaller than $2D_0$ for highly charged latex particles at low concentrations, as discussd in review articles (Ref.5 -7). This situation required us to accept the existence of a substantial attractive interaction between latex particles through the intermediary of counterions. This attraction, together with

the repulsive interaction between the particles per se, would form a secondary minimum. When the particles are not highly charged, the attraction is not intensive because the number of mediating counterions is small. The particles are then, located as far apart as possible from each other, namely at an average distance of $2D_0$. In other words, $2D_{exp} \simeq 2D_0$ for such low charge density particles. The latex samples, which are discussed in Figures 9 - 12, have low charge numbers so that the equality relation mentioned in the text, $a_n \simeq 2D_0$ is reasonable.

Ackowledgments

The present investigations were carried out in the Department of Polymer Chemistry, Kyoto University, in the period from 1980 to 1987.

The author would like to express his sincere gratitude to Professor Norio Ise for his continuous guidance, useful criticisms and encouragement throughout this work. The author expresses his sincere gratitude to Drs. Tsuneo Okubo, Shigeru Kunugi, and Takeji Hashimoto for their guidance and encouragement.

The author would like to express his sincere gratitude to Messrs. Mutsuyuki Sugimura, Kazuyuki Yamamoto, and Yasuo Ishii for their discussions and kind guidance in experimental techniques. Sincere thanks also go to Messrs. Hiroshi Tomiyama, Yukihiro Yoshikawa, Mitsuyuki Tsurumi, and Hideaki Tanaka, who took part in the experimental work. The author expresses appreciation to other investigators in the laboratory for discussions and encouragement.

April, 1987

HIDEKI MATSUOKA

Abstract

Chapter 2

The small-angle X-ray scattering measurements were performed for aqueous solutions of sodium polystyrenesulfonates having narrow molecular weight distributions. As was observed for other synthetic macroions, polynucleotide and proteins, a single, broad peak was observed. The scattering vector at the peak position (q_m) was shifted toward larger values with increasing polymer concentration and toward lower values with increasing salt concentration, which confirmed earlier observations with polyacrylate and poly-L-lysine. The molecular weight dependence of the scattering behavior, which was earlier observed, was confirmed to be true for samples with M_w of 74000, 18000, and 4600. The mixture of two fractions with different M_w's gave a scattering curve which was again different from the composite curve obtained with the parent curves before mixing. A similar situation was observed for the mixture of polystyrenesulfonate and polyacrylate. Thus, it was concluded that the observed single peak indicates the presence of an intermolecular ordering, not an intramolecular ordering. The intermacroion distance ($2D_{exp}$) was thus calculated by using the Bragg equation. $2D_{exp}$ decreased with increasing polymer concentration and increased (not decreased) with increasing concentration of added salt and M_w. The $2D_{exp}$ values thus obtained were smaller beyond the experimental error than $2D_0$, a theoretical distance calculated from concentarion by assuming the uniform distribution of the macroions throughout the

solution and the $2D_0/2D_{exp}$ value amounted to 3.5 for high molecular weight samples. This fact indicates the presence of an intermacroion attractive interaction. When two fractions with differen M_w's were compared at a given number concentration of macroions, the $2D_{exp}$ value for the samples of a larger M_w was smaller than that for the fraction of a smaller M_w. This implies that the attraction must be intensified, though unexpectedly, with increasing valency of the macroions, confirming the earlier interpretation that the attraction could be brought into existence through the intermediary of counterions present between macroions. The larger the number of the counterions, the stronger the intermacroion attraction. With increasing temperature, the peak was slightly lowered and the $2D_{exp}$ became smaller, though very slightly. Rough agreements between X-ray and neutron scattering data were noted. On the basis of the direct microscopic observation of a similar ordering of polymer latex particles, it was suggested that the macroions in the ordered regions were subject to violent thermal motion, and that para-crystalline distortion of the ordered structures allowed us to observe only a single broad peak.

Chapter 3

Dilute aqueous solutions of bovine serum albumin, lysozyme, chondoroitin sulfate and tRNA were measured by small-angle X-ray scattering. The scattering curves showed a single, broad peak characteristic of synthetic polyelectrolytes, indicating the presence of an ordered distribution of charged solutes. The

intermolecular distance evaluated from the peak position ($2D_{exp}$) increased with decreasing polymer concentration and with increasing salt concentration. Except for chondoroitin sulfate, $2D_{exp}$ values were nearly equal to the calculated interparticle distance($2D_0$) calculated based on the assumption of a uniform distribution. For chondoroitin sulfate, $2D_{exp}$ values were smaller than $2D_0$. The observed relationship between $2D_{exp}$ and $2D_0$ was in agreement with the proposal that intermacroion attraction is stronger for highly charged solutes like chondoroitin sulfate and that it is weak for low-charge density particles such as biopolymers under discussion. This attraction and repulsive interparticle interaction create a "secondary" minimum in the potential curve enabling ordering to take place. For tRNA, the scattering peak became lower with rising temperature. The fact, that only a single, broad peak could be observed, was rationalized by invoking the concept of large distortions of an ordered regions such as the paracrystallinity, the thermal motion and the crystalline size effect. The correlation hole theory based on repulsive interaction is critically discussed, particularly in light of the experimental fact that the peak position of albumin shifts toward wider angles with increasing number of charges.

Chapter 4

The small-angle X-ray scattering was carried out for aqueous solutions of polyallylamine hydrochloride. When the polymer concentration was reasonably high and the concentration of coexisting simple salt was low, a single, broad peak was observed. The

peak was interpreted as indicating the presence of an ordered arrangement of macroions in the solutions. The intermacroion spacing was caluculated by the Bragg equation and found to be much smaller than the average intermacroion spacing calculable from the polymer concentration, suggesting that there exist ordered regions and at the same time disordered regions in the solutions. The Bragg spacing decreased with increasing polymer concentration and increased with increasing salt concentration. Mixing of two samples of different molecular weights gave a new scattering peak in between the original peaks of the mother samples, which supports the intermolecular nature of the ordering. The peak height was lowered with increasing temperature. The scattering peak was found to stay unaffected for 21 days.

Chapter 5

The solutions of ionic micelles of dodecyl-, tetradecyl- and hexadecyl-trimethylammonium chlorides were studied by small-angle X-ray scattering (SAXS). The SAXS curves showed a single, broad peak. The interference functions S(q) were obtained from the scattering curves. The radial distribution function g(r) was calculated from S(q) and the distances between nearest neighboring micelles were evaluated. The intermicellar distances(r_m) evaluated from g(r) were close to the average distance calculated by assuming a uniform distribution of the micelles throughout the solution. This fact indicates that the intermicellar attractive force through the intermediary of

counterions was weak, because the number of charges on the micelles was small. A difference between r_m and the Bragg spacing calculated from the overall intensity of scattered X-ray was noticed but it was not large enough to invalidate our previous interpretation that the Bragg spacing is an approximate measure of the ordered structure. By taking into account the paracrystalline distortion, the lattice factor Z(q) was calculated. An excellent agreement was obtained with the structure factor S(q) for a face-centered cubic lattice structure when the distortion factor was assumed to be about 0.2. The number of peaks of the lattice factor decreased with increasing distortion factor. This suggests the incorrectness of the often expressed view that the single broad peak is not reminiscent of some kind of ordering:in this view the large distortion, which exists in solutions and at ambient temperatures, has been overlooked.

Chapter 6

The distribution of colloidal silica particles in suspension was investigated by small-angle X-ray scattering (SAXS). The scattering curves showed a broad, but distinct peak and the second shoulder at low and no salt conditions, which suggests that the particles form more or less ordered array. From the scattering intensity I(q), the interparticle interfernce function S(q) was evaluated, which reflects the distribution of particles more directly. S(q) showed a broad peak and the second shoulder. The peak position shifted to higher angles and became higher with incresing concentration. The peak intensity was lowered with

increasing salt concentration. This fact suggests that the formation of the ordered structure is of an electrostatic origin. The shape of S(q) curve could be well reproduced by the theoretical scattering curve of distorted face-centered cubic paracrystal.

Chapter 7

The three-dimensional paracrystalline lattice factors Z(q) for a face-centered cubic lattice and body-centered cubic lattice in addition to simple cubic lattice were calculated. The Z(q)'s thus calculated could reproduce the diffraction peaks at the characteristic positions for each cubic lattice system in a fairly wide range of g values(g:degree of the paracrystalline distortion). In addition to the paracrystalline distortion, the thermal oscillation and crystal size effects were also considered. The numerically calculated profiles were compared with light and small-angle neutron scattering curves for polymer latex dispersions for quantitative determination of the ordered cubic systems.

List of Publications

Chapter 2 J.Chem.Phys., 81, 3294 - 3306 (1984).

Chapter 3 J.Chem.Phys., 83, 378 - 387 (1985).

Chapter 4 British Polym. J., 18, 242 -246 (1986).

Chapter 5 Ber.Bunsenges.Phys.Chem., 90, 50 - 57 (1986).

Chapter 6 in preparation.

Chapter 7 Phys. Rev. B, in press.